THE UNIVERSITY OF MANITOBA

# THE PETROLOGY, CHEMISTRY AND SULPHIDE MINERALOGY OF THE DIXIE 150 - 17B, 18 and 19 PYRITIC Cu - Zn - Ag PROSPECTS RED LAKE, NORTHWESTERN ONTARIO

BY

DOUGLAS JAMES ANDREWS

A THESIS

SUBMITTED TO THE FACULTY OF GRADUATE STUDIES

IN PARTIAL FULFILLMENT OF THE REQUIREMENTS FOR THE DEGREE

OF MASTER OF SCIENCE

DEPARTMENT OF EARTH SCIENCES

WINNIPEG, MANITOBA

1979

# THE PETROLOGY, CHEMISTRY AND SULPHIDE MINERALOGY OF THE DIXIE 150 - 17B, 18 and 19 PYRITIC Cu - Zn - Ag PROSPECTS RED LAKE, NORTHWESTERN ONTARIO

BY

DOUGLAS JAMES ANDREWS

A dissertation submitted to the Faculty of Graduate Studies of the University of Manitoba in partial fulfillment of the requirements of the degree of

MASTER OF SCIENCE

© 1979

Permission has been granted to the LIBRARY OF THE UNIVERSITY OF MANITOBA to lend or sell copies of this dissertation, to the NATIONAL LIBRARY OF CANADA to microfilm this dissertation and to lend or sell copies of the film, and UNIVERSITY MICROFILMS to publish an abstract of this dissertation.

The author reserves other publication rights, and neither the dissertation nor extensive extracts from it may be printed or otherwise reproduced without the author's written permission.

# ABSTRACT

The Dixie 150 - 17B, 18 and 19 copper - zinc - silver prospects are three of several sulphide lenses which occur along a 45 km greenstone belt composed of regionally metamorphosed mafic volcanic, sedimentary and diapiric granitic rocks of Archean age. The greenstone belt constitutes the southwestern extension of the Uchi - Confederation Lake greenstone belt of the Red Lake (Uchi) subprovince in northwestern Ontario. The prospects are located approximately 32 km southeast of Red Lake, Ontario.

The Dixie 150 - 18 prospect is one of the largest known sulphide occurrences in the area. It is a vertical funnel-shaped sulphide body contained within steeply dipping mafic metavolcanic units comprising massive porphyritic and non-porphyritic basaltic to andesitic flows, lapilli tuffs and siliceous tuffite which have been intruded by several lamprophyric dikes and small feldspar porphyry sills. Similar metavolcanic units with intercalated sequences of greywacke, calcareous siltstone and impure limestone occur east and northeast of the sulphide body.

Major element chemical analysis indicate that the Dixie 150 - 18 massive flows are enriched in sodium when compared to the lapilli tuffs and that both massive flows and lapilli tuffs exhibit a strong iron enrichment trend and an accompanying trend towards alkali enrichment. The volcanic rocks

belong to the sub-alkaline field of volcanic rocks, plot mainly as a tholeiitic suite and are individually classified as high-iron tholeiites of basaltic to andesitic compositions (although some high alumina andesites plot within the calc-alkaline field).

Pyrite, pyrrhotite, sphalerite, chalcopyrite and magnetite are the major metallic minerals and occur as massive and disseminated mineralization. The sulphide mineralization exhibits textural evidence of intense deformation, recrystallization and metamorphic mobilization. Distinct zinc and silver distribution patterns are present within the mineralization. Compositional copper zoning within the central portion of the sulphide body may indicate the location of the discharge source for the hydrothermal solutions.

A large cordierite-anthophyllite alteration zone composed of a complex mineral assemblage of anthophyllite, cordierite, quartz, chlorite and biotite is situated along the footwall of the sulphide body. The cordierite-anthophyllite alteration zone is conformable with the flanks of the sulphide body but thickens, becomes discordant and resembles an alteration pipe beneath the central portion of the sulphide mineralization. Chloritization, cation hydrolysis, silicification and biotitization are locally important alteration processes associated with sulphide mineralization. Major element chemical analyses indicate that strong silica, alkali and lime depletion was accompanied by intense iron,

magnesium, sulphur and manganese enrichment within the zones of sulphide mineralization. This relative enrichment in iron and magnesium and depletion in lime and alkalies within the alteration zone may have been sufficient so that cordierite-anthophyllite assemblages developed within original chloritic alteration zones during high temperature (500 to 800°C) low to moderate pressure (4 to 7 kbars) regional metamorphism.

The 150 - 18 sulphide mineralization may have been precipitated during syngenetic (solfataric) processes contemporaneously with enclosing volcanic sequences or as epigenetic emplacement (stratigraphic trapping and replacement) of mineralization following formation of the volcanic pile.

The Dixie 150 - 17B and 19 prospects are much smaller mineralized veins and lenses of sulphide mineralization contained within granitized metavolcanic tuffs which lie parallel to the contact of nearby granodiorite intrusions. Two main genetic possibilities exist for these prospects. The sulphide mineralization may have been emplaced by hydrothermal fluids emanating from the granodiorite intrusions or by syngenetic processes during volcanism.

# TABLE OF CONTENTS

TABLE OF CONTENTS

TABLE OF CONTENTS

TABLE OF CONTENTS

TABLE OF CONTENTS

# LIST OF FIGURES

# LIST OF FIGURES

# LIST OF FIGURES

# LIST OF TABLES



## APPENDIX

# LIST OF PLATES

# LIST OF PLATES

# CHAPTER 1

# INTRODUCTION

## GENERAL STATEMENT

The Dixie 150 - 17B, 18 and 19 copper-zinc-silver prospects are three of several massive sulphide bodies occurring within the southwestern extension of the Uchi - Confederation Lake greenstone belt. The Uchi - Confederation Lake greenstone belt is easily accessible by water, road or float plane and has been extensively prospected and mined since the turn of the century.

Several gold occurrences were investigated and mined during the latter portions of the 1920 and 1930 decades and the greenstone belt has consequently been extensively mapped, remapped and investigated for additional occurrences of gold and base metals since that time.

Until recently, the southwestern extension of the Uchi - Confederation Lake greenstone belt containing the sulphide occurrences under present examination has been relatively ignored or unmapped, and geological investigations within this area are limited. General inaccessibility, numerous swamps and extensive glacial overburden have hampered geological investigations and mapping. However, the 1968 discovery of the South Bay copper-zinc-silver ores located some 15 km east of the Dixie prospects and recent discoveries of sulphide mineralization including the Dixie prospects has resulted in considerable exploration in the southwestern extension of the

Uchi - Confederation Lake greenstone belt. The area is being actively explored by Selco Mining Corporation and the Ontario Division of Mines is mapping selected portions of the belt.

## SCOPE OF THESIS

The present research is an effort to establish the geology hosting the Dixie 150 - 17B, 18 and 19 prospects and the nature of the mineralization comprising the sulphide bodies. The research is also designed to investigate some aspects of chemical petrology and mineralogy of the enclosing volcanic rocks, alteration zone, metamorphism, metal distribution and textural interpretation of the sulphide minerals with a view to understanding the probable environment of mineralization. Emphasis is primarily given to the 150 - 18 prospect which is currently one of the largest sulphide bodies discovered within the southwestern extension of the Uchi - Confederation Lake greenstone belt. The 150 - 17B and 19 prospects are much smaller and of little economic interest. However, these prospects have been investigated in some detail and compared with the 150 - 18 prospect at the end of this thesis.

The immediate research area is completely covered by an extensive layer of thick glacial overburden which increases the difficulty of geological interpretation and correlation

throughout the area. Consequently, all geological interpretation and research has been based upon diamond drill core intersections which adequately outline the geology and configuration of all three prospects.

The author sampled and logged the diamond drill core from all three prospects during the fall of 1977. Representative samples were collected from lithologically distinct volcanic, sedimentary and mineralized units and analyzed at the University of Manitoba.

Whole rock chemical analyses were obtained for 23 volcanic and sedimentary rocks and 24 rocks from the cordierite-anthophyllite alteration zone. Two hundred and eight thin sections were made for the Dixie prospect rocks and 25 polished sections for the mineralized zones.

The area immediately southwest of the prospects was visited during the field investigations. Approximately one week was devoted to familiarization of the major rock types within this area where outcrop is plentiful and could be studied for comparative purposes and possible correlation with the Dixie prospect volcanic rocks.

## LOCATION AND ACCESS

The Dixie 150 - 17B, 18 and 19 prospects are approximately 32 km southeast of the town of Red Lake and 10 km northeast of the Griffith Iron Mine on the western shores

of Bruce Lake in northwestern Ontario (figure 1). The area is reached by highway #105 to a major forestry access road located approximately 2 km north of Troutlake River. The all-weather access road runs northeast from the highway and terminates near the end of the study area near the drill camp where a footpath runs north, branches off and connects all three prospect locations. The Dixie prospects occur in an area of approximately 25 square km.

## PREVIOUS GEOLOGICAL WORK

Until recently little geological work has been done within the area immediately surrounding the Dixie 150 - $17_B$, 18 and 19 prospects. Selco Mining Corporation unpublished geological maps based upon limited outcrop and magnetic and gravity geophysical data provide the most detailed geological compilations within the area. The geological base map used for the initial interpretation of the area was the Dixie East Part (Selco plan Di 1946) which was continually updated and included information received during the 1977 field season. The progress map also covered almost the entire length and width of the southwestern extension of the Uchi - Confederation Lake greenstone belt.

The closest and most recent government survey includes extensive geological investigations and mapping around the Bruce Lake area by the Ontario Division of Mines (Shklanka,

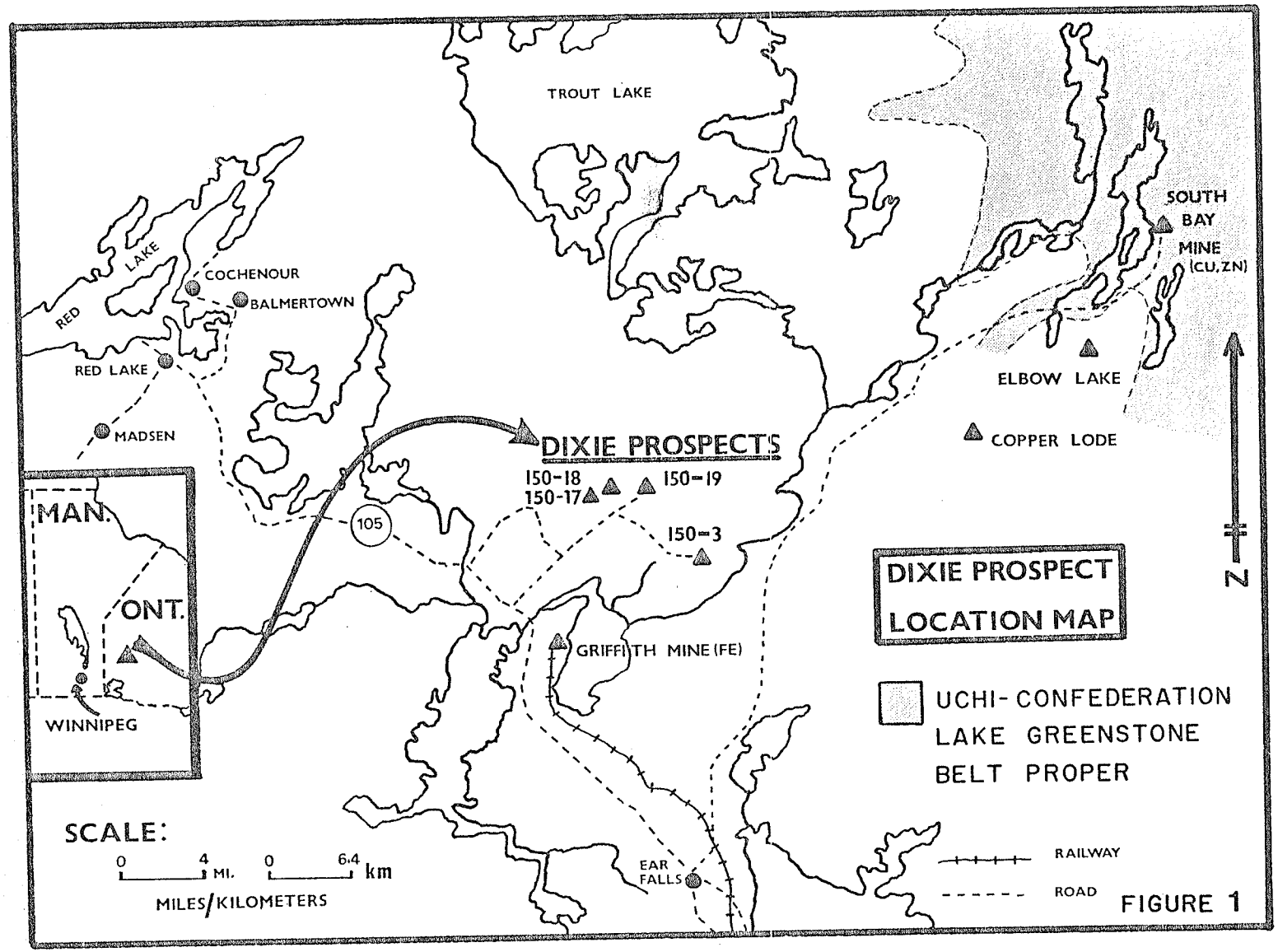
TROUT LAKE
SOUTH BAY MINE (CU, ZN)
RED LAKE
COCHENOUR
BALMERTOWN
RED LAKE
MADSEN
ELBOW LAKE
COPPER LODE
DIXIE PROSPECTS
150-18
150-17
150-19
150-3
105
MAN.
ONT.
WINNIPEG
GRIFFITH MINE (FE)
EAR FALLS
N
DIXIE PROSPECT LOCATION MAP
UCHI-CONFEDERATION LAKE GREENSTONE BELT PROPER
RAILWAY
ROAD
SCALE:
0 4 MI. 0 6.4 km
MILES/KILOMETERS
FIGURE 1

1970). The mapping provided geological information south, southeast of the Dixie prospects which would prove useful when trying to interpret and correlate the volcanic rocks around the Dixie prospects.

ACKNOWLEDGEMENTS

I wish to express my appreciation to Dr. H.D.B. Wilson who suggested the study, helped supervise the research and gave constructive criticism on the presentation of the thesis. I would also like to thank K. Thorsen who helped the author during the initial investigation of the study area and devoted considerable time familiarizing the author with the geology and drill core intersections.

Special appreciation is due Dr. L. D. Ayres and G. Clark for their valuable criticism, direction and patience in listening to numerous problems which arose during the course of investigation.

Thanks are also due Miss I. Berta for the thin and polished sections, K. Ramlal for chemical analyses and R. Pryhitko for photographic development and reductions.

I also acknowledge the co-operation of Selco Mining Corporation which allowed access to the Dixie prospects, provided assays, drill core, drill logs and geophysical data. Without the co-operation of the Company, this thesis would not have been possible.

# CHAPTER 2

## REGIONAL GEOLOGY

The early Precambrian Superior Province in northwestern Ontario comprises seven easterly trending subprovinces. Each represents a primary lithologic sequence which contain characteristic lithologies, structure and metamorphism related to different stages in crustal evolution (Ayres, 1978).

The Dixie 150 - 17B, 18 and 19 sulphide prospects lie within the Red Lake (Uchi) subprovince which is one of the major subprovinces within the Superior Province of northwestern Ontario. The Red Lake (Uchi) subprovince is a block of metavolcanic, metasedimentary and granitic diapiric rocks. The block is dominated by several mafic to felsic volcanic piles which are interconnected by several basaltic flows to form a relatively continuous metavolcanic-metasedimentary-granitic block extending from Lake Winnipeg to Hudson Bay (Thurston and Breaks, 1978).

The Dixie prospects are situated within the southwestern extension of the Uchi - Confederation Lake greenstone belt which is one of the major mafic to felsic volcanic piles contained within the Red Lake (Uchi) subprovince (figure 2). Distinct volcanic cycles have not been recognized within the southwestern extension of the Uchi - Confederation Lake greenstone belt containing the prospects under investigation. However, the volcanic stratigraphy in the northeastern portion of the belt (centred around the Uchi and Confederation Lakes,

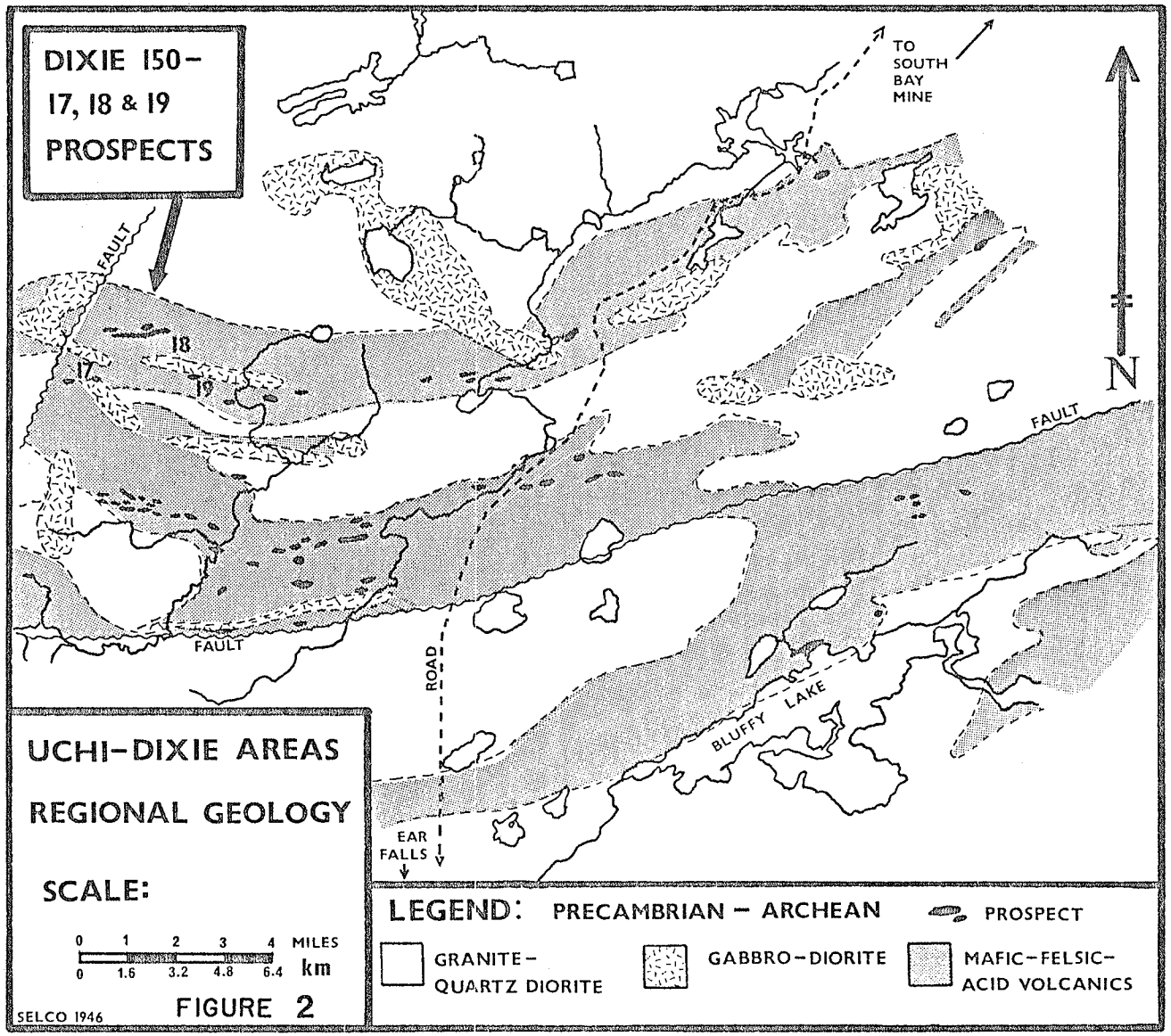
DIXIE 150-
17, 18 & 19
PROSPECTS
TO
SOUTH
BAY
MINE
N
FAULT
18
17
19
FAULT
FAULT
ROAD
BLUFFY
LAKE
EAR
FALLS
UCHI-DIXIE AREAS
REGIONAL GEOLOGY
SCALE:
0 1 2 3 4 MILES
0 1.6 3.2 4.8 6.4 km
SELCO 1946
FIGURE 2
LEGEND: PRECAMBRIAN - ARCHEAN
PROSPECT
GRANITE-
QUARTZ DIORITE
GABBRO-DIORITE
MAFIC-FELSIC-
ACID VOLCANICS

figure 1) is composed of three recognized cycles of volcanism (Thurston et al, 1978). Each of these cycles have been dated by the U - Pb method using zircons (Nunes and Thurston, 1978). Cycle 1 contains a basal pillowed basaltic unit overlain by a mixed unit of felsic pyroclastic and metasedimentary rocks, a second basaltic and intermediate flow unit followed by coarse pyroclastic breccias, marble, sulphide facies iron formation and chert. A small section of felsic vitric crystal tuff and lapilli tuff from the first cycle gave an age of 2959 ± 3 million years.

Cycle II contains a basal amygdaloidal pillowed basaltic unit overlain by oxide facies iron formation, chert and subaqueous pumaceous pyroclastic rocks which are in turn overlain by felsic tuffs and lapilli tuffs (Thurston et al, 1978). The U - Pb zircon age from this cycle is 2800 ± 12 million years.

Cycle III also contains basal pillowed and massive variolitic flows which are succeeded by more pillowed basalts and andesite massive flows. The andesites are overlain by quartz and feldspar phyric flows, welded tuffs, lapilli tuffs with minor rhyolite and rhyolite tuff (Thurston et al, 1978). A quartz and feldspar phyric flow indicated an age of 2738 ± 5 million years for the third volcanic cycle.

## STRUCTURE

The structure of the Dixie prospects is relatively simple. The volcanic rocks and sedimentary sequences have a general east - west strike and dip steeply at angles between 75 and 85 degrees to the south. Major faulting does not occur within the immediate vicinity of the Dixie prospects.

## GEOLOGICAL AREA SELECTION AND GEOPHYSICS

Geological exploration within the southwestern extension of the Uchi - Confederation Lake greenstone belt is primarily restricted to geological areas known to contain base metal occurrences within felsic (siliceous) metavolcanic and metasedimentary rocks and to other linear trends of volcanic rocks containing intercalated intermediate to felsic (siliceous) units. The Dixie 150 - 17B, 18 and 19 prospects were initially indicated by a regional airborne combined Imput EM and magnetic surveys flown over one particular area of interest containing intercalated felsic volcanic rocks. The magnetometer survey conducted over the vicinity of the 150 - 18 sulphide body is shown in figure 3. Two large anomalies reaching maximum intensities of 7000 and 7400 gammas respectively straddle the actual sulphide body.

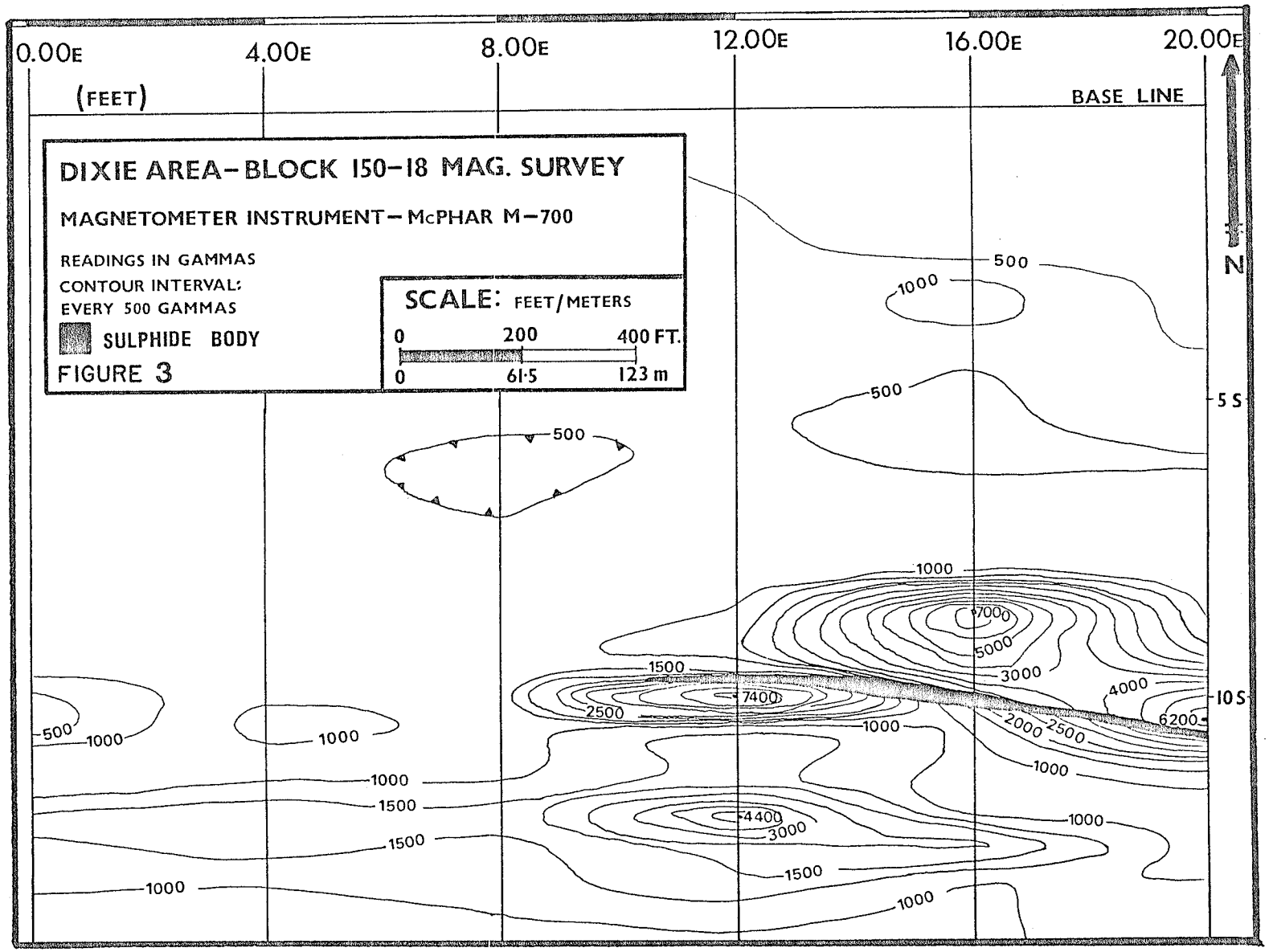
0.00E
4.00E
8.00E
12.00E
16.00E
20.00E
(FEET)
BASE LINE
DIXIE AREA-BLOCK 150-18 MAG. SURVEY
MAGNETOMETER INSTRUMENT-McPHAR M-700
READINGS IN GAMMAS
CONTOUR INTERVAL:
EVERY 500 GAMMAS
SULPHIDE BODY
FIGURE 3
SCALE: FEET/METERS
0 200 400 FT.
0 61·5 123 m
N
5 S
10 S
500
1000
1500
2500
3000
4000
5000
7000
7400
6200
4400
2000

The anomalies overlying the 17B and 19 prospects are much smaller and proportional to the size of the mineralized zones (see figures 34 and 38, Chapter 11).

Horizontal loop electromagnetic surveys were conducted along grid systems in an attempt to pinpoint the exact location and configuration of the mineralized zones. The 150 - 18 prospect responded as two distinct linear electromagnetic conductors along a strike length of 680 m. Single electromagnetic conductors indicated the 150 - 17B and 19 mineralized zones. Although the mineralized zones associated with all three prospects are nowhere exposed, subsequent diamond drilling on the electromagnetic anomalies led to the discovery of copper-zinc-silver mineralization under thick glacial overburden.

## DIAMOND DRILL HOLES AND GRID LOCATIONS

Figure 4 shows the grid and diamond drill hole locations for the Dixie 150 - 17B, 18 and 19 prospects. Figure 5 shows the detail of the 150 - 18 prospect in the insert on figure 4. The geology and mineralization of all three prospects have been well outlined by diamond drill hole intersections. The 150 - 18 sulphide mineralization has been intersected by twelve drill holes located at intervals for 310 m along strike of the electromagnetic anomaly. The holes reach a maximum depth of approximately 150 m.

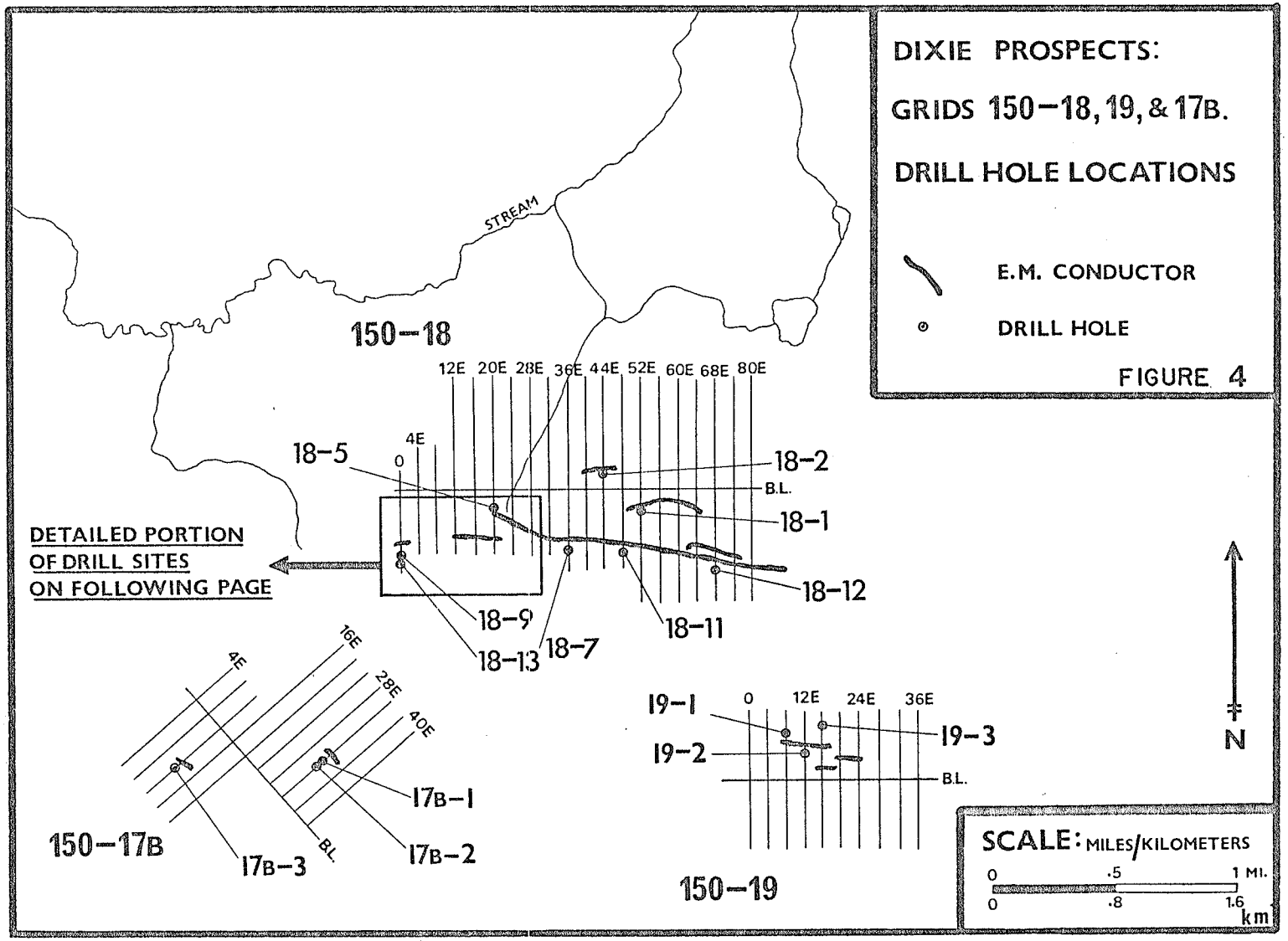
DIXIE PROSPECTS:
GRIDS 150-18, 19, & 17B.
DRILL HOLE LOCATIONS
E.M. CONDUCTOR
DRILL HOLE
FIGURE 4
STREAM
150-18
12E 20E 28E 36E 44E 52E 60E 68E 80E
4E
0
B.L.
18-5
18-2
18-1
18-12
18-9
18-13
18-7
18-11
DETAILED PORTION
OF DRILL SITES
ON FOLLOWING PAGE
16E
4E
28E
40E
17B-1
17B-2
17B-3
B.L.
150-17B
19-1
0
12E
24E
36E
19-3
19-2
B.L.
150-19
N
SCALE: MILES/KILOMETERS
0 .5 1 MI.
0 .8 1.6 km

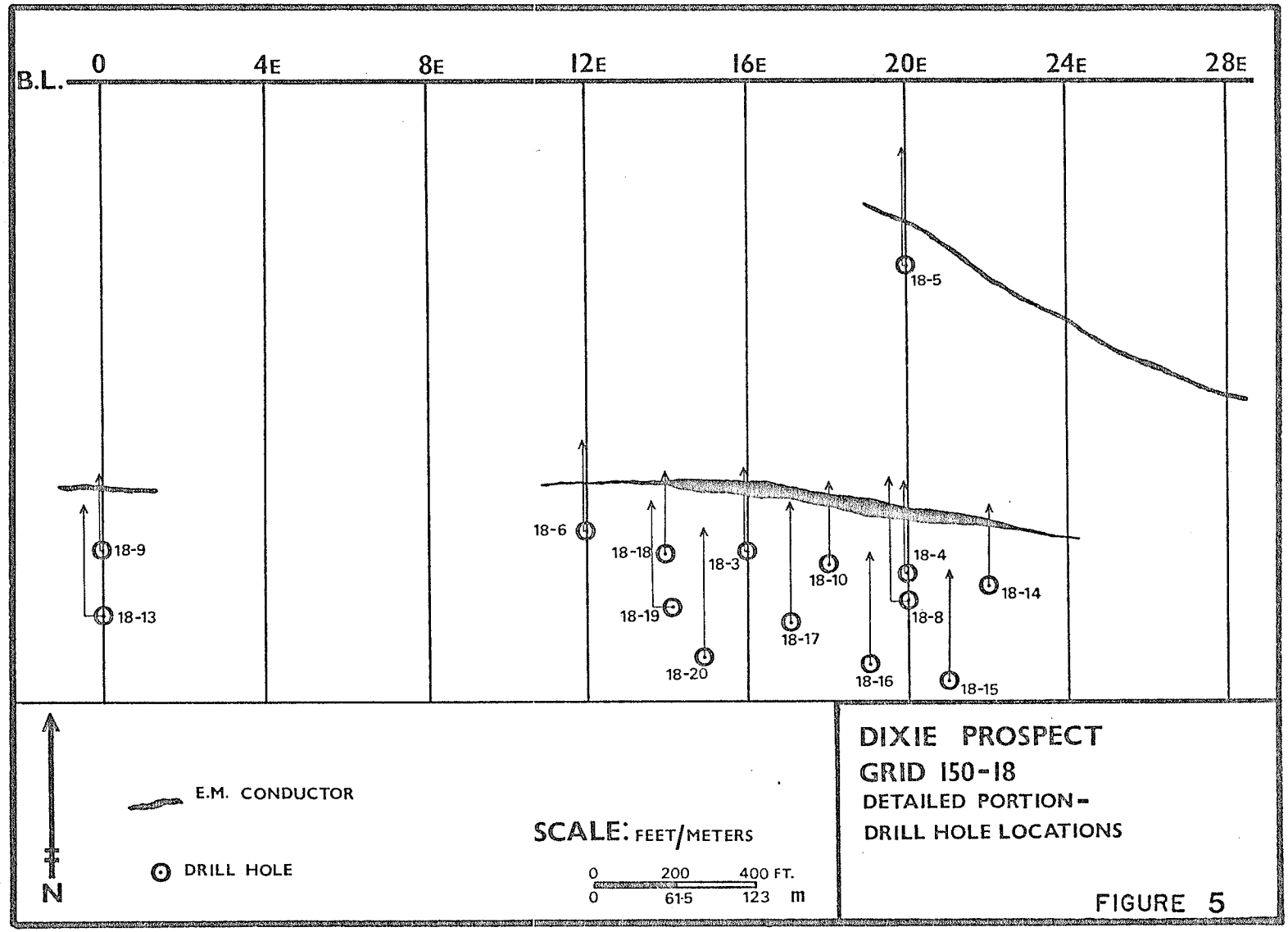
B.L.
0
4E
8E
12E
16E
20E
24E
28E
18-5
18-9
18-13
18-6
18-18
18-19
18-20
18-3
18-17
18-10
18-16
18-4
18-8
18-15
18-14
N
E.M. CONDUCTOR
DRILL HOLE
SCALE: FEET/METERS
0 200 400 FT.
0 61·5 123 m
DIXIE PROSPECT
GRID 150-18
DETAILED PORTION-
DRILL HOLE LOCATIONS
FIGURE 5

Two holes tested the depth and extent of a smaller anomaly located 350 m west and along strike of the larger anomaly (figure 5). All drill holes dip between 40 and 50 degrees into the sulphide body and enclosing volcanic rocks.

Three diamond drill holes outline the 150 - 19 prospect. Two drill holes dip south and the other north at angles of approximately 45 degrees (figure 4). The 150 - 17B prospect (figure 4) has been intersected by two drill holes, both dipping northeast at angles of approximately 45 degrees. Drill hole 150 - 17B - 3 failed to intersect mineralization and is not of interest in this study.

Four additional electromagnetic anomalies were tested by eight reconnaissance drill holes (18 - 1, 2, 5, 7, 9, 11, 12 and 13). These drill holes are located within 2 km east and northeast of the 150 - 18 prospect. All holes failed to intersect sulphide mineralization but provide useful documentation of the geology in those areas.

# CHAPTER 3

# LOCAL AND HOST ROCK GEOLOGY

## LOCAL GEOLOGY

The rocks within the immediate vicinity of the Dixie 150 - 17B, 18 and 19 prospects comprise mafic metavolcanic rocks with minor intercalated sequences of metasedimentary and sporadic ultramafic to felsic intrusive rocks.

The metavolcanic rocks consist of massive and porphyritic andesitic to basaltic flows and lapilli tuffs with minor siliceous tuffite horizons. The metasedimentary rocks consist of predominantly greywacke sequences with calcareous siltstones and minor impure limestone. The intrusive rocks comprise granodiorite and quartz diorite stocks with smaller diorite and gabbro sills, feldspar porphyry sills and lamprophyre dikes.

The geology immediately enclosing the Dixie 150 - 18 sulphide body consists almost entirely of metavolcanic flows and lapilli tuffs with greywacke, calcareous siltstone and impure limestone occurring east and northeast of the sulphide body. The geology hosting the 150 - 17B and 19 prospects consists of volcanic rocks which have been intensely metasomatically granitized into highly altered, schistose, felsic volcanic tuffs intruded by several large granodiorite stocks, smaller quartz diorite, feldspar porphyry and gabbro sills and lamprophyre dikes.

Further discussion concerning the geology hosting the 150 - 17B and 19 prospects is reviewed in detail in Chapter 11 and is not considered in this chapter.

## HOST ROCK GEOLOGY OF THE DIXIE 150 - 18 SULPHIDE PROSPECT

### VOLCANIC ROCKS

#### GENERAL

The volcanic rocks within the immediate vicinity of the Dixie 150 - 18 sulphide body are massive and porphyritic flows, lapilli tuffs and siliceous tuffite. Figure 6 shows the diagramatic stratigraphic column for the Dixie 150 - 18 section. The vertical thickness of the section is approximately 215 m and the section has been generalized. The volcanic rocks have been broadly subdivided according to distinct lithofacies characteristics recognized within the volcanic pile. Each lithofacies has been termed a unit and given an informal alphabetical designation in order of stratigraphic development or decreasing age. A possible time break imposed by the deposition and precipitation of the sulphide mineralization and weathering and erosional development of the siliceous tuffite suggests that lithofacies unit A may belong to a separate formation entitled formation A and lithofacies units B through D belong to a second younger

ARCHEAN

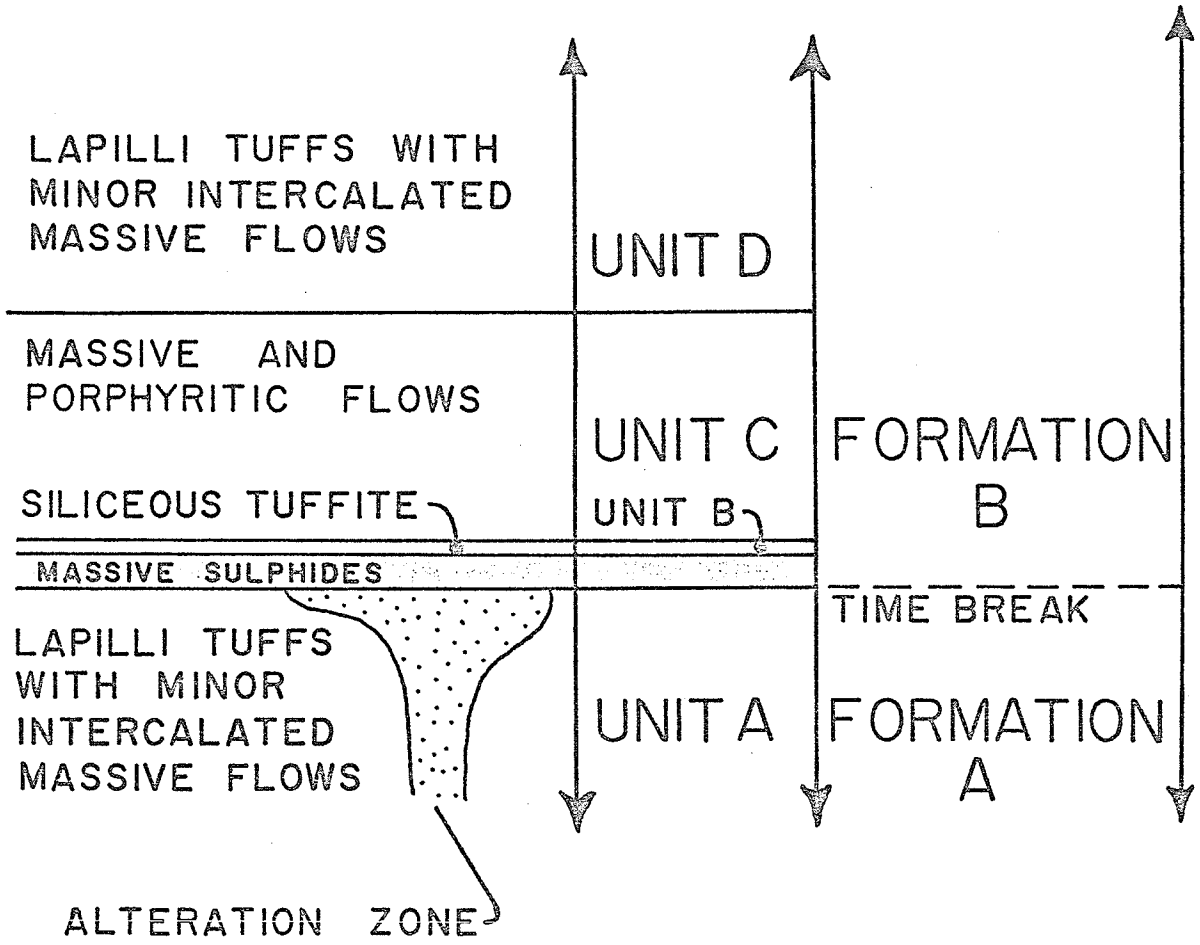


# DIXIE 150-18 PROSPECT

## GENERALIZED STRATIGRAPHIC SECTION

FIGURE 6

volcanic formation entitled formation B (figure 6). Lithofacies contacts are generally poorly defined and range from sharp to conformable and gradational.

## LITHOLOGY

### MASSIVE FLOWS

Thick continuous sequences of massive flows are confined to Unit C. Thinner individual massive flows are intercalated with sequences of lapilli tuffs in units A and D. The massive flows are fine-grained, dark green-gray to black units. The flows locally contain as much as 10% elliptical quartz phenocrysts 1 to 2 mm in diameter set in a fine-grained to aphanitic matrix (plate 1).

The flows have an average composition of 8.5% quartz, 36% oligoclase or andesine, 36.5% hornblende, 5.5% biotite, 4% actinolite, 4% garnet (almandine) with minor amounts of epidote, carbonate, sericite, microcline and opaque iron ore minerals; pyrite, pyrrhotite and magnetite (table 1).

The quartz grains are relatively evenly distributed throughout all sections and range in size from 0.1 to 0.2 mm, in concentration from 6.3 to 15% and average 8.5%. Individual grains are polygonal, equidimensional, equally sized and recrystallized. Sutured grain boundaries and intense undulatory extinction are common in most grains.

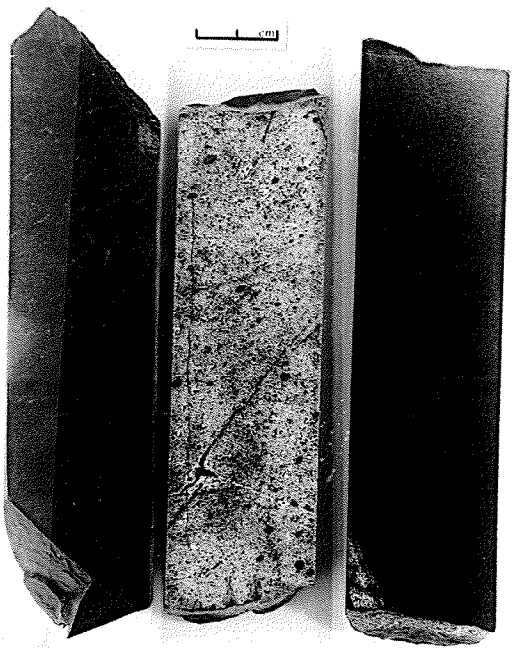


# PLATE 1

## MASSIVE FLOWS

CENTRE CORE ETCHED WITH CONC. HF – SHOWING ELLIPTICAL QUARTZ EYE PHENOCRYSTS (BLACK).

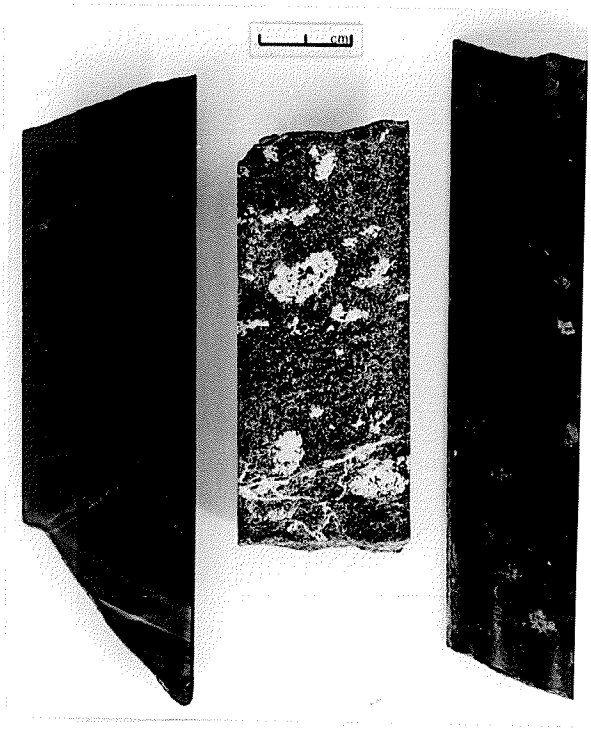


# PLATE 2

## PORPHYRITIC FLOWS

CENTRE CORE ETCHED WITH CONC. HF – SHOWING LARGE PLAGIOCLASE PHENOCRYSTS (WHITE).

Quartz eyes are present in some sections and range in size from 1 to 2 mm, and usually account for 5 to 10% of the total quartz. The quartz eyes are usually evenly distributed throughout the sections but some local bead-like concentrations aligned parallel to foliation are present. Individual eyes are usually composed of a mosaic of broken subhedral to anhedral crystals or fractured, lenticular aggregates of shattered crystal fragments. Stringers of small equidimensional quartz grains are commonly aligned parallel to foliation. Lenses and stringers of large composite quartz grains occur in a few sections.

Oligoclase or andesine ranges in concentration from 21.6 to 50% and averages 36% (table 1). The mineral occurs as small equidimensional recrystallized grains intimately associated with quartz. Some large poikiloblastic grains as much as 10 mm in diameter are present. Alteration of oligoclase or andesine to sericite or epidote is minor or nonexistent.

Hornblende is the most abundant mafic mineral in the massive flow units and ranges in concentration from 22 to 48% and averages 36%. Individual laths and prisms range in size from 0.1 to 0.3 mm. Orientation relative to foliation is moderate to strong and some laths are moderately poikiloblastic. Hornblende almost invariably occurs in elongated elliptical pods and as long continuous stringers

## TABLE I

## MODAL ANALYSES FOR THE MASSIVE FLOWS

| DRILL HOLE | 18-13-397 | 18-10-77 | 18-4-126 | 18-14-123 | 18-9-38 | 18-7-128 |
|---|---|---|---|---|---|---|
| QUARTZ | 150 | 63 | 88 | 77 | 78 | 47 |
| PLAGIOCLASE | 332 | 403 | 500 | 307 | 216 | 403 |
| HORNBLENDE | 475 | 300 | 218 | 390 | 429 | 370 |
| BIOTITE | 12 | 50 | 57 | 86 | 112 | 8 |
| ACTINOLITE | | 138 | | | | 82 |
| GARNET | | | | 123 | 103 | 23 |
| EPIDOTE | | | 32 | | | |
| CARBONATE | | 35 | 49 | 7 | | 17 |
| SERICITE | | | 50 | | | |
| MICROCLINE | 4 | 7 | 6 | 7 | 10 | 6 |
| OPAQUES | 27 | 4 | | 3 | 52 | 44 |
| TOTAL | 1000 | 1000 | 1000 | 1000 | 1000 | 1000 |

## TABLE II

## MODAL ANALYSES FOR THE PORPHYRITIC FLOWS

| DRILL HOLE | 18-8-57 | 18-17-248 | 18-13-262 | 18-10-11 | 18-8-177 |
|---|---|---|---|---|---|
| QUARTZ | 38 | 90 | 48 | 61 | 63 |
| PLAGIOCLASE | 601 | 320 | 452 | 336 | 414 |
| HORNBLENDE | 100 | 231 | 327 | 208 | 316 |
| BIOTITE | 21 | 103 | 149 | 42 | |
| ACTINOLITE | 118 | 111 | | 109 | 70 |
| GARNET | | 88 | | 81 | 53 |
| EPIDOTE | | 42 | | 8 | 56 |
| CARBONATE | | | | 44 | |
| SERICITE | 101 | | | 94 | |
| MICROCLINE | 11 | 3 | 4 | 7 | 7 |
| OPAQUES | 10 | 12 | 20 | 10 | 21 |
| TOTAL | 1000 | 1000 | 1000 | 1000 | 1000 |

which contain only minor quantities of oligoclase or andesine and quartz.

Biotite occurs as subhedral laths and prisms and ranges in concentration from 1 to 12% and averages 5.5%. The laths and prisms range in size from 0.1 to 0.3 mm and are always fresh and unaltered. The crystals are moderately to strongly aligned relative to foliation and occur as small disseminations, individual scattered laths and in places as long continuous chains. Biotite is usually associated with other mafic minerals such as hornblende and actinolite.

Actinolite is closely associated with hornblende and ranges in concentration from 0.5 to 14% and averages 4%. Individual laths and prisms exhibit a preferred orientation parallel to foliation and range in size from 0.1 to 4 mm poikiloblastic prisms.

Garnet occurs in most sections and ranges in concentration from 0.5 to 12% and averages 4%. Individual anhedral crystals range in size from 0.3 to 2 mm and are commonly red-brown. All grains are stretched and elongated parallel to foliation and are highly poikiloblastic with innumerable quartz grain inclusions.

The distribution of epidote is erratic. Epidote ranges in concentration from 0.5 to 3% and averages 1%. The mineral occurs as elongated angular crystal masses moderately aligned parallel to foliation and relict crystal segments are commonly observed. Epidote is usually altered to clinozoisite and is

concentrated preferentially near oligoclase or andesine grains.

Carbonate occurs locally as randomly distributed tiny blebs which range in size from 0.1 to 0.3 mm and in concentration from 0.5 to 5%, averaging 2%. The close spatial association of carbonate with oligoclase or andesine and epidote suggests that carbonate may be forming from the alteration of plagioclase minerals and epidote.

Sericite ranges in concentration from 0.5 to 5% and averages 1%. The mineral is always associated with oligoclase or andesine where it occurs as minor to pervasive replacements of whole oligoclase or andesine grains.

Opaque iron ore minerals are represented by magnetite with lesser amounts of pyrite and pyrrhotite. Magnetite occurs as euhedral to subhedral cubes and octahedra and the iron sulphides form irregular disseminations and stringers which are commonly aligned parallel to foliation. The iron ore minerals range in concentration from 0.5 to 6% and average 2%. The minerals are usually contained within hornblende-actinolite-rich layers.

Trace amounts of zircon occur in all sections. Zircon usually occurs in biotite where it is surrounded by a pleochroic halo.

## PORPHYRITIC MASSIVE FLOWS

Compositionally, the porphyritic massive flows are similar to the non porphyritic massive flows. The porphyritic

sequences are homogenous in appearance over their entire exposure in the drill holes and are essentially confined to the central portions of unit C (plate 2).

The porphyritic flows are characterized by a fine-grained assemblage of approximately 42% oligoclase or andesine, 6% quartz, 24% hornblende, 6% biotite, 8% actinolite, 3% garnet with minor amounts of epidote, carbonate, sericite, microcline and opaque iron ore minerals (table II).

The oligoclase or andesine phenocrysts have a uniform size (0.6 to 1.5 cm) and distribution and may commonly constitute 15% of the rock volume. The anhedral phenocrysts are strongly recrystallized and their primary euhedral tabular shapes are poorly preserved. Some of the oligoclase or andesine phenocrysts are partially replaced by hornblende and biotite with minor sericite and are commonly difficult to distinguish from the groundmass. Rare quartz phenocrysts ranging in size from 0.3 to 2 mm occur in some zones where they maintain their well-preserved subhedral equant shapes.

The groundmass in all porphyritic units has been recrystallized into a fine-grained assemblage of hornblende, biotite, quartz and oligoclase or andesine.

Apart from the zone of sulphide mineralization, the porphyritic unit is the only unit which can be correlated between drill holes with accuracy and serves as an excellent marker horizon within the volcanic pile.

## SILICEOUS TUFFITE

The siliceous tuffite is an indurated unit composed of a mixture of pyroclastic and sedimentary detritus, especially fine ash and sediment. The unit is siliceous, fine-grained, bleached white to gray-white and is restricted to a narrow zone immediately above the zone of sulphide mineralization. It is characterized by large concentrations of quartz and continuous intercalated bands or laminations of biotite ranging from 5 mm to 2 cm in thickness (plate 3).

The tuffite has an average composition of 39% quartz, 34% oligoclase or andesine, 18% biotite, 3% microcline with minor amounts of actinolite, garnet, carbonate, epidote and opaque iron ore minerals (table III). Quartz, the most characteristic and abundant mineral in the tuffite ranges in concentration from 35 to 41% and averages 39%. Individual grains are equidimensional and polygonal and range in size from 0.1 to 3 mm except for larger elongated composite grains which are concentrated into distinct lenses, stringers and narrow bands aligned parallel to foliation. The smaller polygonized grains are concentrated into distinct bands which are devoid of any other minerals. The bands range in width from a few millimeters to several centimeters. Contacts between the bands, lenses and stringers of larger composite crystals and the fine polygonized quartz bands are sharp.

Quartz eyes are abundant in some polygonized quartz bands and range in size from 0.4 to 1 mm, averaging

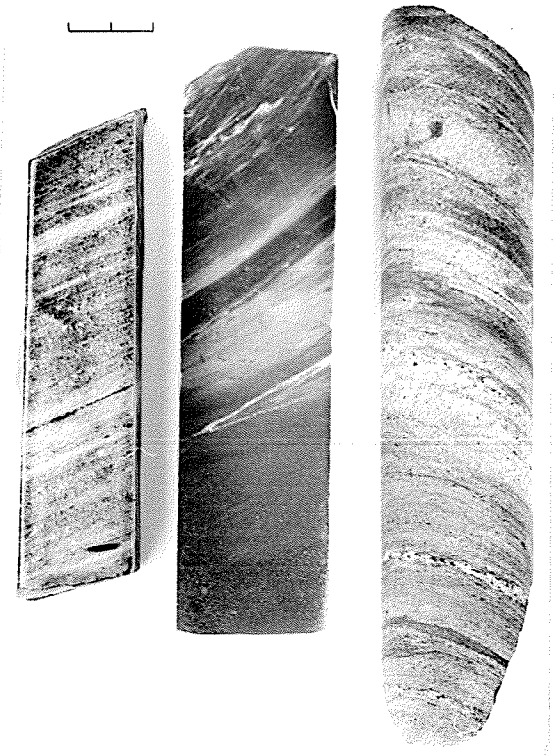

# PLATE 3

SILICEOUS TUFFITE WITH WHITE BANDS OF QUARTZ, DARK BANDS OF BIOTITE.

## TABLE III

## MODAL ANALYSES FOR THE SILICEOUS TUFFITE

| DRILL HOLE | 18-8-260 | 18-4-148 | 18-17-376 |
|---|---|---|---|
| QUARTZ | 412 | 354 | 406 |
| PLAGIOCLASE | 301 | 358 | 360 |
| HORNBLENDE | | | |
| BIOTITE | 196 | 146 | 198 |
| ACTINOLITE | | 34 | 2 |
| GARNET | 12 | | 2 |
| EPIDOTE | 2 | 27 | 4 |
| CARBONATE | 6 | 38 | 8 |
| SERICITE | | | |
| MICROCLINE | 55 | 25 | 14 |
| OPAQUES | 16 | 18 | 6 |
| TOTAL | 1000 | 1000 | 1000 |

## TABLE IV

## MODAL ANALYSES FOR THE LAPILLI TUFFS

| DRILL HOLE | 18-12-201 | 18-4-296 | 18-13-172 | 18-13-207 | 18-8-97 |
|---|---|---|---|---|---|
| QUARTZ | 156 | 136 | 126 | 147 | 81 |
| PLAGIOCLASE | 239 | 311 | 243 | 256 | 233 |
| HORNBLENDE | 187 | 254 | 256 | 286 | 233 |
| BIOTITE | 157 | 172 | 194 | 181 | 251 |
| ACTINOLITE | 104 | | | | 68 |
| GARNET | | 58 | 57 | 83 | 52 |
| EPIDOTE | 80 | | | 30 | |
| CARBONATE | 52 | | 51 | | 46 |
| SERICITE | | | | | |
| MICROCLINE | 21 | 20 | 30 | 5 | 5 |
| OPAQUES | 4 | 49 | 43 | 12 | 21 |
| TOTAL | 1000 | 1000 | 1000 | 1000 | 1000 |

0.6 mm. The quartz eyes consist of unbroken anhedral to subhedral crystals.

Biotite ranges in concentration from 15 to 20% and averages 18%. The subhedral laths and prisms range in size from 0.1 to 1 mm and occur as elongated disseminations or long continuous bands and chains. Narrow bands are most common where biotite concentrations are high. The bands range in width from 0.3 to 15 mm and contain minor amounts of quartz, oligoclase or andesine and actinolite. Sharp contacts occur between the biotitic and quartz-rich layers. All of the grains are aligned parallel to foliation and are unaltered.

Oligoclase or andesine ranges in concentration from 30 to 36% and averages 34%. Individual grains are equidimensional and polygonal and range in size from 0.1 to 3 mm, averaging 2 mm. The polygonized grains are concentrated into distinct bands which are intercalated with similar quartz-rich bands. Contacts between the quartz and oligoclase or andesine bands are gradational into one another.

Microcline is erratically distributed throughout the siliceous tuffite. It occurs in trace amounts in most sections but does reach concentrations as much as 12% by volume in two sections. Microcline usually occurs as randomly distributed equant grains which range in size from 0.1 to 0.7 mm although distinct lenses and bands as much as 8 mm in width and 2 cm in length occur in a few sections. The mineral is rarely altered to sericite.

Carbonate occurs locally as randomly distributed tiny blebs which range in size from 0.1 to 0.3 mm. The close spatial relationship between carbonate and oligoclase or andesine and epidote suggests that carbonate may be forming from the alteration of plagioclase minerals and epidote.

Actinolite is present in a few sections and is usually contained within the biotite-rich bands. Individual laths are much larger than biotite and exhibit a strong orientation parallel to foliation.

Garnet is a rare constituent in the siliceous tuffite. The large poikiloblastic grains are stretched parallel to foliation, excessively fractured and corroded and contain abundant quartz grain inclusions. The grains are commonly 5 to 7 mm in size.

Epidote is rare and occurs as tiny irregular crystal masses aligned parallel to foliation.

Opaque iron ore minerals occur in minor amounts in all sections. Magnetite is the most common mineral accompanied by lesser concentrations of pyrite and pyrrhotite. Magnetite occurs as small (0.1 to 0.5 mm) cubes and octahedra and the iron sulphides as irregular disseminations and stringers aligned parallel to foliation.

## LAPILLI TUFFS

The tuffaceous units are strongly characterized by dominantly lapilli-size fragments set in a fine-grained

medium green-gray to black matrix. Thick continuous sequences of lapilli tuffs are confined to Units A and D although minor sequences are intercalated with massive flows in Unit C. The grayish-white to brown fragments are commonly deformed and stretched parallel to foliation (plate 4). Many fragments are almost completely incorporated into the matrix and the distribution of the fragments is erratic. Quartz eyes are abundant throughout the units and some sections consist of a fine-grained tuff which exhibits well-defined banding or possibly bedded characteristics (plate 5).

The lapilli tuffs have an average composition of 13% quartz, 26% oligoclase or andesine, 24% hornblende, 19% biotite, 3% actinolite, 5% garnet (almandine), 2% epidote, 3% carbonate, 3% opaque iron ore minerals with traces of zircon and sericite (table IV).

Quartz ranges in concentration from 8 to 15% and averages 13%. The grains are polygonal, equidimensional, recrystallized and range in size from 0.1 to 0.3 mm, averaging 0.2 mm. Bands, stringers and lenses of quartz grains are common and are aligned parallel to foliation. Many lenses are elliptical and average 2 cm in length and 0.5 cm in width. Lenses of much larger composite quartz grains are also common in certain sections and attain widths as much as 2 cm and lengths between 2 and 4 cm.

Quartz eyes are common in the tuffaceous units. They are usually restricted to specific linear zones parallel

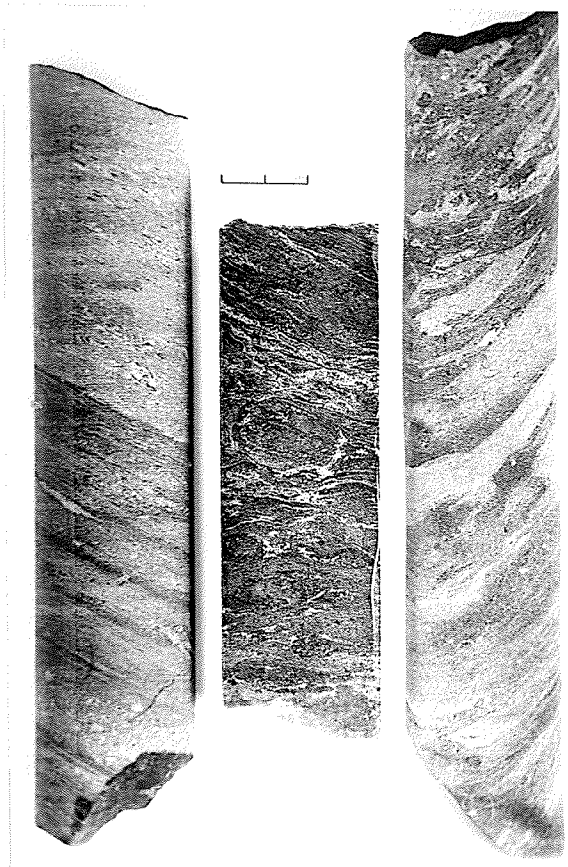

# PLATE 4

## LAPILLI TUFFS

WITH STRETCHED LAPILLI SIZE FRAGMENTS (WHITE) IN FINE GRAINED (DARK GRAY) MATRIX.

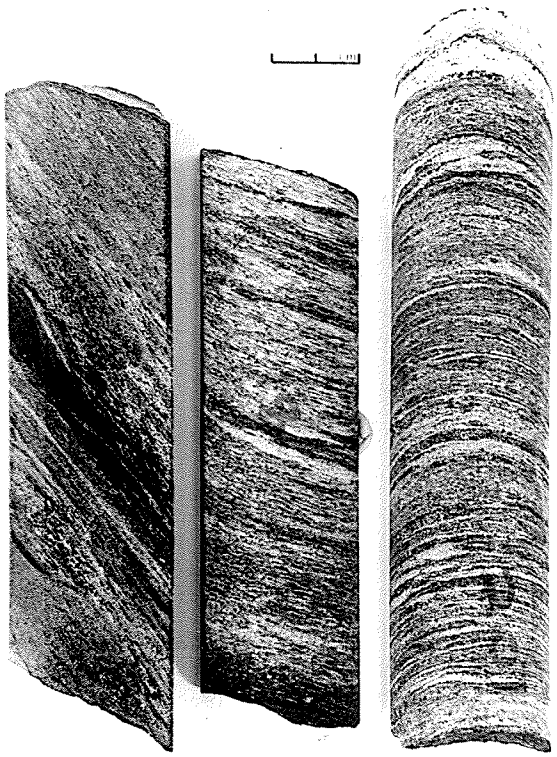

# PLATE 5

## LAPILLI TUFFS

WITH WELL DEFINED BANDING OR POSSIBLY BEDDED CHARACTERISTICS

to foliation and range in concentration from 10 to 15%. The eyes are usually 2 to 3 times larger than the surrounding polygonized quartz grains and differ in their degree of perfection from unbroken anhedral crystals to shattered crystals and lenticular aggregates of broken quartz fragments. Unbroken quartz eyes are spherical and exhibit undulatory extinction.

Oligoclase or andesine is intimately associated with quartz and occurs as small equidimensional recrystallized grains and rarely as large individual poikiloblastic grains. The mineral ranges in concentration from 23 to 31% and averages 26%. Most grains are relatively unaltered but the larger poikiloblastic grains exhibit minor alteration to sericite or epidote.

Hornblende and biotite are the most characteristic minerals in the tuffaceous units. Hornblende, the most abundant ranges in concentration from 18 to 29% and averages 24%. The mineral ranges in size from 0.1 to 3 mm and occurs as stubby, well developed prism faces concentrated into distinct bands, lenses and rods of segregated crystals. The larger crystals tend to be highly poikiloblastic and all crystals show a strong orientation parallel to foliation. Biotite ranges in concentration from 16 to 25% and averages 19%. The subhedral laths and prisms range in size from 0.1 to 0.8 mm and are strongly aligned parallel to foliation. The mineral commonly occurs in distinct bands 1 cm in width and as elliptical lenses 1.5 cm in length. Individual

grains are commonly scattered about within hornblende-actinolite rich zones. The biotite laths are always unaltered.

Actinolite ranges in concentration from 0.5 to 10% and averages 3%. Individual subhedral laths and prisms range in size from 0.1 to 0.3 mm and are commonly scattered throughout hornblende-rich zones or concentrated into distinct bands. All grains exhibit a pronounced orientation parallel to foliation. Particular sections contain actinolite grains which are concentrated into well-defined elliptical clots with minor amounts of quartz and oligoclase or andesine. The clots are commonly elongated and in some places broken apart, boudinaged and sinuous in shape. Some actinolite grains exhibit various degrees of alteration to epidote and carbonate.

Garnet (almandine) is present in all sections examined and ranges in concentration from 0.5 to 8%, averaging 5%. Individual poikiloblastic crystals are large, ranging in size from 0.5 to 3 mm. They are reddish-brown, stretched or elongated relative to foliation and contain many quartz grain inclusions. Grain boundaries are commonly excessively corroded and numerous grains have been shattered into angular fragments.

Carbonate ranges in concentration from 0.5 to 5% and averages 3%. The mineral occurs as randomly distributed blebs and continuous elongated masses aligned parallel to foliation. Individual blebs range in size from 0.1 to

0.2 mm and elongated masses commonly reach 6 to 8 mm in length with widths as much as 0.4 mm. Carbonate is commonly associated with actinolite and oligoclase or andesine and appears to form from the alteration of these two minerals. A few carbonate veinlets are scattered about some sections.

Sericite, epidote, microcline and the opaque iron ore minerals in the tuffaceous units are similar in distribution and characteristics to those described in the massive and porphyritic flow units although the concentrations differ slightly.

## SEDIMENTARY ROCKS

Sedimentary rocks within the vicinity of the Dixie 150 - 18 prospect comprise intercalated sequences of greywacke, calcareous siltstone and impure limestone. Relative ages of the sediments are uncertain but the occurrence of sediments intercalated with volcanic sequences suggests that the sediments are approximately the same age as the volcanics.

## METAGREYWACKES

Metagreywackes are generally confined to the areas north and east of the 150 - 18 sulphide body. Extensive units were encountered in drill holes 150 - 18 - 5, 7, 11 and 12.

The greywacke is a light to medium gray fine-grained

unit composed of poorly foliated to moderately schistose sequences. All units are bedded although graded bedding was never seen. Identifiable rock fragments were not found within any sequences.

Biotite and hornblende-bearing greywackes are the most prevalent. These rocks are composed of oligoclase or andesine, quartz, and biotite or hornblende which may constitute as much as 30% of the rock volume. Garnet porphyroblasts and microcline occur locally. Carbonate grains occur in all units and commonly attain as much as 10% of the rock volume. Secondary minerals include chlorite, sericite, opaque iron ore minerals and epidote (table V).

## CALCAREOUS SILTSTONE

Calcareous siltstones are essentially confined to drill holes 150 - 18 - 1 and 2 with minor intersections in drill holes 150 - 18 - 11 and 12 northeast and east of the 150 - 18 sulphide body. The calcareous siltstone units are light to dark gray, finely-laminated to thinly-bedded graphitic sequences commonly containing narrow beds or lenses of light gray carbonate, quartz and fine pyritic lamellae lying parallel to the bedding. Some larger angular quartz fragments are also contained within the units.

The siltstones commonly contain approximately 40% fine equigranular masses of carbonate with subordinate biotite

TABLE V
MODAL ANALYSES FOR THE GREYWACKES

| DRILL HOLE | 18-11-55 | 18-5-200 | 18-1-166 |
|---|---|---|---|
| QUARTZ | 143 | 288 | 301 |
| PLAGIOCLASE | 314 | 476 | 304 |
| HORNBLENDE | | | |
| BIOTITE | 172 | 157 | 278 |
| ACTINOLITE | | 54 | 28 |
| GARNET | | | |
| EPIDOTE | 4 | | |
| CARBONATE | 28 | | |
| SERICITE | | | |
| MICROCLINE | 228 | 12 | 51 |
| OPAQUES | 8 | 3 | 38 |
| TOTAL | 1000 | 1000 | 1000 |

and hornblende, minor quartz, oligoclase or andesine, epidote and garnet. Cryptocrystalline semi-opaque masses of irregular to finely disseminated bands and lenses of graphite, clay minerals and iron oxides usually constitute as much as 80% of the rock volume. Extensive bands and lenses of sericite with minor carbonate and epidote are intercalated with the cryptocrystalline semi-opaque masses in other sections of the siltstone units.

## IMPURE LIMESTONE

Narrow units of crystalline limestone were intersected in drill holes 150 - 18 - 11 and 12 located to the east of the 150 - 18 sulphide body. The units are light gray to white, moderately bedded and contain small lenses of well-sorted quartz grains with minor dark gray to black laminae which commonly contain disseminations of quartz and clay minerals. The limestone is almost entirely composed of interlocking equigranular anhedral calcite crystals with smaller quartz grains scattered about the intersticies between the calcite grains.

## INTRUSIVE ROCKS

Intrusive rocks within the vicinity of the Dixie 150 - 18 prospect include quartz diorite and feldspar porphyry sills and lamprophyre dikes. Distinct cross cutting contact and

structural relationships of the intrusive rocks suggests that they are all younger than the enclosing volcanic units.

## QUARTZ DIORITE

Quartz diorite occurs as large sill-like bodies north and northeast of the 150 - 18 sulphide body. Continuous intersections as much as 75 m thick were encountered in drill holes 150 - 18 - 2 and 5. A much narrower dike was encountered in drill hole 150 - 18 - 12 east and along strike of the sulphide body.

The quartz diorite is a medium-grained, grayish-green, spotted rock composed of anhedral plagioclase, hornblende and actinolite phenocrysts contained in a fine-grained matrix of quartz, plagioclase, carbonate, epidote and sericite. Plagioclase laths are extensively altered to epidote and sericite and the amphiboles have been slightly altered to epidote and possibly magnetite. Contact zones appear to be marked by a finer-grained quartz diorite with some weak laminations composed of hornblende and actinolite aligned parallel to the contact with the enclosing volcanics.

## FELDSPAR PORPHYRY

Feldspar porphyry occurs as small irregular sills and dikes within the immediate vicinity of the 150 - 18 sulphide body. Dikes are usually less than 6 m and the sills average

THE UNIVERSITY OF MANITOBA LIBRARIES

between 10 and 20 m. The rock is a medium gray to black, medium-grained intrusion that is characterized by subhedral laths of plagioclase from 0.5 to 1 cm in length. The laths are sparsely distributed or concentrated into distinct clusters which constitute as much as 30% of the rock volume. Quartz phenocrysts are common and are much smaller than the plagioclase phenocrysts. The matrix consists of biotite, plagioclase and interlocking fused granular aggregates of quartz with minor amounts of hornblende, carbonate, sericite, muscovite and epidote with trace magnetite and apatite.

The feldspar porphyry is in part spherulitic. Spherulitic intergrowths of plagioclase and quartz form a matrix around the plagioclase and quartz phenocrysts. Epidote and sericite occur as alteration products of plagioclase and the porphyry is not as intensely metamorphosed as the other intrusive rocks or enclosing volcanic and sedimentary rocks. Contact relationships are sharp and fine-grained chilled margins are not present.

## LAMPROPHYRE

Narrow dikes of lamprophyric composition are scattered throughout the entire sequence of volcanic rocks hosting the 150 - 18 sulphide body. The dikes range in width from 0.1 to 1 m and average 0.5 m. The largest dike is located near the 150 - 18 sulphide body and is closely associated

with a large feldspar porphyry sill.

The dikes are dark gray-green and fine-grained with distinct medium-grained biotite porphyroblasts or concentrations. Biotite is the dominant mafic mineral and occurs throughout the matrix and also as large porphyroblasts. Hornblende and actinolite also occur in the matrix but rarely form porphyroblastic aggregates. Minor concentrations of quartz, plagioclase, carbonate, magnetite and zircon are present. The dikes are highly metamorphosed and intrusive contacts are sharp with well-defined chilled margins.

# CHAPTER 4

## MINERALOGICAL CLASSIFICATION OF THE VOLCANIC ROCKS

The lapilli tuffs, massive flows and porphyritic flows were classified according to their mineral compositions previously shown in tables I, II and IV. Sixteen specimens were classified according to Streckeisen (1967) in the Q A P triangle where Q, A and P represent total quartz, alkali feldspar and plagioclase within the rock. The modal analyses are based upon 1000 point counts throughout a thin section representative of that specific volcanic rock. Five of the sixteen calculations were from the lapilli tuff sequences, six from the massive flows and five from the porphyritic flow sequences directly above and along strike of the Dixie 150 - 18 sulphide body.

The tuffs and flows have similar mineralogical compositions and plot essentially as andesites and basalts with a few specimens of quartz andesite. The plots also correspond to the tholeiitic basalt and andesite fields (figure 7).

## GRADE OF METAMORPHISM

The mafic metavolcanic rocks are characterized by two distinct mineralogical assemblages. The first assemblage comprises colourless to pale green actinolite and hornblende - Ca plagioclase ± chlorite and epidote. The second and more diagnostic mineral assemblage comprises dark green

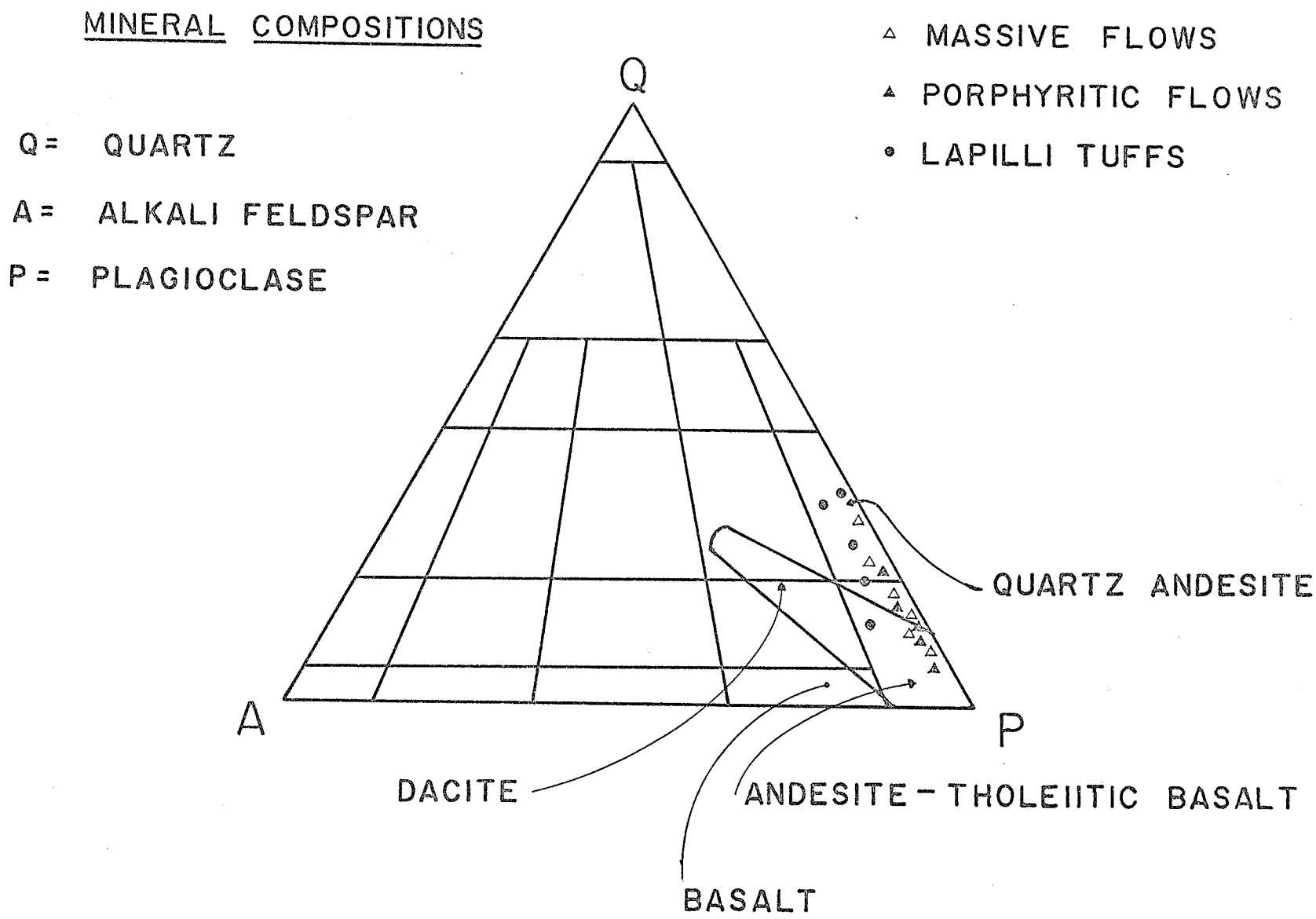


FIGURE 7 MINERALOGICAL CLASSIFICATION OF THE DIXIE VOLCANIC ROCKS (STRECKEISEN, 1967)

hornblende - plagioclase (oligoclase or andesine) - biotite ± garnet. More felsic metavolcanic rocks contain plagioclase (oligoclase or andesine) - quartz - biotite ± garnet mineral assemblages (see tables I - IV).

The first mineral assemblage is characteristic of the upper greenschist facies (Winkler, 1976). The second assemblage is distinctive of the lower to middle amphibolite facies and reflects low to intermediate pressure facies conditions (Winkler, 1976). Consequently, the volcanic rocks enclosing the Dixie 150 - 18 sulphide body belong to the medium grade metamorphic domain which ranges from upper greenschist to lower - middle amphibolite facies of metamorphism (Winkler, 1976).

## METAMORPHIC TEXTURES IN THE VOLCANIC ROCKS

The most obvious metamorphic texture found throughout the tuffaceous and massive flow units is schistosity. The schistosity is accompanied by parallel alignment of biotite, hornblende, actinolite, stretched garnet grains, lithic fragments and in places by narrow bands and lenses of quartz and plagioclase. Poikiloblastic biotite, hornblende, garnet and to a lesser extent actinolite developed in a syntectonic environment as they are all aligned parallel to foliation.

The second most pronounced metamorphic texture is a distinctive granoblastic texture which occurs in the quartz - plagioclase groundmass in all volcanic units. Extensive

recrystallization which polygonized the quartz and plagioclase groundmass also developed porphyroblasts of actinolite, hornblende and biotite.

Sutured quartz grain boundaries and excessive undulatory (strained) extinction in many sections may have resulted from a later stage of deformation. This later stage of deformation may have also been responsible for retrograde alteration of plagioclase to sericite, epidote and carbonate; actinolite to epidote; and rarely biotite to chlorite observed in some of the volcanic tuffs.

The metamorphic textures indicate a moderately complex deformational history. Initial deformation created the strongly pronounced foliation (schistosity) in all volcanic units and resulted in oriented growth of poikiloblastic biotite, hornblende, actinolite and garnet along with stretching, corrosion, crushing and fracturing of quartz eyes, plagioclase phenocrysts, some garnet porphyroblasts and lithic fragments.

The period of initial intense deformation was probably followed by a period of extensive recrystallization which produced the strongly polygonized nature of the quartz and plagioclase grains and the granoblastic appearance of the groundmass.

This period was then followed by a less intense deformational period which produced local sutured borders and excessive undulatory extinction in many of the quartz grains. This deformational period may have also induced

minor retrograde alteration of plagioclase to sericite, epidote and carbonate; actinolite to epidote; and rarely biotite to chlorite.

## PRIMARY VOLCANIC-SEDIMENTARY TEXTURES

Quartz and plagioclase phenocrysts represent the only recognizable primary texture remaining in the massive and porphyritic flows. Quartz eyes, bedding and relict lithic fragments are the only remaining primary textures preserved in the tuffaceous sequences. Biotite layers and laminations, graded bedding and sorting of quartz, plagioclase and microcline grains, and high modal concentrations of microcline are the only relict primary textures within the siliceous tuffite.

The relict fragments, although severely deformed and altered, only occur within the tuffaceous units. Most fragments are less than 1 cm in length and average 3 mm. A few larger fragments as much as 3 cm in length occur in one section. The distribution of the fragments is erratic but many have been stretched, elongated and fractured along specific linear zones. Many fragments are almost completely incorporated into the matrix.

The fragments occur as lenticular clots of quartz and plagioclase with minor amounts of biotite, actinolite and hornblende. The borders of the fragments differ from distinct to ghostly and gradational. Many irregular patches

of quartz and plagioclase with minor biotite and hornblende occur but cannot be called fragments with certainty. In other sections, the fragments occur as actinolite - biotite-rich clots separated by granoblastic quartz and plagioclase matrix. The foliation in all the mafic minerals in the volcanic units is also apparent in the fragments. All fragments are lenticular and stretched parallel to foliation (see plate 4).

Primary bedding in the tuffaceous units is commonly obliterated through extensive metamorphic foliation and recrystallization. The units appear to be layered but bedding is not always substantiated (see plate 5). However, in some sections bedding may be preserved and is characterized by the following features. The tuffaceous units are thinly bedded with bedding thicknesses ranging from 1 to 10 cm. The bedding is usually defined by compositional or grain size variations throughout the sequences. Bedding planes are commonly delineated by a gradational increase in concentrations and size of hornblende, biotite and actinolite laths.

Linear arrangements of stretched relict fragments also define bedding planes and size variation in quartz and plagioclase grains represent bedding planes in the more felsic tuffaceous sequences.

Quartz eyes occur throughout all the volcanic units but exhibit a pronounced increase in abundance in the tuffaceous sequences. The quartz eyes are characterized

by several distinctive features which suggest primary phenocryst or amygdaloidal development. Each feature is listed below in order of recurrence.

(1) The quartz eyes are always much larger than the quartz grains in the matrix.

(2) Many of the large crystals contain embayments which are diagnostic of volcanic quartz phenocrysts.

(3) Many lenticular aggregates of shattered, unsutured or recrystallized quartz fragments and granular quartz mosaics may represent extensively deformed and crushed former quartz phenocrysts. Various stages of metamorphic destruction of single quartz phenocrysts can be detected in several sections.

(4) The quartz eyes are evenly distributed throughout the massive and porphyritic flows.

(5) Those quartz eyes containing a core of altered plagioclase surrounded by a radial mosaic pattern of intergranular quartz may represent a two stage mineral growth within vesicles in the massive and porphyritic flows. Subsequent deformation produced the fractured mosaic pattern of quartz grains and retrograde alteration of the plagioclase core.

The quartz eyes probably represent relict quartz phenocrysts grown within a magma chamber and ejected with volcanic debris, crystallizing phenocrysts contained within massive and porphyritic flows or relict amygdaloidal fillings within vesicles in the flow sequences. The phenocrysts or amygdules

were then subjected to various stages of metamorphic deformation within their respective rock types.

Initial low grade regional metamorphism of potassium bearing illitic and chloritic clays gives rise to the development of muscovite and chlorite. At higher grades of regional metamorphism, muscovite and chlorite become progressively unstable and react to form biotite (Winkler, 1976). Similar mineralogical transformations resulting in the development of biotite may have occurred within the siliceous tuffite.

Continuous layers of biotite invariably cap graded sequences of quartz and plagioclase in the siliceous tuffite. Smaller laminations are usually intercalated with fine grained well sorted layers of quartz and plagioclase. The biotite layers and laminations probably represent former argillaceous (shaly) horizons deposited through the action of water carrying a load of argillaceous sediment. Similarly, graded bedding and sorting in many layers and lenses of quartz, plagioclase and microcline clearly indicate deposition through the action of water carrying detrital quartz, plagioclase and possibly microcline. These minerals were probably derived from the weathering and erosion of surrounding volcanic and sedimentary units within the area.

# CHAPTER 5

## THE DIXIE 150 - 18 CORDIERITE-ANTHOPHYLLITE ALTERATION ZONE

A hydrothermal cordierite-anthophyllite alteration zone situated immediately beneath the footwall of the sulphide body is composed of volcanic rocks which are compositionally, texturally and chemically distinct from all other rocks in the study area. The cordierite-anthophyllite alteration zone occurs as a narrow conformable zone beneath the outer edges of the upper portion of the sulphide body. The alteration zone gradually thickens, becomes discordant and resembles an alteration pipe near the centre of the sulphide body which extends some 70 m into the footwall volcanic rocks (figure 11).

As the sulphide body decreases in size and lateral extent with increasing depth, the cordierite-anthophyllite alteration zone also decreases considerably in lateral extent. However, with increasing depth, the cordierite-anthophyllite alteration zone begins to thicken and attains maximum thicknesses of at least 85 m beneath the sulphide mineralization. The total extent of the cordierite-anthophyllite alteration zone beneath the central portion of the sulphide body is not known. Drill holes 150 - 18 - 3, 16 and 17 terminated within cordierite and anthophyllite-bearing rocks. This central portion of the alteration zone continues to greater depth, appears to be thickening and may contain a number of undiscovered sulphide lenses at depth.

# TABLE VI

## MODAL ANALYSES FOR THE ALTERATION ROCKS

| DRILL HOLE | 18-17 419 | 18-17 408 | 18-3 176 | 18-10 231 | 18-17 421 | 18-18 210 | 18-18 220 | 18-16 523 | 18-6 120 | 18-17 393 | 18-18 206 | 18-4 276 |
|---|---|---|---|---|---|---|---|---|---|---|---|---|
| QUARTZ | 18 | | | 269 | 295 | 310 | 540 | 356 | 307 | 315 | 638 | 428 |
| PLAGIOCLASE | 73 | | 104 | 82 | 45 | 110 | 2 | 46 | 7 | 5 | 33 | 10 |
| ANTHO-PHYLLITE | 165 | 21 | 333 | 253 | 145 | 51 | 163 | 136 | 131 | 208 | 10 | 129 |
| BIOTITE | 179 | | 4 | 42 | 42 | 134 | 55 | 12 | 3 | 112 | 59 | 24 |
| ACTINOLITE | | | | 100 | 161 | | | 118 | | | | |
| CORDIERITE | 35 | | | 154 | | | | | 435 | | | 276 |
| CHLORITE | 190 | 738 | 189 | 16 | 34 | 248 | 55 | 40 | 32 | 53 | 184 | 27 |
| GARNET | 40 | | 26 | | 48 | 13 | 23 | | 1 | 220 | 16 | |
| EPIDOTE | | 14 | | | 9 | | | 14 | | | | |
| SERICITE | 35 | | | | | | | 32 | | | | |
| ZIRCON | 7 | | | | | 1 | | | | 4 | | |
| OPAQUES | 258 | 227 | 344 | 34 | 281 | 133 | 162 | 246 | 84 | 83 | 60 | 106 |
| TOTAL | 1000 | 1000 | 1000 | 1000 | 1000 | 1000 | 1000 | 1000 | 1000 | 1000 | 1000 | 1000 |

Several mineralogical assemblages occur throughout the cordierite-anthophyllite alteration zone. Modal analyses of various rocks from the alteration zone are given in table VI. The major alteration assemblages based upon modal and estimated visual mineralogical abundance are shown below:

(1) quartz - cordierite - anthophyllite

(2) quartz - chlorite - biotite ± anthophyllite

(3) quartz - anthophyllite - actinolite ± garnet

(4) chlorite

(5) anthophyllite - chlorite ± biotite and plagioclase

High modal abundances of pyrite, pyrrhotite, chalcopyrite and magnetite occur with all assemblages.

Rocks within the alteration zone are dark green to gray, very coarse-grained, siliceous and weakly foliated. The altered volcanic rocks are generally characterized by a coarse-grained porphyroblastic growth of anthophyllite and cordierite enclosed within a medium-grained matrix of quartz and/or chlorite and biotite with minor garnet. Foliation is weakly defined by alignment of biotite grains and to a lesser extent cordierite and anthophyllite laths.

## MINERALS OF THE ALTERATION ZONE

Cordierite ranges in concentration from 0.5 to 45% and averages 8%. The mineral occurs as large (8 mm to 2 cm) poikiloblastic laths which contain numerous

inclusions of quartz, sulphides, biotite and anthophyllite. Extensive alteration of cordierite to chlorite is common.

Anthophyllite ranges in concentration from 2 to 34% and averages 15%. Anthophyllite exhibits a great variation in grain size but usually occurs as large (1 to 3 cm) poikiloblastic subhedral to euhedral laths and prisms. It also occurs as sheafs or fibrous radial aggregates of much smaller (2 to 8 mm) prismatic crystals. Biotite and chlorite commonly replace the large anthophyllite laths along cleavage planes and fractures.

Chlorite ranges in concentration from 1 to 74% and averages 15%. The mineral generally occurs in massive form or as continuous felted mats and commonly constitutes almost the entire rock. Chlorite also occurs as small individual blades and as small reaction rims around cordierite, biotite and anthophyllite. The chlorite is always dark green and replaces all other minerals present.

Biotite ranges in concentration from 0.5 to 18% and averages 6%. The grains occur as small (2 to 4 mm) randomly distributed subhedral laths aligned parallel to foliation or as radiating divergent clots or felted mats within the matrix between larger cordierite and anthophyllite laths. Biotite is always partially chloritized.

Quartz ranges in concentration from 0.5 to 64% and averages 39%. The quartz grains are extremely variable and irregular in size and shape (0.6 to 6 mm) but are generally coarse-grained and occur as a conglomeration of highly

irregular and multi-sized forms. The mineral usually occurs within the matrix between larger cordierite and anthophyllite laths, as inclusions in cordierite and commonly as small cross-cutting veinlets.

Actinolite ranges in concentration from 0.5 to 12% and averages 3%. The actinolite laths resemble anthophyllite but the individual actinolite laths are usually much smaller and tend to be more prismatic or fibrous.

Garnet (spessartite) ranges in concentration from 0.5 to 23% and averages 3%. The mineral occurs as large, green, inclusion-free, euhedral, porphyroblastic crystals which occur most profusely in association with large concentrations of anthophyllite. A few euhedral crystals are contained within very large anthophyllite laths. Elsewhere, small excessively corroded, stretched and inclusion riddled anhedral porphyroblasts are randomly distributed throughout the altered volcanic rocks.

Plagioclase (oligoclase or andesine) ranges in concentration from 0.5 to 11% and averages 4%. The mineral resembles quartz and usually occurs with quartz as variably-sized individual grains in intersticies between larger cordierite and anthophyllite laths. Plagioclase is commonly partially altered to sericite, epidote and rarely biotite and chlorite.

Opaque iron ore minerals range in concentration from 6 to 35% and average 17%. Pyrite and pyrrhotite form approximately 90% of the opaque iron ore minerals with

minute concentrations of chalcopyrite and magnetite throughout the alteration zone. Pyrite is generally more abundant than pyrrhotite but both iron sulphides have a wide range in concentration.

The sulphide minerals occur as randomly distributed highly irregular clots and elongated sinuous masses in fracture and cleavage planes in numerous minerals and form a continuous sulphide matrix that encloses many of the grains. Many of the sulphide masses are weakly aligned parallel to foliation. Silicate mineral replacement by the iron sulphides is a common and extensive feature observed throughout the alteration zone and does not exhibit a preference for one particular silicate mineral over another.

Magnetite usually occurs as small randomly distributed poikiloblastic euhedral to subhedral crystals and irregular disseminations.

Sericite and epidote occur in minor concentrations within the matrix where they represent alteration products of plagioclase. Minor zircon is distributed within biotite and chlorite as minute prismatic crystals commonly surrounded by a pleochroic halo.

# CHAPTER 6

## STRATIGRAPHIC CORRELATION OF THE VOLCANIC ROCKS ENCLOSING THE DIXIE 150 - 18 SULPHIDE BODY

The Dixie 150 - 18 sulphide body is defined by twelve diamond drill holes all situated immediately south of the mineralized zone (figure 8). The drill holes are located along three linear arrays on the surface which intersect the sulphide body at three different levels. The three linear arrays are shown on figure 9 along with the east - west stratigraphic plane corresponding to the approximate depths reached by each array. Individual vertical north - south sections could not be constructed at various depths throughout the sulphide body because the drill holes are not located along the same section lines.

All drill holes dip at an angle of approximately 40 ± 5 degrees north into the sulphide body and enclosing volcanic rocks which dip at an angle of approximately 70 ± 5 degrees south. The resultant angle between each drill hole and the dip of the volcanic rocks is approximately 70 ± 5 degrees and large enough so that perpendicular stratigraphic sections can be drawn along each drill hole intersection without too much concern for the variability in true thickness of each volcanic unit and the sulphide body.

Stratigraphic correlation of the individual volcanic rock types into distinct lithological members or subunits has been developed along each linear array of drill holes

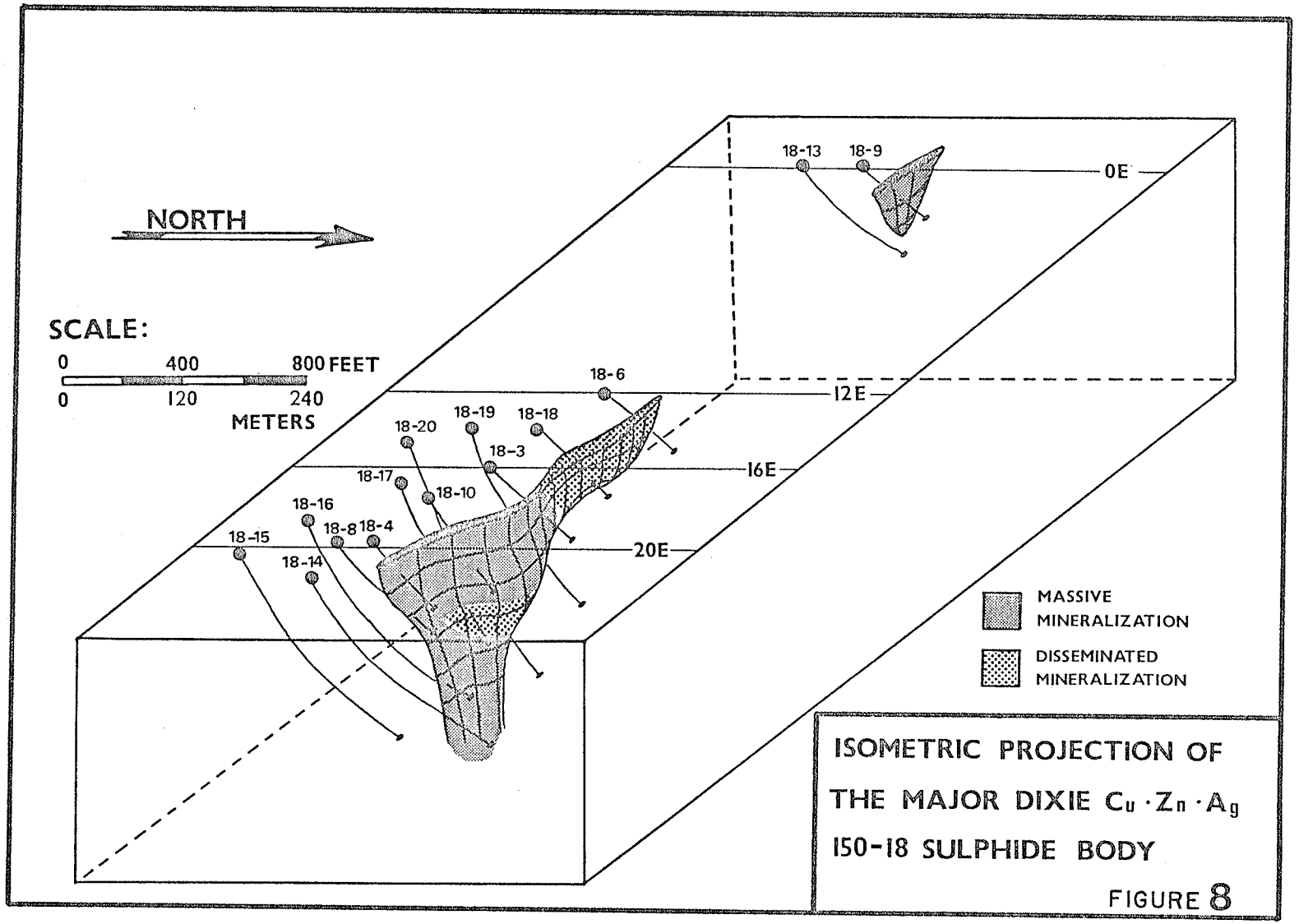


ISOMETRIC PROJECTION OF THE MAJOR DIXIE Cu · Zn · Ag 150-18 SULPHIDE BODY

FIGURE 8

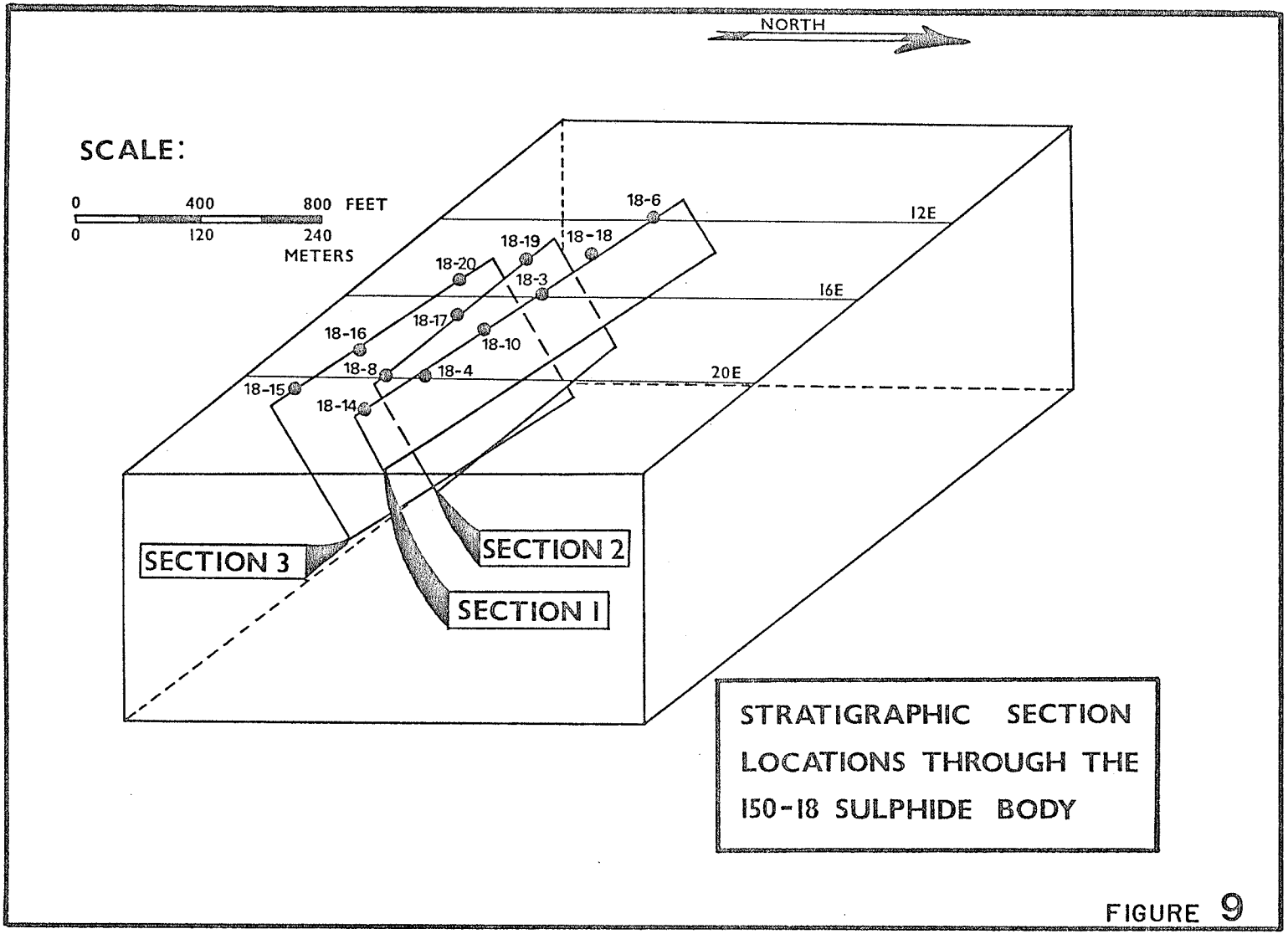


STRATIGRAPHIC SECTION LOCATIONS THROUGH THE 150-18 SULPHIDE BODY

FIGURE 9

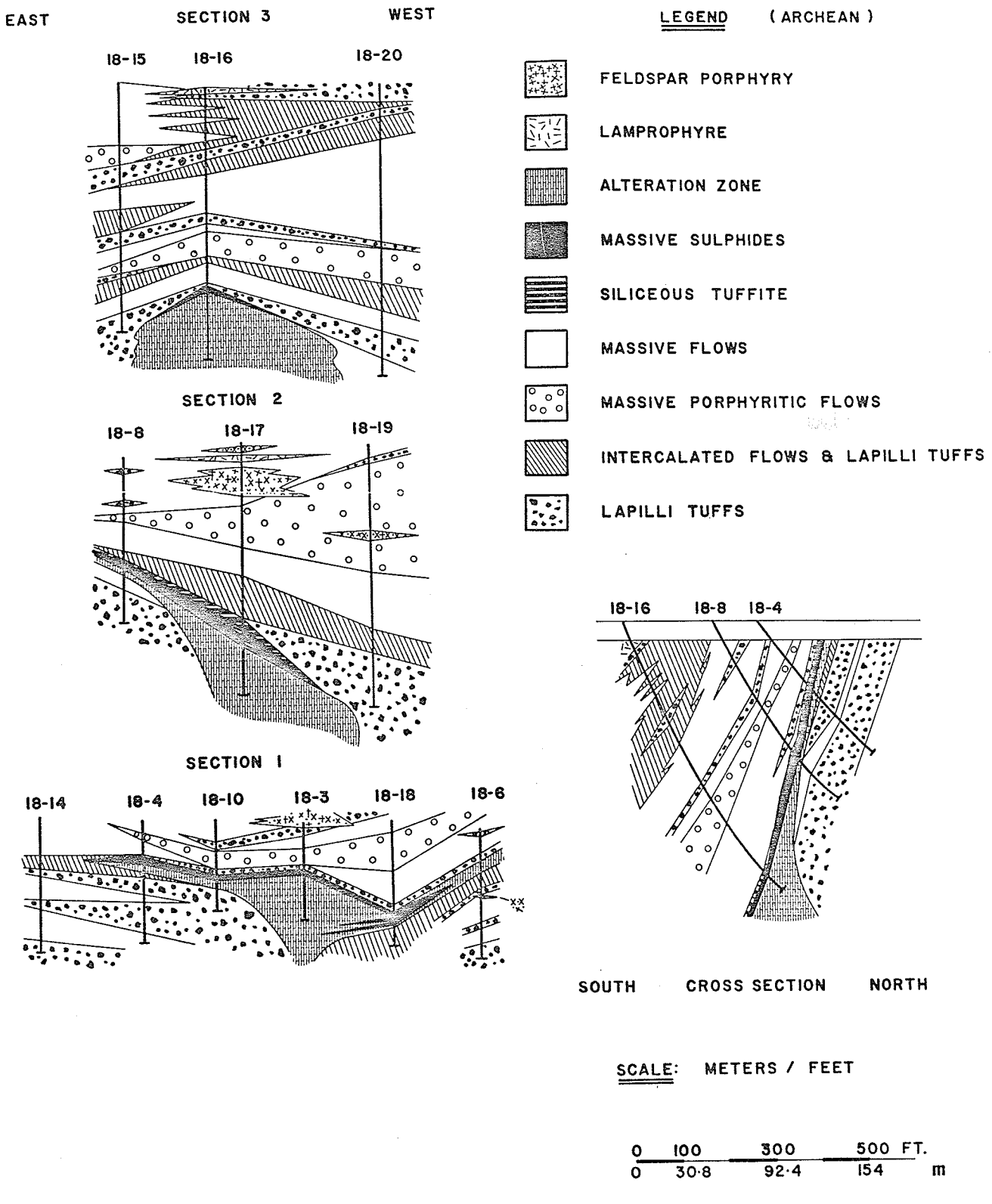


FIGURE 10 STRATIGRAPHIC SECTIONS THROUGH THE DIXIE 150-18 SULPHIDE BODY

(figure 10). Section 1 is closest to the sulphide body and correlates the volcanic rocks immediately above and along the entire strike length of the sulphide body. The section is approximately 308 m in length and reaches an average depth of 77 m. Section 2 intersects the sulphide body at intermediate depths and correlates the volcanic stratigraphy further south or higher up in the stratigraphic sequence above the sulphide body. The section is approximately 246 m in length and reaches an average depth of 140 m. Section 3 outlines the sulphide body at the greatest depths and correlates the volcanic stratigraphy even further south or at the highest stratigraphic levels above the sulphide body. This section is approximately 230 m in length and attains a maximum depth of 170 m.

The only vertical cross section of the Dixie 150 - 18 sulphide body is shown in figure 10. This section is outlined by three drill holes intersecting the mineralized zone and volcanic rocks down to a depth of 178 m.

## THE VOLCANIC UNITS ENCLOSING THE DIXIE 150 - 18 SULPHIDE BODY

The relative lack of structural deformation enables a reasonable interpretation of the volcanic stratigraphy and depositional history in the immediate vicinity of the Dixie 150 - 18 sulphide body. The porphyritic flows act as the stratigraphic marker horizon in all sections. Figure 10

shows the following significant stratigraphic features:

(1) Thick sequences of massive and porphyritic flows are stratigraphically situated above the sulphide body.

(2) The porphyritic flows appear as a thin unit which thickens considerably over the central portion of the sulphide body and thins again farther south.

(3) The sulphide body is partially capped by a thin discontinuous siliceous tuffite which is well developed at intermediate depths over the central portion of the sulphide body. The unit does not appear elsewhere in the volcanic stratigraphy.

(4) The sulphide body is situated primarily within tuffaceous units which also cap the mineralization in places.

(5) The alteration zone, situated immediately below the sulphide body also lies within tuffaceous units.

(6) Another unit of tuffs with some minor intercalated flows reappears near the top of the stratigraphic sections immediately above the massive and porphyritic flows.

(7) Large lamprophyric dikes and smaller feldspar porphyry sills intrude all of the volcanic units but are more prevalent near the central portion of the sections and above the sulphide body.

All drill hole alteration intersections lie immediately north or on the footwall of the Dixie 150 - 18 sulphide body (figure 10) and suggest that the volcanic units enclosing the mineralization are stratigraphically younger south or

above the mineralized zone. Furthermore, graded bedding preserved in the siliceous tuffite indicates that the volcanic units are progressively younger south or towards the top of each section shown in figure 10. Many of the volcanic sequences comprise intercalated flows and lapilli tuffs which are too small or discontinuous to allow correlation from one drill hole to the next. One continuous sequence may represent as many as a dozen individual flows or segments of flows and lapilli tuffs. Several of these sequences have been grouped together as "intercalated flows and lapilli tuffs" (figure 10).

Apart from the twelve drill holes outlining the configuration and enclosing volcanic rocks of the Dixie 150 - 18 sulphide body, eight reconnaissance drill holes were drilled over small electromagnetic anomalies north, northeast and east of the 150 - 18 prospect. Two drill holes, 150 - 18 - 9 and 13 outlined a small mineralized zone approximately 400 m along strike of the larger sulphide body. All other drill holes failed to intersect mineralization but provide an account of the outlying geology.

The drill hole locations and respective geology are shown on figure 11. Although correlation between drill holes is not possible, one distinctive change in the geology is evident. Large continuous sequences of greywacke, calcareous siltstone with minor beds of impure limestone occur north, northeast and east of the Dixie 150 - 18 sulphide body.

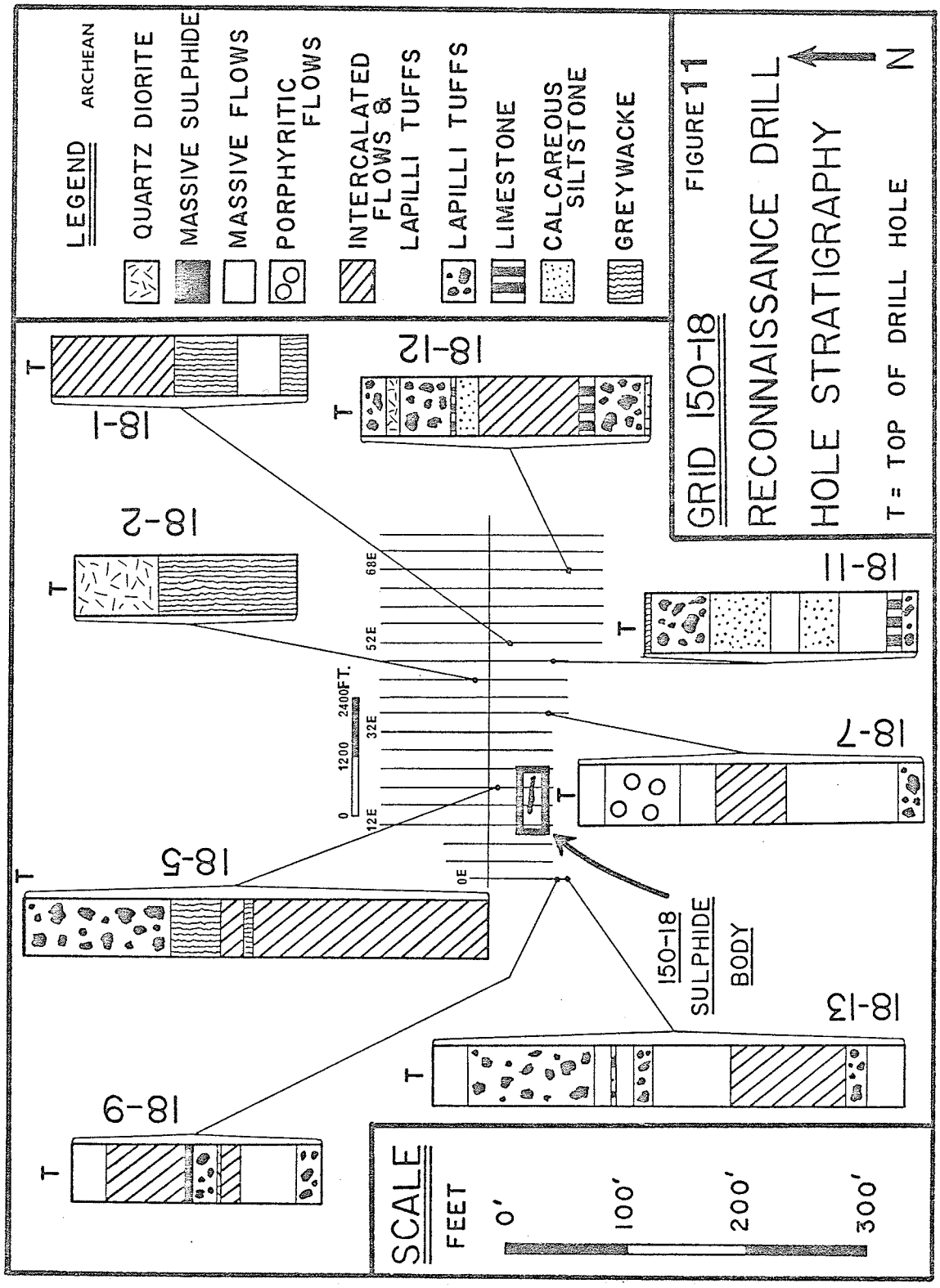
LEGEND ARCHEAN
QUARTZ DIORITE
MASSIVE SULPHIDE
MASSIVE FLOWS
PORPHYRITIC FLOWS
INTERCALATED FLOWS & LAPILLI TUFFS
LAPILLI TUFFS
LIMESTONE
CALCAREOUS SILTSTONE
GREYWACKE
GRID 150-18
RECONNAISSANCE DRILL HOLE STRATIGRAPHY
T = TOP OF DRILL HOLE
N
18-1
18-2
18-3
18-5
18-7
18-9
18-11
18-12
18-13
T
0E
12E
32E
52E
68E
0
1200
2400FT.
150-18 SULPHIDE BODY
SCALE
FEET
0'
100'
200'
300'

FIGURE 11

## DEPOSITIONAL HISTORY OF THE VOLCANIC UNITS ENCLOSING THE DIXIE 150 - 18 SULPHIDE BODY

The generalized volcanic lithological sequences and depositional history is as follows:

(1) Initial deposition of a tuffaceous unit with minor intercalated massive flows (bottom of sections 1 - 3, figure 10).

(2) Deposition of the sulphide - base metal mineralization with coincident development of the alteration zone (sections 1 - 3, figure 10)[1].

(3) Deposition of the siliceous tuffite immediately above and only along the extent of the sulphide body (section 2, figure 10).

(4) Period of volcanism primarily associated with extrusion of large massive and prophyritic flows (top of section 1 and 2, middle of section 3, figure 10).

(5) Period of volcanism primarily associated with extrusion and deposition of tuffaceous debris (top of section 3, figure 11).

(6) Intrusion of small lamprophyric dikes and feldspar porphyry sills (sections 1 - 3, figure 11).

1 There remains a possibility that the sulphide - base metal mineralization may have been incorporated into the volcanic units well after stratigraphic development.

Continuous sequences of greywacke, calcareous siltstone and impure limestone may indicate a distinct environmental transgression eastward from a subaerial or subaqueous volcanic environment near the vicinity of the Dixie 150 - 18 sulphide body into a deeper offshore marine environment.

# CHAPTER 7

# THE DIXIE 150 - 18 SULPHIDE BODIES

## GENERAL

The Dixie 150 - 18 sulphide prospect consists of two conformable, steeply-dipping, lenticular sulphide bodies. Both sulphide bodies, one of which is much larger than the other strike east - west and dip steeply to the south (figure 8).

The larger sulphide body is continuous along strike for at least 280 m. The width is variable, attaining a maximum of approximately 5 m in massive mineralization and 12 m in disseminated mineralization. Disseminated mineralization is generally confined to the shallow western end of the sulphide body and transforms downdip and along strike into narrow massive mineralization. The disseminated mineralization extends to a depth of approximately 66 m and the massive mineralization reaches depths of approximately 145 m (figure 8).

The smaller lensoid body located 390 m west and along strike of the larger sulphide body is composed of massive mineralization which attains a maximum thickness of 2 m down to a depth of approximately 60 m.

The estimated in place mineral reserve for both lenses of sulphide mineralization is 330,000 tons grading 0.48% copper, 6.9% zinc and 0.43 ounces of silver per ton. The larger sulphide body is open downdip and along strike for

other sulphide lenses.

Figure 12 illustrates the main sulphide compositional differences between the massive and disseminated mineralization. The compositional diagram is based upon visual estimations and assays of sulphide mineralization at 60 cm intervals throughout all mineralized sections of drill core. The sulphide mineralization contains substantial quantities of pyrite and pyrrhotite and only minor variation occurs in the distribution of chalcopyrite and sphalerite in the massive and disseminated mineralization. Zinc-rich mineralization is generally massive and copper-rich mineralization is disseminated (figure 12).

## DISSEMINATED MINERALIZATION - MEGASCOPIC FEATURES

Pyrite, pyrrhotite and subordinate amounts of sphalerite, chalcopyrite and magnetite occur in the disseminated mineralization. The disseminated mineralization consists of a mixture of silicate and sulphide minerals with total sulphide content ranging between 10 and 30% by volume. Relatively thin sulphide layers in many sections alternate with sulphide-poor gangue silicate layers of approximately equal thickness resulting in a pronounced layering. The silicate layers are characterized by diffuse accumulation of pyrite, pyrrhotite, and chalcopyrite in discrete grains or stringers aligned parallel to foliation. Zones of intense deformation within the sulphide-poor silicate layers are represented by relict

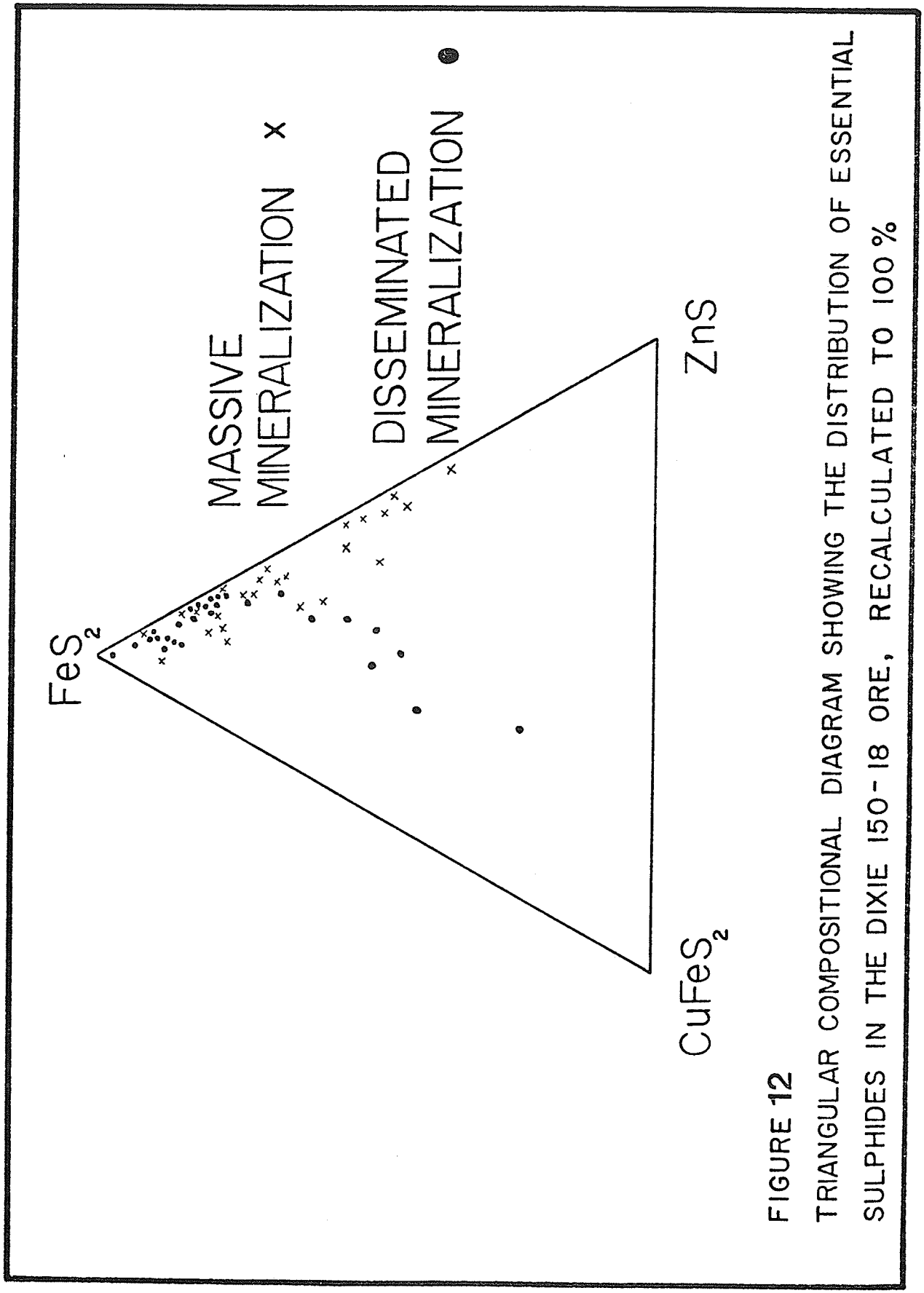


FIGURE 12

TRIANGULAR COMPOSITIONAL DIAGRAM SHOWING THE DISTRIBUTION OF ESSENTIAL SULPHIDES IN THE DIXIE 150-18 ORE, RECALCULATED TO 100 %

streaks or stringers of granulated pyrite aligned parallel to foliation in the silicate minerals and chalcopyrite and pyrrhotite along cleavages in the silicate minerals. Lenticulation and boudinage of earlier pyrite aggregates throughout all of the disseminated mineralization is common.

## MASSIVE MINERALIZATION - MEGASCOPIC FEATURES

The massive mineralization contains 60 to 95% sulphide minerals by volume which are generally concordant with the foliation of the enclosing volcanic rocks and cordierite - anthophyllite alteration zone. Pyrite, pyrrhotite and sphalerite with subordinate amounts of chalcopyrite, magnetite and tetrahedrite are the sulphide and oxide minerals.

The massive sulphide layers are pyrite- or pyrrhotite-rich and sphalerite is closely associated with pyrite. Some parts of the massive mineralization contain silicate lenses which are aligned parallel to the foliation in the enclosing wallrock. The sulphide mineralization commonly shows minor folding of the gangue silicate minerals and conspicuous banding is exemplified by variation in the proportions of pyrite, sphalerite and to a lesser extent pyrrhotite. Banding is also obvious in monominerallic pyrite layers by variation in grain size and texture.

Prominent features of the massive mineralization include a streaky layering of pyrrhotite parallel to foliation

in the wallrock and plicative gneissic textures (plates 6 & 7). Granoblastic texture is characterized by mosaic development of equigranular pyrite crystals. Porphyroblasts of pyrite are commonly embedded in an optically continuous sphalerite matrix (plates 8 & 9). Brecciation of the more competent pyritic layers and plastic flowage of chalcopyrite and pyrrhotite deflecting around silicate mineral fragments is common (plates 10 & 11).

## PYRITE

Pyrite is the most abundant sulphide mineral observed in the Dixie 150 - 18 sulphide body. The mineral is commonly present as subhedral cubes which range in size from 0.1 mm to coarse crystals 2 cm across. Idiomorphic crystals are commonly enclosed by sphalerite and pyrrhotite (plates 8 & 9). Where a number of crystals are massed together, outlines are not well defined and resemble an aggregate that is contained within an interstitial sphalerite or pyrrhotite matrix.

Many crystals show extensive corrosion along crystal boundaries, fractures and parting planes which act as hosts to embayments and tiny veinlets of pyrrhotite, sphalerite and silicate minerals. The embayments are of the normal rounded form and range in size from small indentations to large cavities. Rounded inclusions of one or more sulphide minerals (primarily sphalerite) are commonly enclosed within the grains.

## PLATE 6

STREAKY LAYERING OF PYRRHOTITE PARALLEL TO FOLIATION IN WALL ROCK. (4 X)

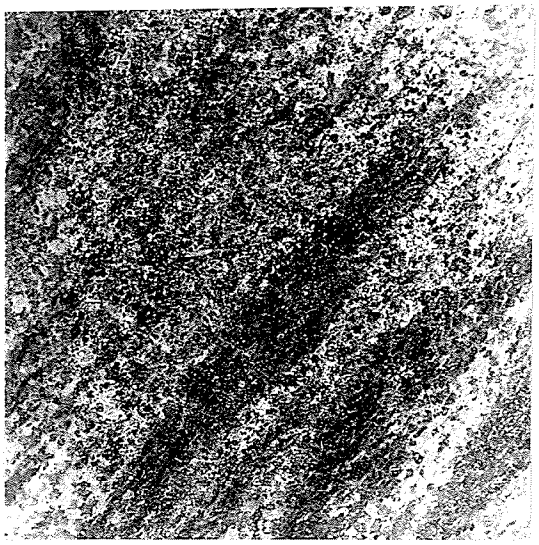

## PLATE 7

PLICATIVE GNEISSIC TEXTURES OF PYRITE AND PYRRHOTITE (WHITE) IN GANGUE SILICATES (BLACK). (4 X)

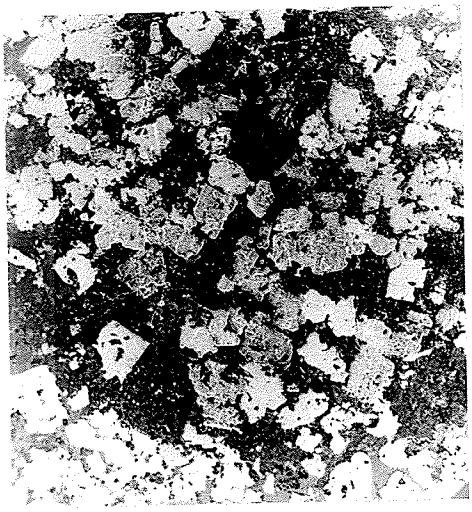

## PLATE 8

POIKILOBLASTIC PYRITE (WHITE) EMBEDDED IN A SPHALERITE – MINOR PYRRHOTITE MATRIX (DARK GRAY TO BLACK). (4 X)

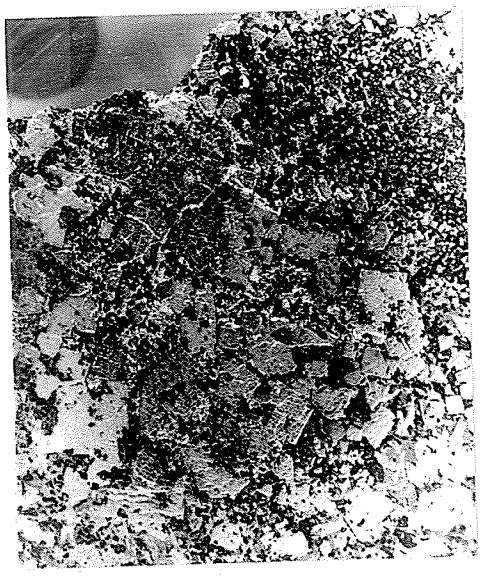

## PLATE 9

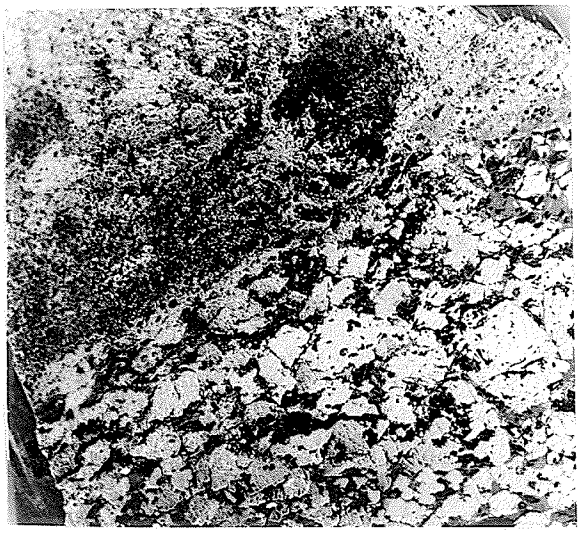

## PLATE 10

BRECCIATION AND GRANULATION OF COMPETENT PYRITE LAYERS (WHITE) IN A SPHALERITE – MINOR PYRRHOTITE MATRIX (DARK GRAY TO BLACK). 4 X

## PLATE 11

PLASTIC FLOWAGE OF CHALCOPYRITE AND PYRRHOTITE (WHITE AND LIGHT GRAY) AROUND GANGUE SILICATE FRAGMENTS ( DARK GRAY TO BLACK ). 4 X

Tectonic brecciation and cataclastic deformation of pyrite crystals occur in many sections (plate 12). Many grains have been fractured or completely shattered to form zones of sharply angular fragments enclosed in a matrix of sphalerite and pyrrhotite (plates 14, 15 & 16). The alignment of the fractures in many crystals suggests a possible crystallographic control on the breakage direction (plates 12 & 15). Fractures are always filled by either pyrrhotite, sphalerite and/or chalcopyrite (plate 13). Zoned structure is conspicuous in a few euhedral crystals and colloform or framboidal textures of pyrite were not observed.

## PYRRHOTITE

Pyrrhotite is a major constituent of the Dixie 150 - 18 sulphide body. It commonly forms equigranular multi-grained patches and allotriomorphic aggregates of various sizes with gangue silicate minerals and sphalerite. Individual grains are equidimensional and exhibit an elongated form which coalesces to form ribbons or foliated masses. A weak dimensional orientation of individual grains occurs in the ribbons and numerous grains exhibit simultaneous extinction (plate 6).

The foliated granular aggregates of pyrrhotite commonly contain a few exsolution granules of sphalerite. The granules are aligned along crystallographic boundaries in

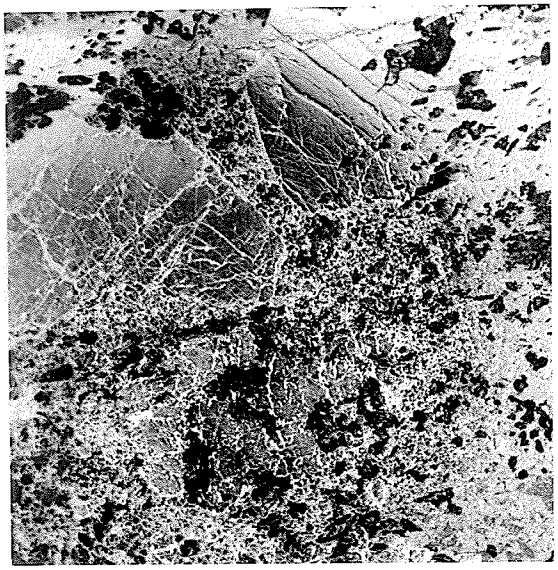

## PLATE 12

SEVERE TECTONIC BRECCIATION AND CATACLASTIC DEFORMATION OF PYRITE PORPHYRO-BLASTS — WITH ALIGNMENT OF FRACTURES SUGGESTING CRYSTALLO-GRAPHIC CONTROL ON THE BREAKAGE DIRECTION. 4 X

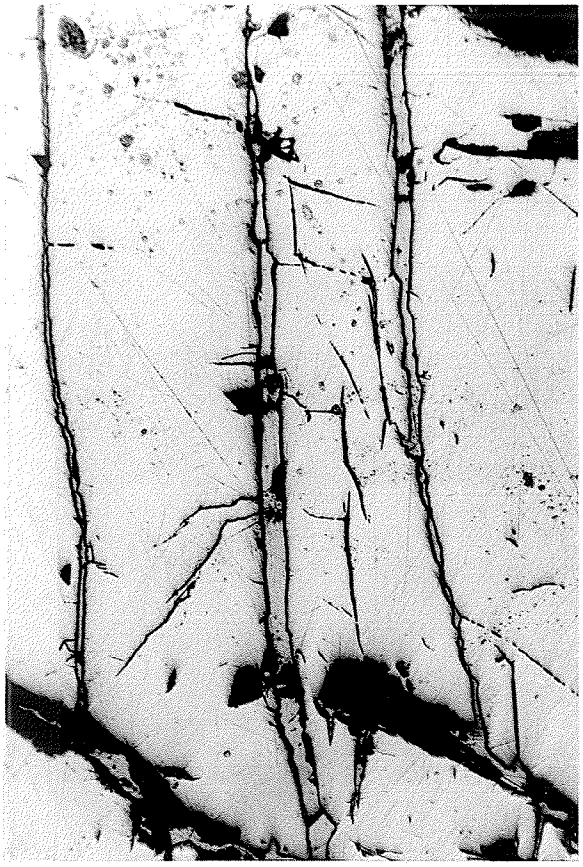

## PLATE 13

MAGNIFIED PYRITE PORPHYROBLAST FROM ABOVE SHOWING LARGE FRACTURES FILLED WITH CHALCOPYRITE AND MINOR PYRRHOTITE. 40 X

PLATE 14

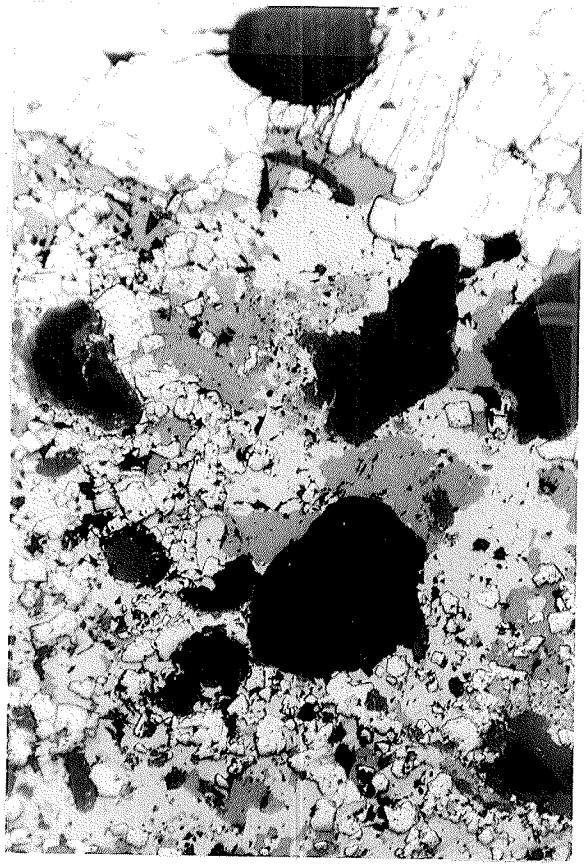

PLATE 15

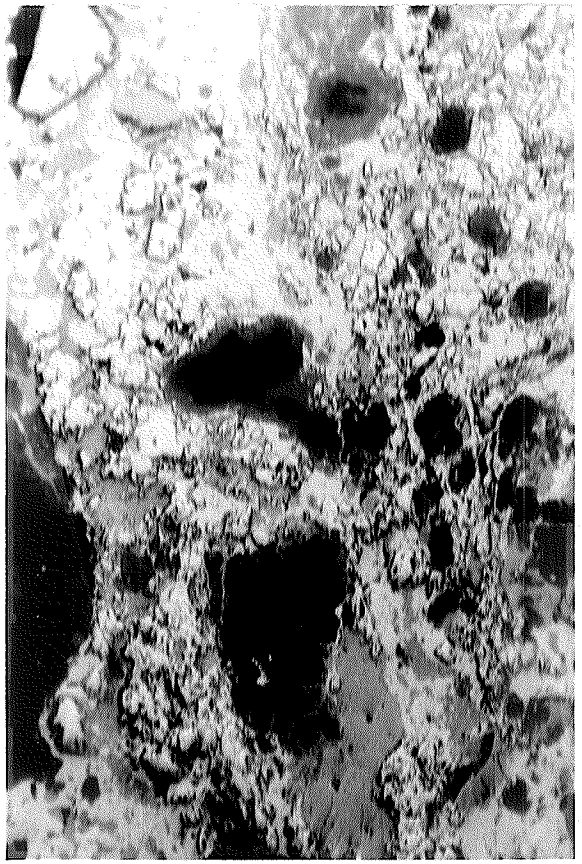

PLATE 16

PROGRESSIVE DEFORMATION AND MOBILIZATION OF PYRITE PORPHYROBLASTS. (40X)

PLATE 14 INITIAL BRECCIATION OF A LARGE PYRITE PORPHYROBLAST (EXTREME LEFT) INTO SMALL ANGULAR FRAGMENTS (WHITE) IN A PYRRHOTITE — SPHALERITE MATRIX (GRAY).

PLATE 15 CONTINUAL BRECCIATION OF A PYRITE PORPHYROBLAST (TOP) WITH MOBILIZATION OF FRAGMENTS (WHITE) IN A PYRRHOTITE (LIGHT GRAY) — SPHALERITE (DARK GRAY) — GANGUE (BLACK) MATRIX.

PLATE 16 PYRRHOTITE — SPHALERITE SHOWING PLASTIC DEFORMATION AND CARRYING INNUMERABLE PYRITE AND GANGUE FRAGMENTS.

pyrrhotite. More commonly, innumerable exsolution granules of pyrrhotite occur in sphalerite and also align along crystallographic boundaries.

Pyrrhotite commonly occurs in intersticies between silicate minerals and in many places appears to have been forced out of a "mush" of idiomorphic silicate minerals. Pyrrhotite always exhibits mutual grain boundaries with sphalerite. Chalcopyrite replaces pyrrhotite along fractures and grain boundaries.

## SPHALERITE

Sphalerite is the most abundant ore mineral. It generally occurs as extensive monominerallic aggregates that are composed of small equigranular grains which invariably show dihedral angles at grain boundaries in pyrrhotite and repeated twinning when etched. Some aggregates form small lensoid bodies that commonly lie parallel to the foliated silicate minerals.

Sphalerite is characterized in all sections by profuse exsolution of pyrrhotite and less commonly chalcopyrite. The exsolution granules are aligned along crystallographic boundaries and twinning directions in sphalerite and fluidal textures of exsolved pyrrhotite and chalcopyrite are present (plates 17 & 18). Inclusions and embayments of sphalerite in pyrite, magnetite and pyrrhotite are common. Mechanical dislocation features occur in some sections where sphalerite

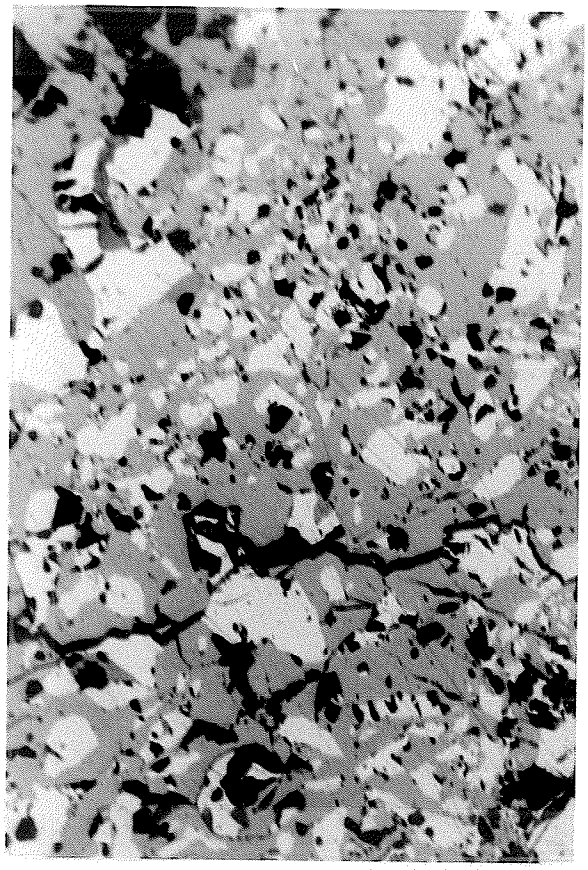

## PLATE 17

COMPLEX EXSOLUTION OF PYRRHOTITE IN SPHALERITE (DARK GRAY).
40 X

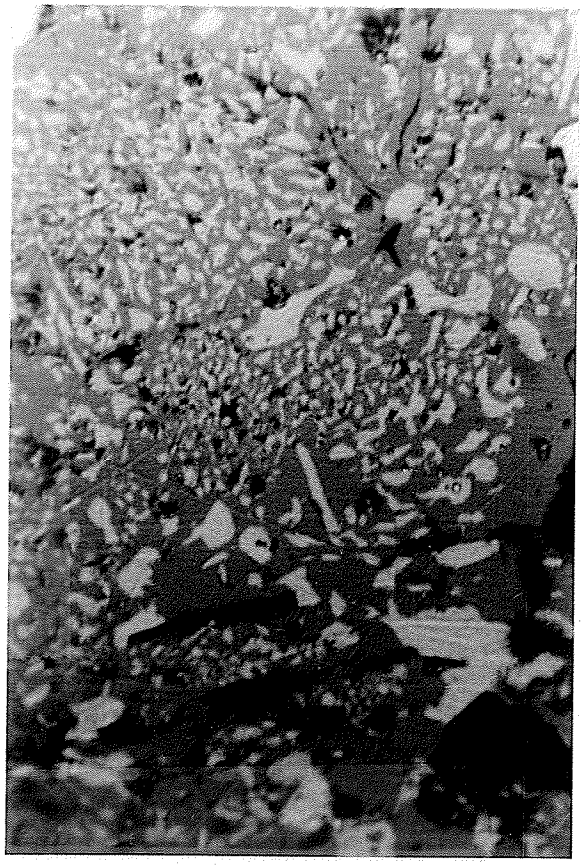

## PLATE 18

PROFUSE LACE-LIKE EXSOLUTION ARRANGEMENT OF CHALCOPYRITE EMULSOID BODIES IN SPHALERITE (DARK GRAY).
100 X

is fractured into a series of narrow shards.

## CHALCOPYRITE

Chalcopyrite is commonly contained within sphalerite and rarely magnetite as minute inclusions in a variety of exsolution patterns. Observed patterns include rounded emulsoid bodies randomly distributed, trains of emulsoid bodies depicting cleavage directions in sphalerite (plate 19) and rarely as rims around sphalerite grain boundaries.

Chalcopyrite has a strong affiliation with gangue silicate minerals and commonly occurs in anhedral form in veins, veinlets and intersticies in the gangue silicate minerals (plate 20). It also fills fractures and cleavage planes in pyrite and pyrrhotite and occurs in late stage fractures cutting across all sulphide and silicate minerals.

Chalcopyrite rarely occurs as equigranular and allotriomorphic aggregates in pyrrhotite and strain shadows around pyrite grains. The mineral also mantles many pyrite, pyrrhotite and silicate mineral grain boundaries.

## MAGNETITE

Magnetite is not a common constituent of the Dixie 150 - 18 sulphide body. It is anhedral, intimately intergrown with the silicate minerals and follows the foliation in the silicate mineral layers. Most magnetite occurs as irregular

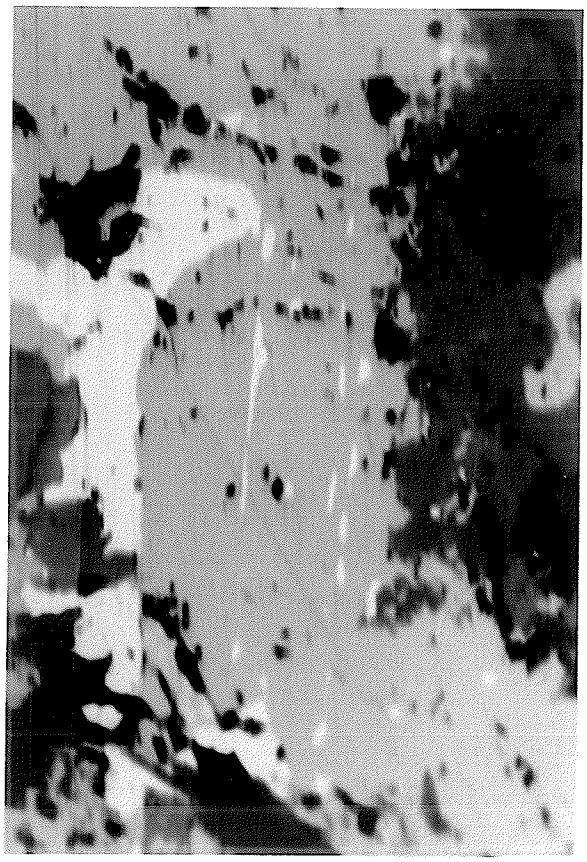

## PLATE 19

TRAINS OF CHALCOPYRITE EMULSOID BODIES DEPICTING CLEAVAGE DIRECTIONS IN SPHALERITE (GRAY). 40 X

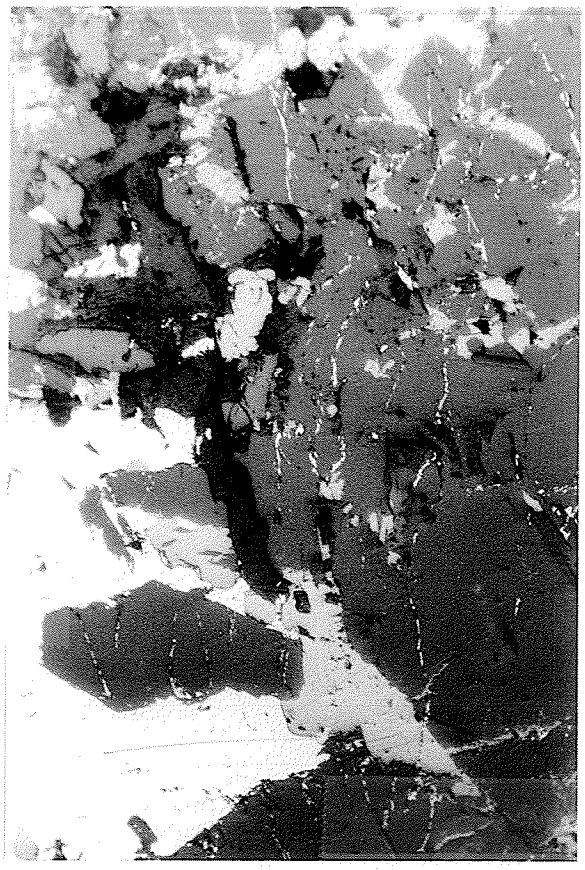

## PLATE 20

CHALCOPYRITE (WHITE) FILLING FRACTURE VEINLETS AND CLEAVAGE PLANES IN GANGUE (ANTHOPHYLLITE) SILICATES (DARK GRAY). 40 X

to elongated grains which have undergone cataclastic fracturing. Pyrrhotite and sphalerite commonly mould about the grains, invade many of the fractures and occur as small inclusions in others. In some sections, magnetite is very fine-grained and stretched into elongated shredded masses which contain well developed sub-myrmekitic-graphic intergrowths with surrounding pyrrhotite and rarely chalcopyrite (plate 21). Idiomorphic euhedral crystals of magnetite were not observed in any sections.

## TETRAHEDRITE

Tetrahedrite is a rare constituent in the Dixie 150 - 18 sulphide body. The mineral only occurs in sections which contain considerable sphalerite. Tetrahedrite usually occurs as minute exsolution granules and irregular shaped grains in sphalerite and rarely gangue silicate minerals, magnetite and chalcopyrite (plate 22).

## Cu, Zn, Ag AND IRON SULPHIDE COMPOSITIONAL ZONATIONS

The copper, zinc and silver zonation profiles for the Dixie 150 - 18 sulphide body are shown in figures 13 and 14. Figure 13 represents a horizontal or lateral zonation east to west across the upper portion of the sulphide body at an average depth of approximately 30 m. Figure 14 represents a vertical zonation profile with depth at the eastern edge

## PLATE 21

SHEARED AND ELONGATED SHREDDED MASSES OF MAGNETITE IN GANGUE (DARK GRAY). 40 X

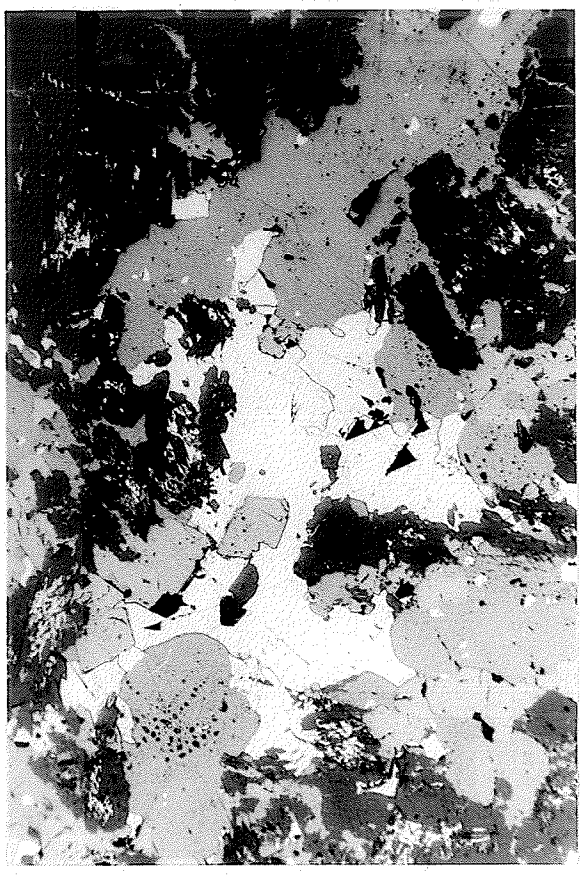

## PLATE 22

TETRAHEDRITE (WHITE) IN CHALCOPYRITE ENCLOSED BY EUHEDRAL MAGNETITE (GRAY). 40 X

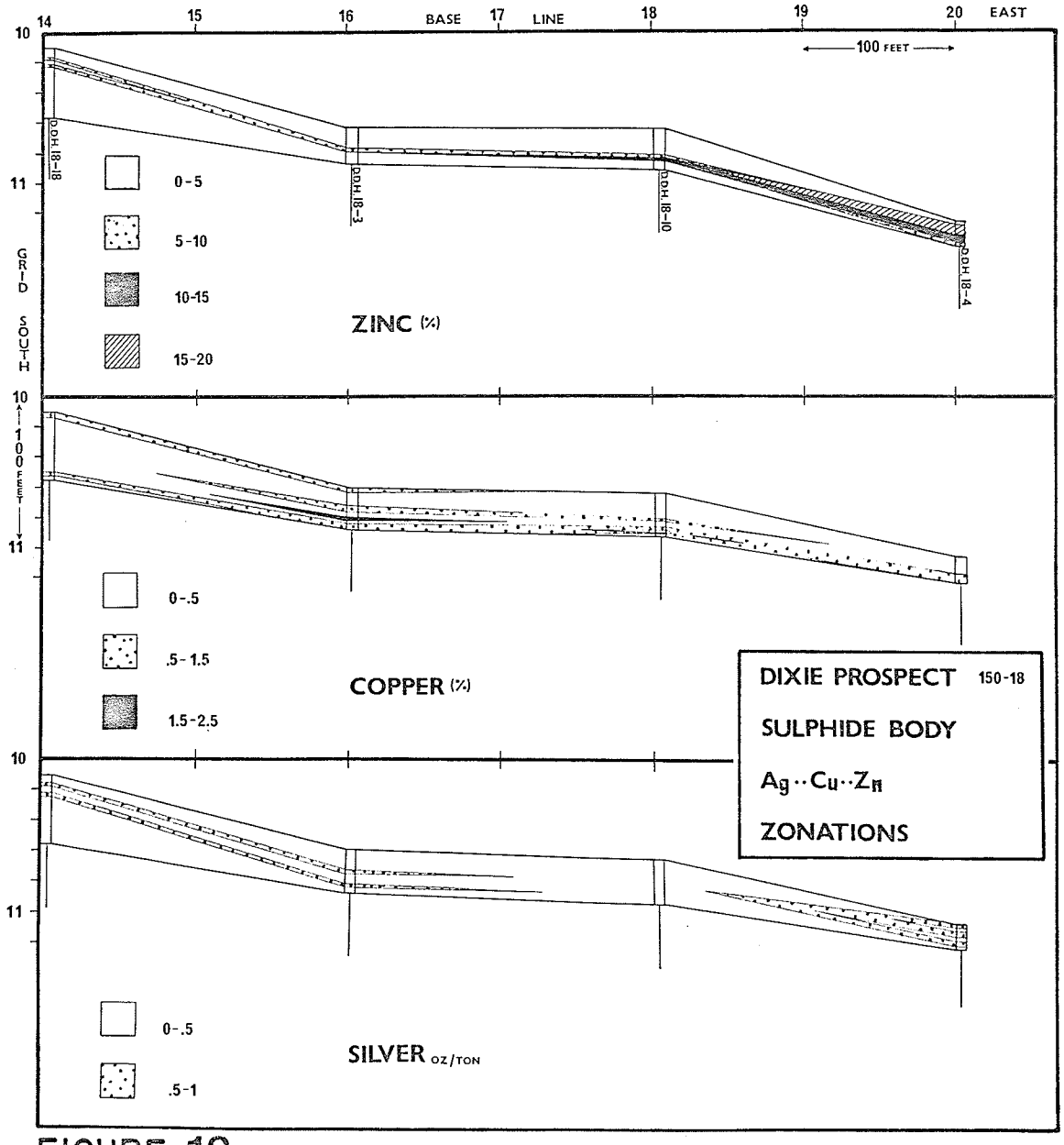


FIGURE 13

HORIZONTAL PLAN VIEW

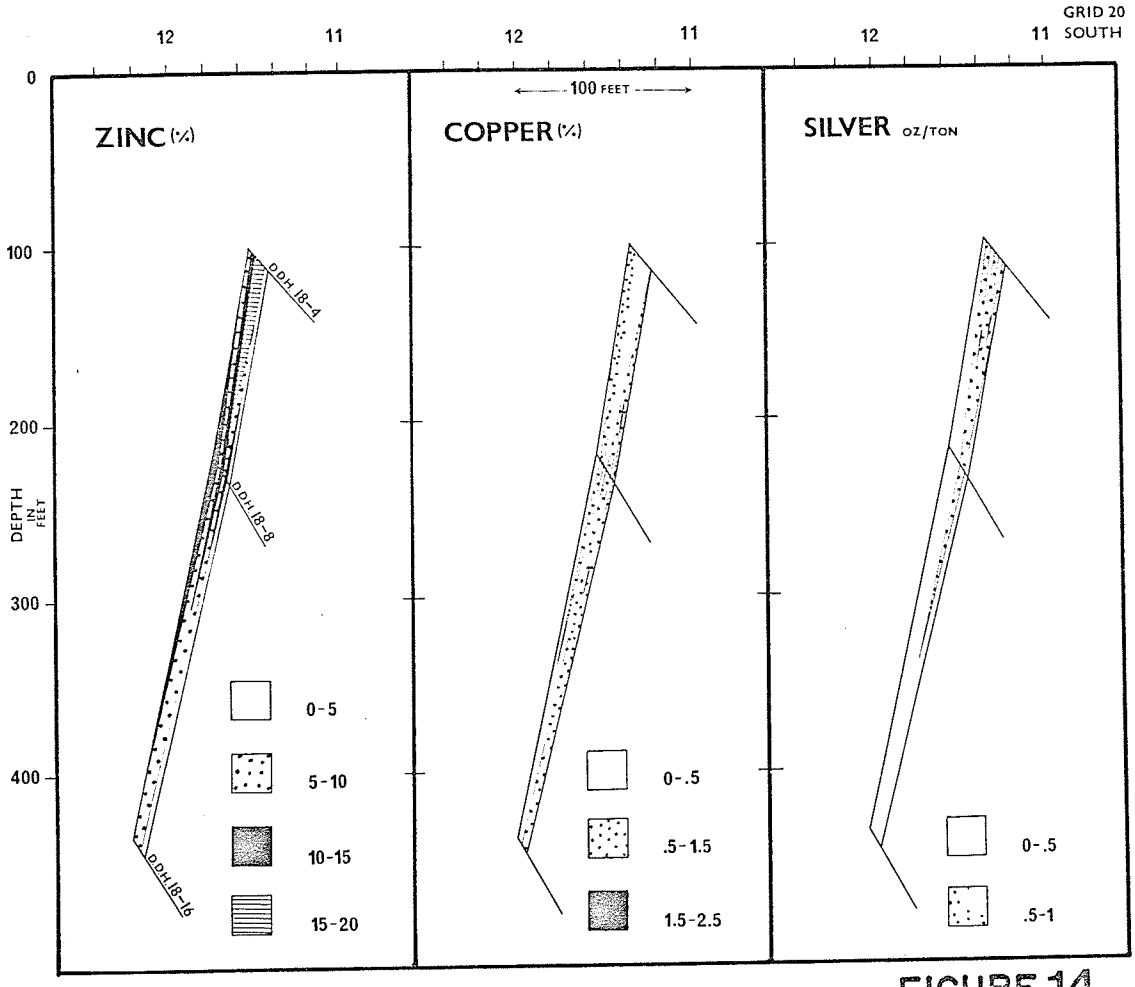


FIGURE 14

VERTICAL SECTION

DIXIE PROSPECT 150-18

SULPHIDE BODY

Ag··Cu··Zn

ZONATIONS

of the sulphide body.

Several zonation relationships are illustrated in the profiles. Zinc forms an enriched core throughout the entire sulphide body and increases in concentration towards the eastern extremities of the sulphide zone. High concentrations of zinc are confined to the upper portion of the sulphide body and gradually decrease with depth. Copper is somewhat more variable. The highest concentrations of copper occurs in drill hole 150 - 18 - 3. A uniform distribution of copper occurs with depth and a slight enrichment of copper appears along the margins of the sulphide body. Silver is associated with the higher concentrations of zinc and forms an enriched central core in the western portion of the sulphide zone and a larger concentration at the western edge where zinc is commonly in excess of 15% by volume. Silver, like zinc, gradually decreases in concentration with depth.

Mineral - metal variation diagrams for each mineralized section intersected by 5 major drill holes at various depths throughout the Dixie sulphide body are shown in figure 15. The drill holes extend over a distance of 600 feet along strike of the sulphide body. Drill holes 150 - 18 - 17 and 18 represent disseminated mineralization.

A few more relationships are shown in this figure. Magnetite is primarily concentrated within the disseminated mineralization near the western edge of the sulphide body. The greatest concentration of pyrite and pyrrhotite are

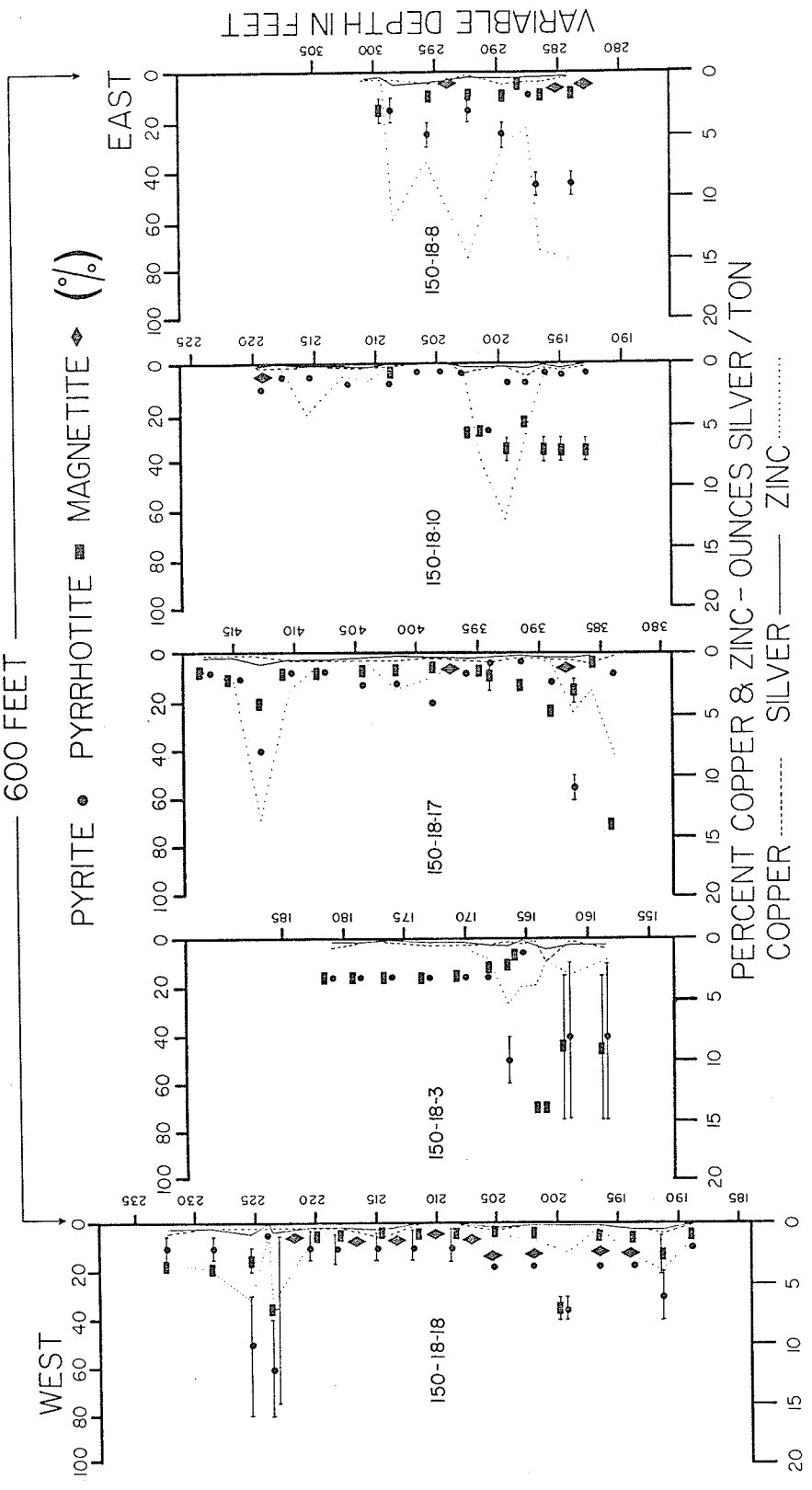


FIGURE 15 PERCENTAGES OF MAGNETITE, PYRRHOTITE AND PYRITE WITH COPPER, ZINC AND OUNCES OF SILVER PER TON FOR THE DIXIE 150-18 PROSPECT

superimposed upon the highest concentrations of zinc. Pyrrhotite exhibits a weak association with copper-rich intersections and pyrite exhibits a similar association with zinc-rich intersections. The highest concentrations of copper, zinc and silver are erratically distributed throughout the massive mineralization. All three metals tend to be concentrated at or near the margins of the sulphide body in disseminated mineralization.

## INTERPRETATION OF THE SULPHIDE TEXTURES

The megascopic and microscopic features of the Dixie 150 - 18 sulphide mineralization indicate that the present characteristics and textures of the mineralization resulted from the interplay of differential stress, metamorphic recrystallization and mobilization. The occurrence of large pyrite porphyroblasts in the mineralization is indicative of nucleation and growth resulting from metamorphism, and the characteristic fracturing of the porphyroblasts is evidence that the pyrite grains were subjected to subsequent tectonic stress.

Healing of fractured pyrite porphyroblasts by chalcopyrite and pyrrhotite can be explained by plastic deformation and mobilization of chalcopyrite and pyrrhotite whereas pyrite tends to fail by brittle behaviour (Clark and Kelly, 1973; Graf and Skinner, 1970). Furthermore, characteristic lenticulation, boudinage and cataclastic brecciation of

former pyrite aggregates, plicative gneissic sulphide textures and streaky layering of pyrrhotite parallel to foliation indicate that metamorphism has modified the sulphide mineralization from its initial configuration.

The intensity of metamorphism would effectively mask or annihilate any primary textures such as colloform and framboidal structures that may have developed during precipitation and deposition of the sulphide mineralization. Consequently, environmental interpretation and paragenesis of sulphide deposition based on sulphide textures and assemblages is invalid. Clearly the initial mineralization must have been syn- or pre-metamorphic.

## INTERPRETATION OF Cu, Zn, Ag AND IRON SULPHIDE COMPOSITIONAL ZONATIONS

Plastic flowage and remobilization of chalcopyrite and pyrrhotite is clearly evident throughout the Dixie 150 - 18 sulphide body. Rearrangement of the metals within the metamorphosed sulphide mineralization is possible as chalcopyrite and to a lesser extent pyrrhotite have responded plastically to deformative and chemical processes either by solid state flow or hydrothermal dissolution and redeposited elsewhere. Metamorphism may have mobilized chalcopyrite out of its original position and redeposited the mineral along the outer more dilatent margins of the sulphide body as is indicated by the distribution of copper within the western

portion of the mineralized zone (figure 13).

The behaviour of ore forming solutions in seawater and physico-chemical problems involving Koroko mineralizing processes have been studied in detail by Sato (1972; 1973). Sato determined that copper-rich and lead-poor ores probably precipitate from higher temperature, lower salinity brines which tend to be sulphur excess. Because the fluids are sulphur excess and low density, chalcopyrite accumulations would be expected to form in the vicinity of the discharge vent. Conversely, sphalerite and galena ores would form in relatively low temperature systems and be precipitated from highly saline sulphur deficient brines. Such brines will have a high density and tend to accumulate away from the discharge vent (Sato, 1972).

Similarly, the relative solubilities, transport and deposition of sphalerite, chalcopyrite and galena in hydrothermal solutions has been reviewed by Large (1977). Chalcopyrite solubility is susceptible to subtle changes in oxygen fugacity in the Koroko type environment and to decreasing pH in copper - zinc mineralization typified by deposits in the Archean greenstone belts of Canada (Noranda, Matagami and Timmins districts). Such changes can lead to an abrupt decrease in chalcopyrite solubility which causes precipitation of chalcopyrite at the discharge vent or within the hydrothermal pipe (as stringer or massive replacement ore) while sphalerite and galena solubilities are unaffected and remain in solution (Large, 1977).

The highest concentrations of copper in the Dixie 150 - 18 sulphide body occur in samples from drill hole 150 - 18 - 3. Also, the copper/zinc ratio throughout this drill hole averages 0.26 whereas the average copper/zinc ratio throughout the entire sulphide body is 0.07. Drill hole 150 - 18 - 3 terminated within cordierite - anthophyllite rocks (figure 10). This central portion of the sulphide body continues to greater depth, appears to be thickening and resembles an alteration pipe (figure 10).

The occurrence of high grade copper intersections throughout drill hole 150 - 18 - 3 suggests that the discharge vent or source for the hydrothermal ore solutions lies within the west central portion of the sulphide body (figure 10). This location also coincides with the thickest extension of the cordierite - anthophyllite alteration that represents the fissure or channel through which the hydrothermal ore solutions have migrated. The highest concentrations of zinc occur along the eastern extension of the sulphide body (figure 13) suggesting that zinc precipitation and deposition occurred at considerable distances from the proposed discharge vent or source for the hydrothermal solutions.

The approximate location of the discharge vent or source for the hydrothermal solutions becomes a major priority when searching for additional lenses of sulphide mineralization. Chalcopyrite precipitation will tend to occur at

the discharge vent or within the hydrothermal (alteration) pipe. Therefore, the extension of the cordierite - anthophyllite alteration zone beneath drill hole 150 - 18 - 3 (figure 10) represents an area that should be favoured in the search for additional copper-rich sulphide lenses.

# CHAPTER 8

# CHEMISTRY OF THE UNALTERED DIXIE 150 - 18 VOLCANIC ROCKS

## INTRODUCTION

Twenty three representative samples of unaltered volcanic rocks were selected for major element chemical analyses[1]. The unaltered volcanic rock samples were subdivided as follows:

8 samples from massive and porphyritic flows

8 samples from the lapilli tuffs

4 samples from the siliceous tuffite

3 samples from greywacke sequences

Samples were selected from the massive and porphyritic flows and lapilli tuffs located stratigraphically above the 150 - 18 sulphide body and from reconnaissance drill holes east and along strike of the sulphide body.

The analyses are shown in tables A1 to A3 in the appendix. The range and average chemical composition for each unaltered volcanic rock and sedimentary rock type are shown on figure 16.

Barth norms were calculated for all unaltered samples, volatile-free after removing $H_2O$, $CO_2$ and S recalculating the analyses to 100%. The norm calculations are shown in tables A7 to A9 in the appendix. The $Fe_2O_3/FeO$ ratio is

1 Unaltered volcanic rocks represent the least altered volcanic rocks not contained within the cordierite - anthophyllite alteration zone.

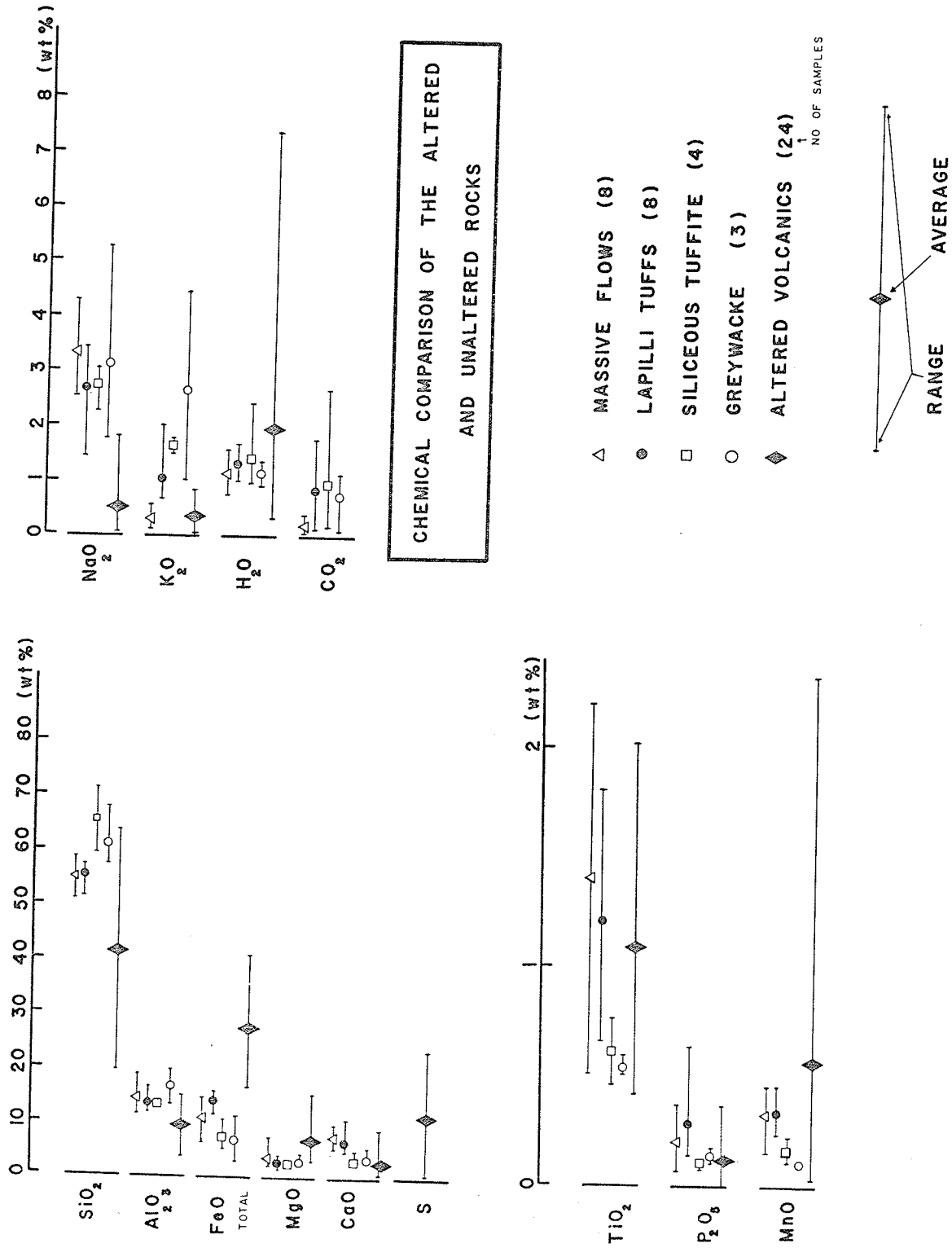
CHEMICAL COMPARISON OF THE ALTERED AND UNALTERED ROCKS
MASSIVE FLOWS (8)
LAPILLI TUFFS (8)
SILICEOUS TUFFITE (4)
GREYWACKE (3)
ALTERED VOLCANICS (24)
NO OF SAMPLES
AVERAGE
RANGE
0 10 20 30 40 50 60 70 80 (wt%)
0 1 2 3 4 5 6 7 8 (wt%)
0 1 2 (wt%)
SiO2
Al2O3
FeO TOTAL
MgO
CaO
S
Na2O
K2O
H2O
CO2
TiO2
P2O5
MnO

FIGURE 16

low in all analyses and only a few of the samples exceed the upper limit for $Fe_2O_3$ determined from the equation % $Fe_2O_3$ = % $TiO_2$ + 1.5 (Irvine and Baragar, 1971). The excess $Fe_2O_3$ determined from the equation should be converted to FeO but the amount of $Fe_2O_3$ in excess was negligible in all samples. Furthermore, magnetite is not abundant in any samples analysed. Therefore, the norm calculations were not adjusted for oxidation of FeO.

A rejection limit of 3.8% total $H_2O$ + $CO_2$ and abnormally high sulphur contents was applied to all samples to minimize the metasomatic introduction of $H_2O$, $CO_2$ and S into the unaltered volcanic and sedimentary rocks (Wilson et al, 1965). This criteria was also facilitated during sampling procedures because samples with quartz, carbonate, epidote and sulphide veins or clots were excluded. All samples are well below the rejection limit and detectable sulphur is not present. In general, volatile contents of the unaltered volcanic and sedimentary rocks are low and not indicative of metasomatism.

Plots of the chemical data are represented on various diagrams (figures 17 - 27). The diagrams aid in determining major chemical changes, delineating trends, detecting specific forms of metasomatism and facilitating classification of the various unaltered volcanic rocks.

Twenty four representative samples from the cordierite - anthophyllite alteration zone were collected for major element chemical analyses. The analyses are shown in tables

A4 to A6. The cordierite - anthophyllite alteration samples are utilized as a direct comparative suite of highly altered volcanic rocks on several of the diagrams. In addition to acting as a good comparative suite, metasomatic chemical trends of these highly altered volcanic rocks are exemplified on the diagrams.

Analyses of three greywacke and four siliceous tuffite samples are plotted on a few of the diagrams. The sedimentary rocks are plotted on volcanic diagrams to facilitate classification and ensure that the sedimentary rocks are chemically distinct from the unaltered volcanic rocks.

All diagrams are interpreted in conjunction with the bulk chemical analyses in tables A1 to A3 in the appendix.

## CHEMISTRY OF THE UNALTERED VOLCANIC ROCKS

The weight percent of each oxide is plotted against silica for the unaltered massive and porphyritic flows and lapilli tuffs in figures 17 and 18. The trends have been delineated by visual estimation. Figure 17 shows an increase in total FeO and a uniform decrease in MgO, $Al_2O_3$ and CaO with increasing silica content in both volcanic rock types. Similarly, figure 18 shows an increase in $Na_2O$ and $P_2O_5$, a constant distribution of $K_2O$ in the massive flows and a somewhat variable decrease in $K_2O$ in the lapilli tuffs with increasing silica. $TiO_2$ is relatively constant in both volcanic rock types. Perhaps the

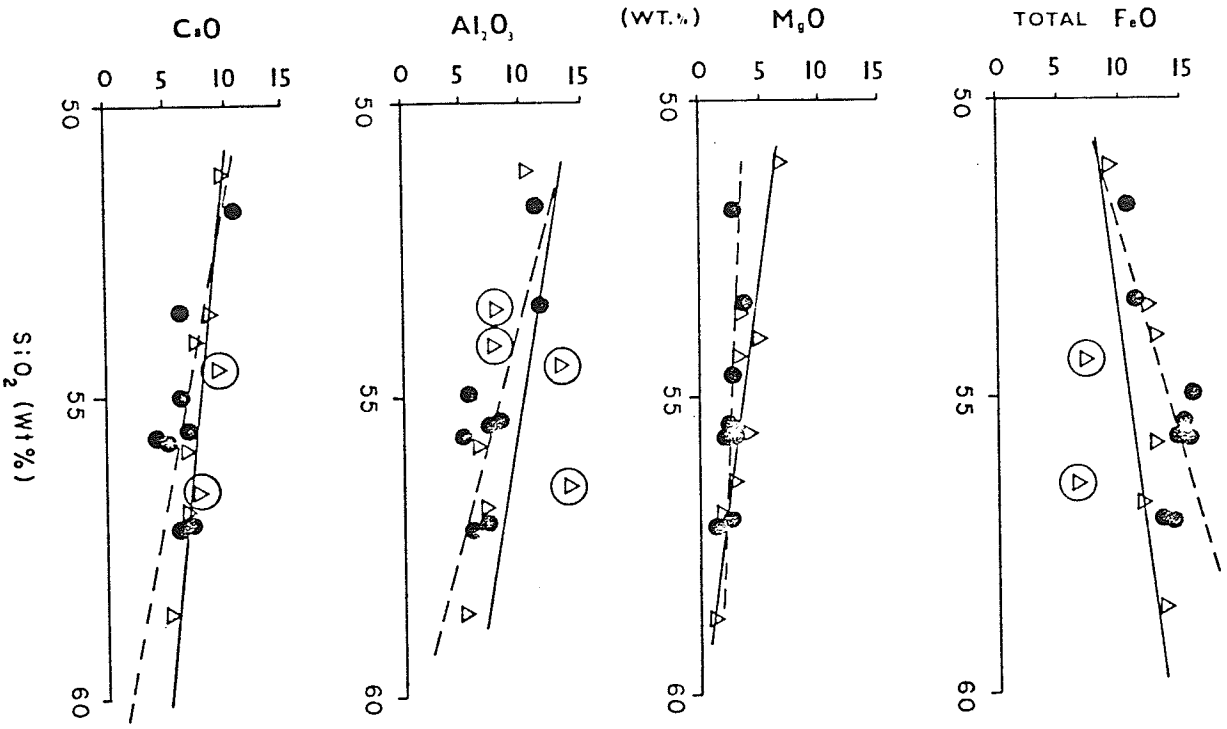


FIGURE 17 PLOTS OF MAJOR ELEMENTS VERSES SILICA FOR THE DIXIE VOLCANIC ROCKS. △MASSIVE FLOWS ——— ● LAPILLI TUFFS — — —

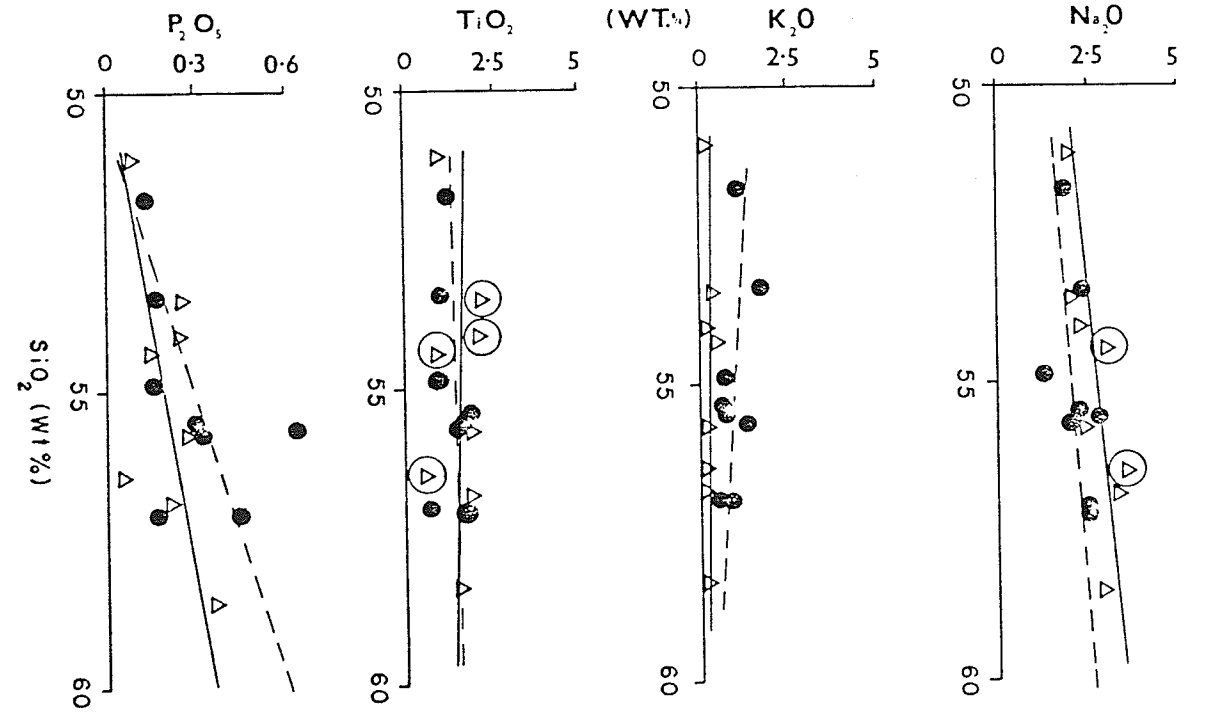


FIGURE 18 PLOTS OF MAJOR ELEMENTS VERSES SILICA FOR THE DIXIE VOLCANIC ROCKS. △MASSIVE FLOWS ——— ● LAPILLI TUFFS — — —

most striking aspect of figures 17 and 18 are the sympathetic trends between certain elements in the massive flows (shown by enlarged circles on figures 17 and 18). Flows with high $Al_2O_3$ contents are also characterized by high CaO and $Na_2O$ with correspondingly low $TiO_2$ and total FeO contents. Those flows which are characterized by high $TiO_2$ and total FeO contents have low $Al_2O_3$ contents (figures 17 and 18).

The behaviour of the individual alkalies can be examined on the alkali igneous spectrum diagram (figure 19) of Hughes (1972) with modification from Stauffer et al (1975) to include island arc tholeiities. Most unaltered igneous rocks should plot within the "igneous spectrum" and those lying outside the boundary have undergone various degrees of potassium or sodium metasomatism. The flows and tuffs form two distinct groupings on the alkali igneous diagram. The flows cluster near the bottom of the sodium field and exhibit a slight increase or enrichment in sodium. The lapilli tuffs exhibit a larger lateral spread but remain within the unaltered igneous spectrum.

The CaO versus $Al_2O_3$ verses total alkali ternary diagram (figure 20) illustrates the similarity between the massive flows and lapilli tuffs. There is a strong trend towards the CaO apex of the diagram, at a constant $Al_2O_3$/ total alkali ratio.

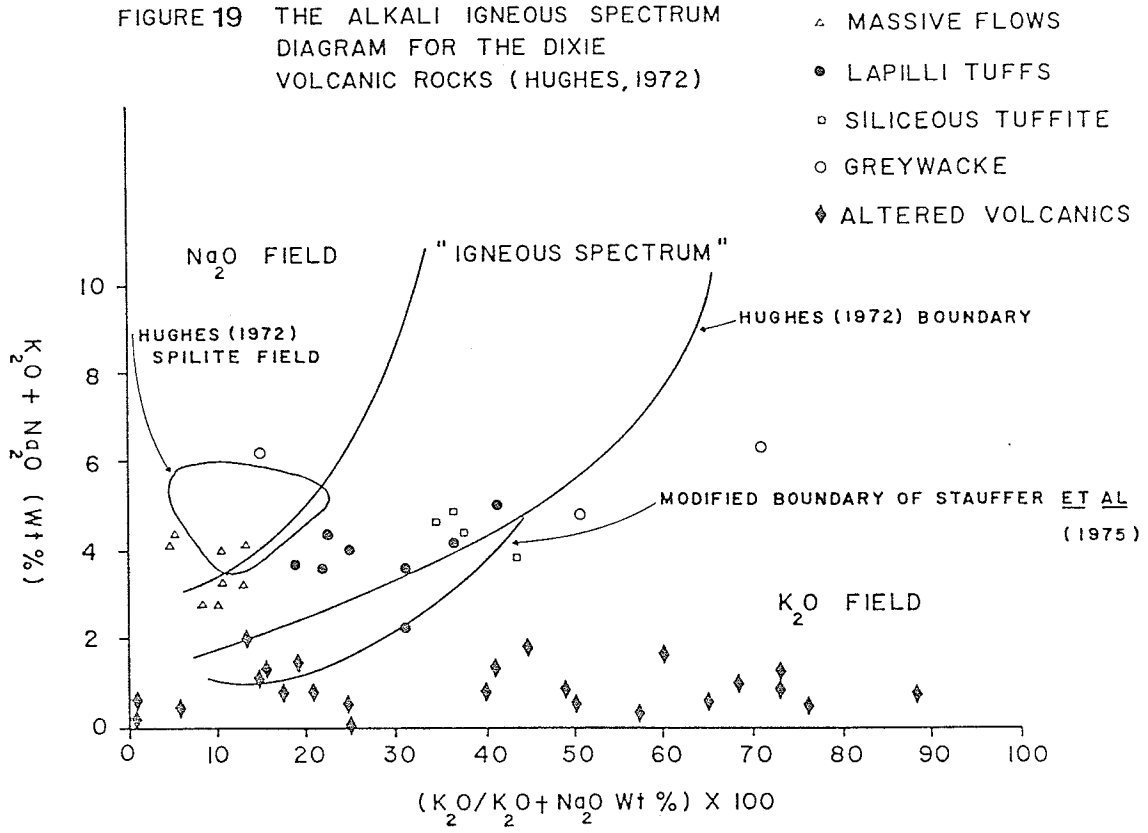


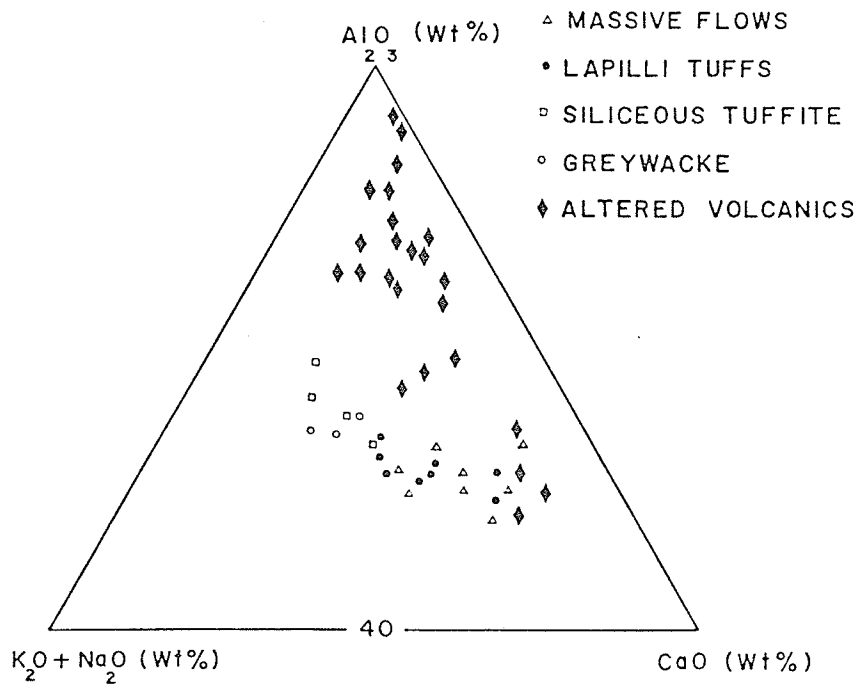


FIGURE 19 THE ALKALI IGNEOUS SPECTRUM DIAGRAM FOR THE DIXIE VOLCANIC ROCKS (HUGHES, 1972)

FIGURE 20 ALUMINA - ALKALI - LIME TERNARY PLOT OF THE DIXIE VOLCANICS

A plot of total alkalies versus silica content for the massive flows and lapilli tuffs from the Dixie 150 - 18 prospect (figure 21) illustrates their sub-alkalic nature (Irvine and Baragar, 1971). The massive flows show a trend towards increasing total alkali content with increasing silica.

The sub-alkalic field comprises tholeiitic and calc-alkaline suites. Four diagrams were employed to determine which suite the Dixie volcanic rocks belong to. The most significant chemical difference between the two suites is their alumina content which is shown by the $Al_2O_3$ - normative plagioclase diagram (figure 22). Most of the samples plot within the tholeiitic field and have normative plagioclase compositions between $An_{25}$ and $An_{50}$. The high alumina massive flows (150 - 18 - 4 - 126 and 150 - 18 - 7 - 56) plot separately within the calc-alkaline field.

The A F M variation diagram (figure 23) indicates that the massive flows and lapilli tuffs plot within the tholeiitic field although the high alumina flows plot within the calc-alkaline field. The massive flows and lapilli tuffs exhibit a well-defined elongate iron enrichment trend sub-parallel to the FeO total - MgO side of the diagram. An accompanying trend towards slight enrichment in total alkalies is also evident. The trend of evolution of the massive flows and lapilli tuffs closely corresponds to the trends of the Skaergaard liquids (Wager and Brown, 1968) the Hawaiian tholeiitic suite (MacDonald and Katsura, 1964)

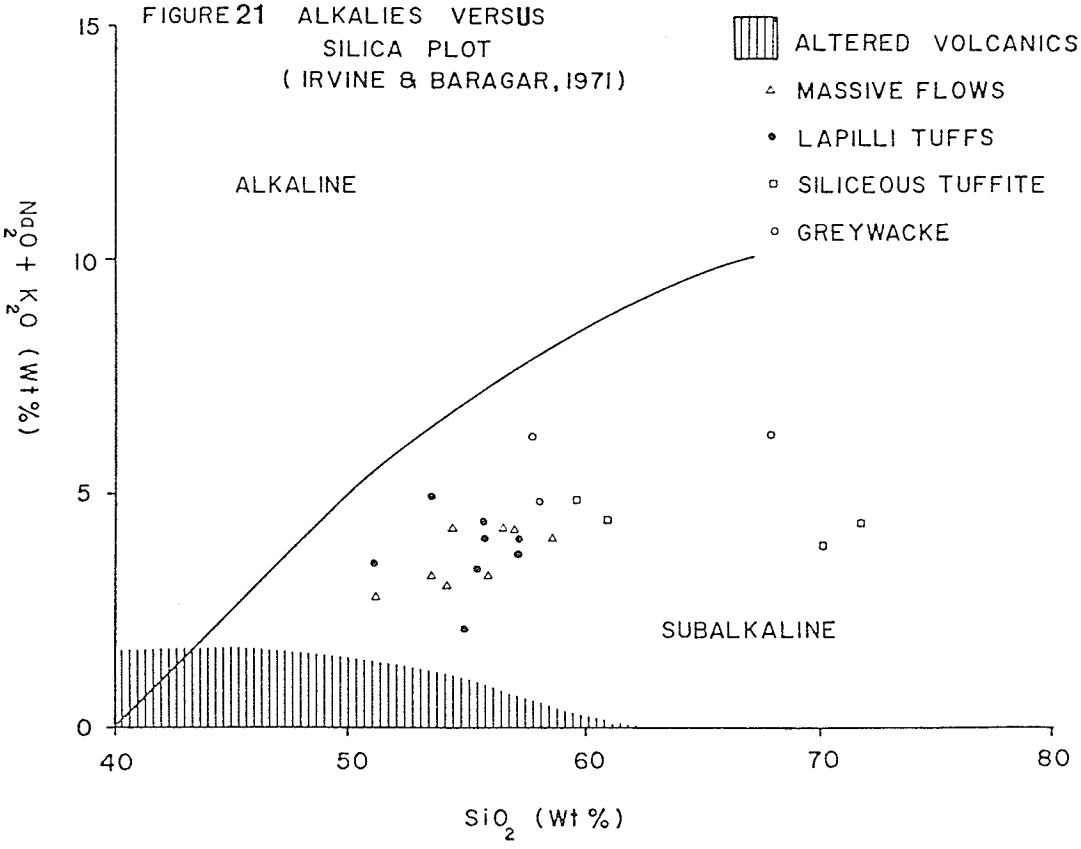


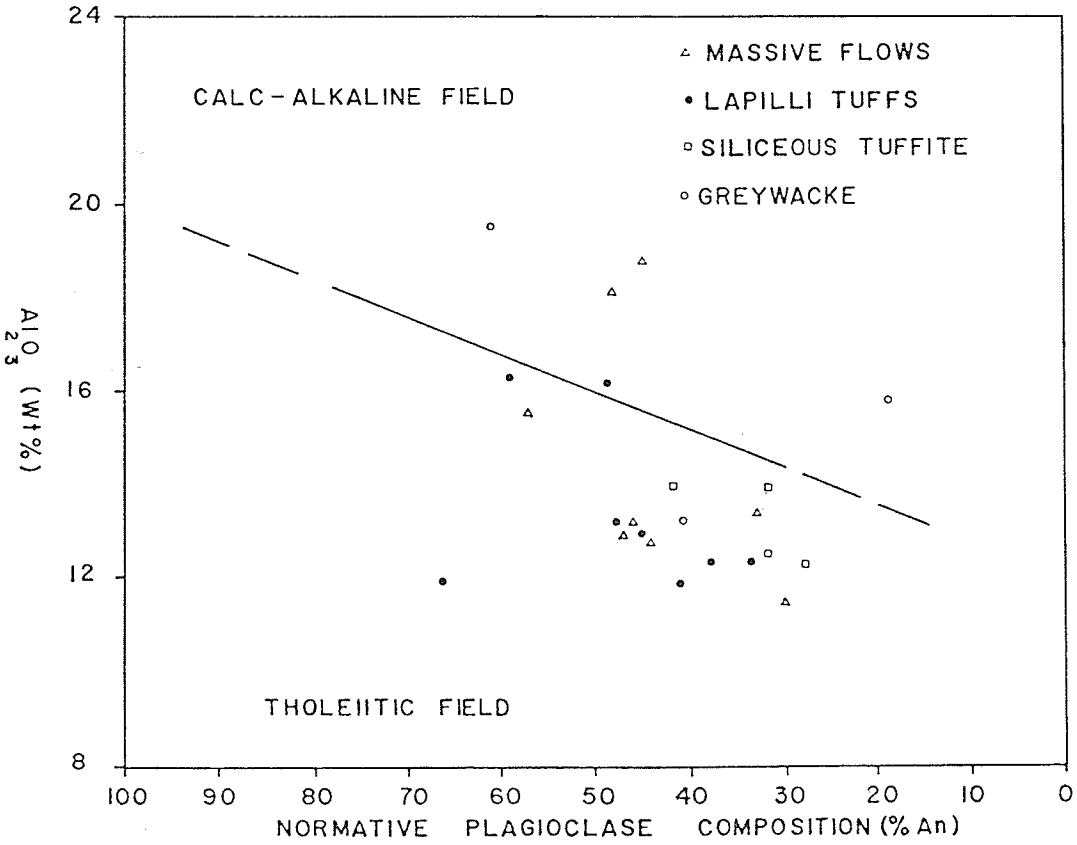


FIGURE 22 ALUMINA VERSUS NORM. PLAG. COMP. DIAGRAM (IRVINE & BARAGAR, 1971)

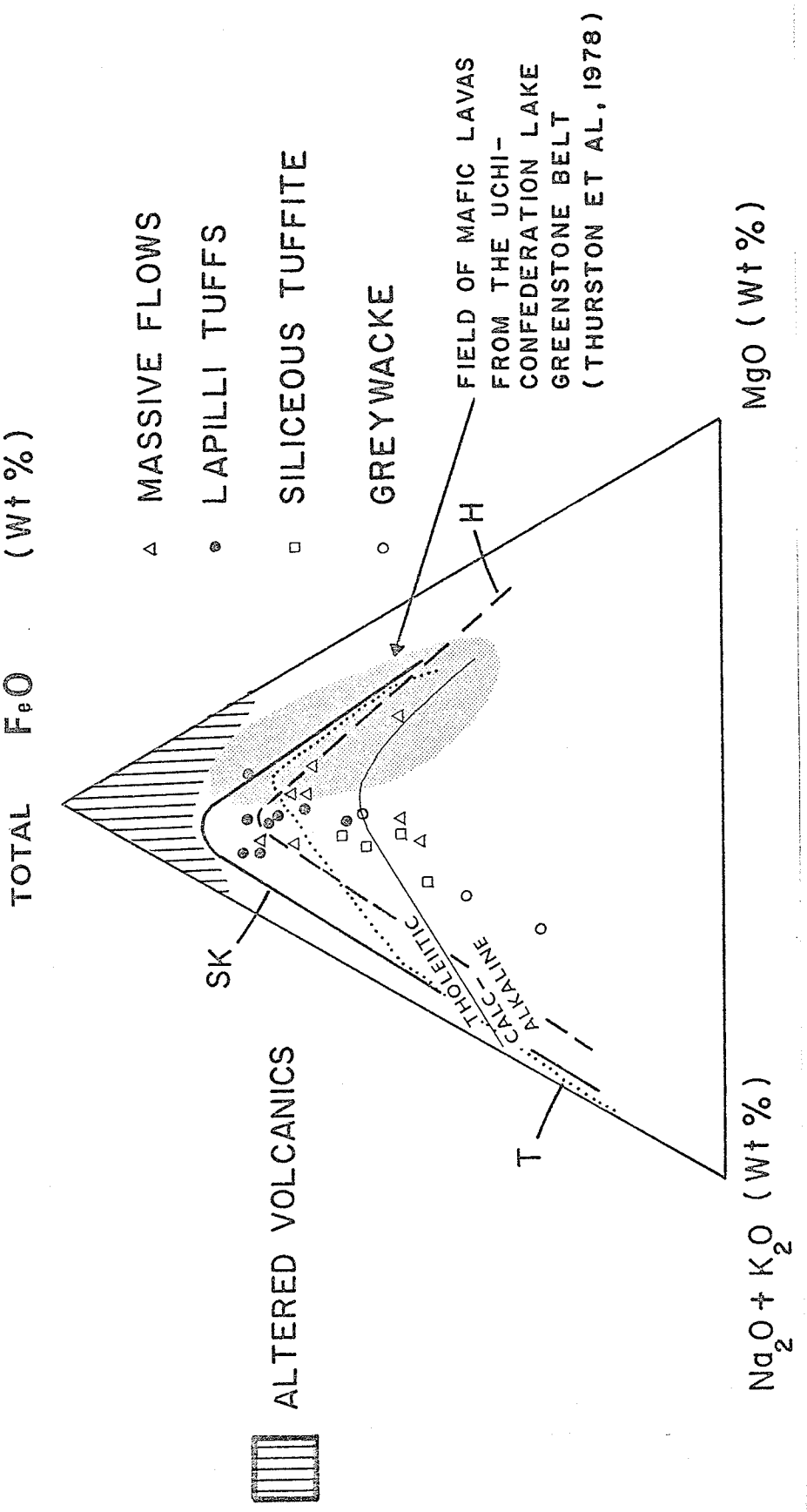


FIGURE 23 A F M DIAGRAM FOR THE DIXIE VOLCANIC AND SEDIMENTARY ROCKS
SKAERGAARD TREND (SK) FROM WAGER & BROWN (1968); HAWAIIAN THOLEIITIC
TREND (H) FROM MACDONALD & KATSURA (1964) AND THE THINGMULI TREND
(T) FROM CARMICHAEL (1964).

and the Thingmuli volcanic rocks in Iceland (Charmichael, 1964). In contrast, the shaded region represents 70 analyses of mafic volcanic rocks (basalts and andesites) from the Uchi - Confederation Lake greenstone belt (Thurston et al, 1978). The Uchi - Confederation Lake lavas exhibit a well-defined elongate iron enrichment trend sub-parallel to the FeO total - MgO side of the diagram but do not show an accompanying trend towards alkali enrichment that characterizes the Dixie 150 - 18 volcanic lavas.

The Jenson Cation Plot has been proposed as an alternative method for classifying sub-alkaline volcanic rocks (Jenson, 1976). The cation plot discriminates between differentiation trends of komatiitic, tholeiitic and calc-alkaline suites of volcanic rocks encompassing various rock types such as komatiitic basalt, magnesium and iron rich tholeiitic basalts, tholeiitic andesite to rhyolite and calc-alkaline basalt to rhyolite. The Jenson Cation Plot (figure 24) once again is compatible with the tholeiitic nature of the Dixie volcanic rocks and vaguely defines a tholeiitic trend of iron enrichment. Most flows and lapilli tuffs plot individually as high iron tholeiitic basalts and andesites. The high alumina massive flows plot separately within the calc-alkaline field as calc-alkaline andesites.

Miyashiro (1974) advocated the use of a silica versus total FeO/MgO diagram to classify the calc-alkaline and tholeiitic suites from island arcs. All of the Dixie 150 -

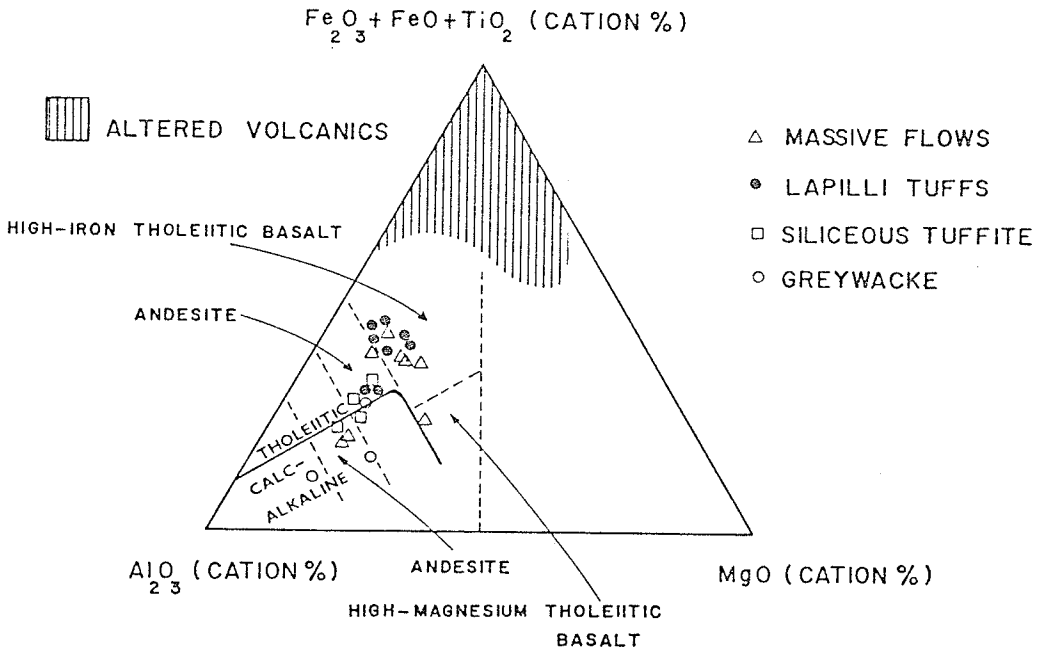


FIGURE 24 JENSEN (1976) CATION PLOT FOR THE DIXIE VOLCANIC ROCKS

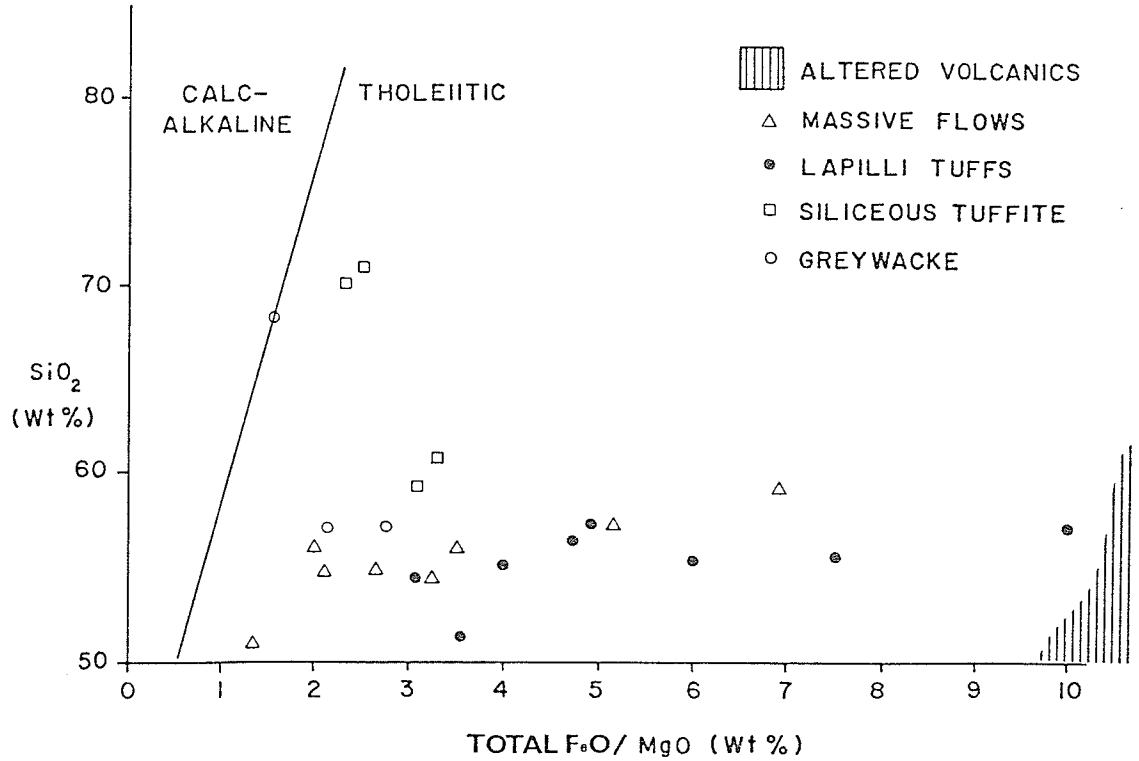


FIGURE 25 SILICA VERSUS TOTAL IRON / MAGNESIUM DIAGRAM (MIYASHIRO, 1974)

18 volcanic rocks lie well within the tholeiitic field and emphasize the high iron concentrations which characterize the massive flows and lapilli tuffs (figure 25).

Further subdivision of the unaltered volcanic rocks into "K - poor", "average" and "K - rich" rock types is possible on the An-Ab-Or diagram (figure 26) after Irvine and Baragar (1971). Most of the lapilli tuffs plot within the "average" rock field and show little variation in sodium or potassium. However, the massive flows cluster within the sodic field and around the K - poor andesite region. This feature was depicted earlier on the Hughes (1972) alkali diagram and again reflects higher concentrations of sodium and low concentrations of potassium within the massive flows when compared to the lapilli tuffs.

The final and perhaps most important classification of the sub-alkaline volcanic rocks involves the use of the normative colour index versus normative plagioclase composition which classifies all sub-alkaline basalts, andesites, dacites and rhyolites (Irvine and Baragar, 1971). The Dixie 150 - 18 volcanic rocks exhibit considerable scatter but plot individually as basalts and tholeiitic andesites (figure 27).

## DISCUSSION

Several of the variation diagrams illustrate some of the main chemical traits of the Dixie 150 - 18 volcanic rocks.

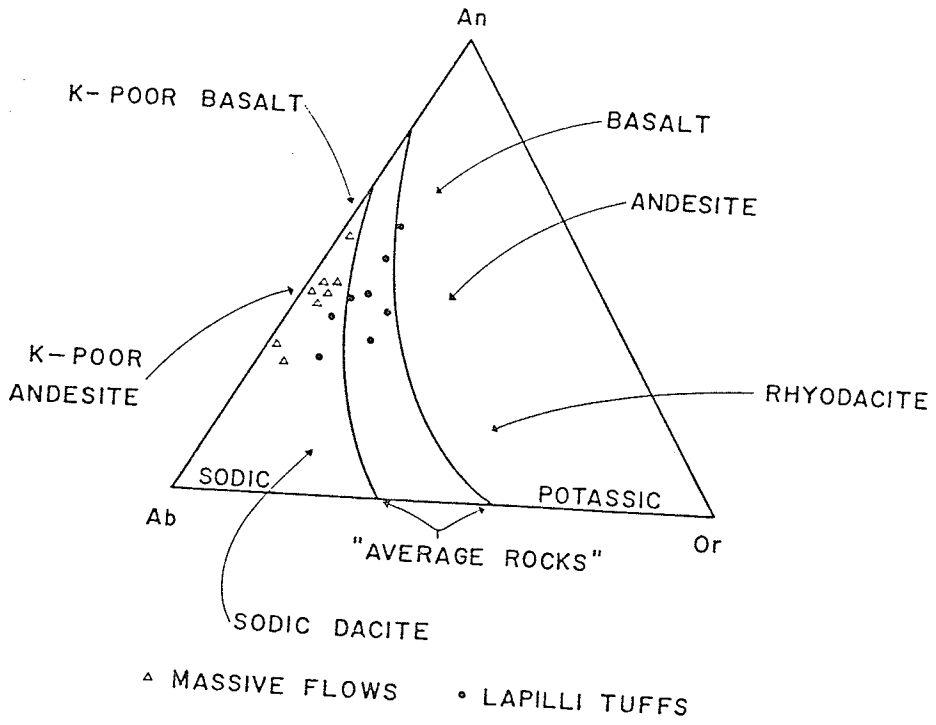


FIGURE 26 An-Ab-Or DIAGRAM FOR THE DIXIE 150-18 VOLCANIC ROCKS (IRVINE & BARAGAR, 1971)

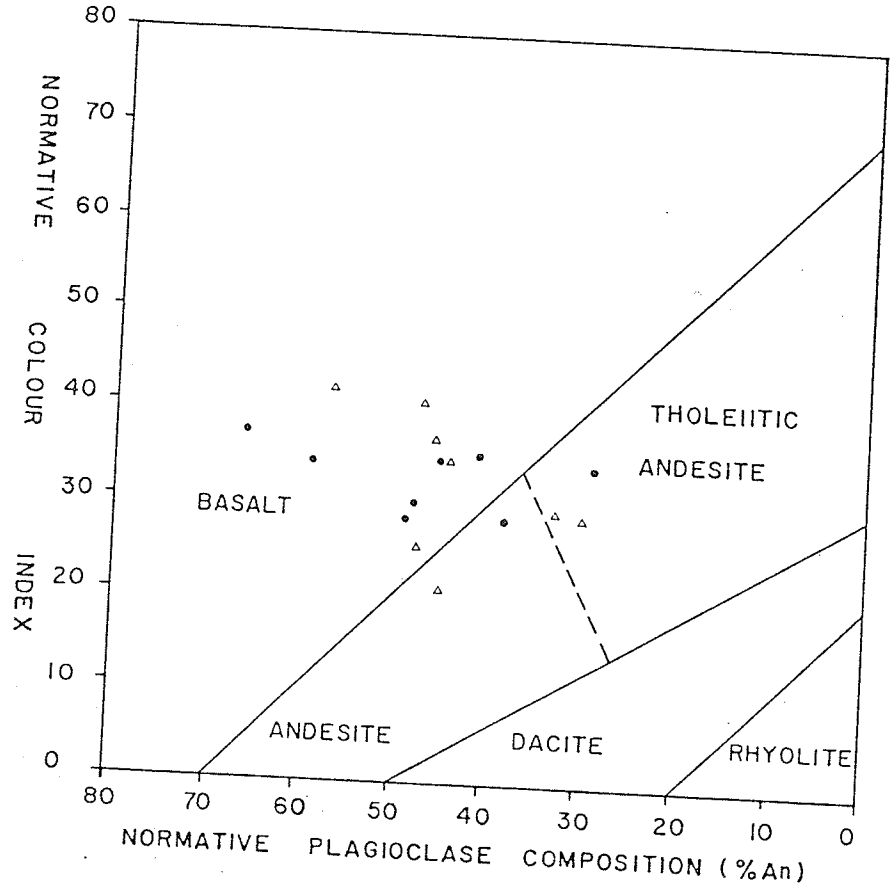


FIGURE 27 NORMATIVE COLOUR INDEX VERSUS NORMATIVE PLAGIOCLASE COMPOSITION DIAGRAM (IRVINE & BARAGAR 1971)

Although there are only a limited number of analyses, a few general observations may be made. The volcanic rocks are sub-alkalic in nature (figure 21) and plot within the tholeiitic field with the exception of two high alumina massive flows which plot in the calc-alkaline field (figures 22 to 25).

The massive flows are characterized by low $K_2O$ and high $Na_2O$ contents when compared to the lapilli tuffs. Both rock types exhibit an iron enrichment trend and an accompanying trend towards alkali enrichment (figures 23 to 25). The iron enrichment trend corresponds to the trends of the Skaergaard liquids, the Hawaiian tholeiitic trend and the Thingmuli volcanic rocks (figure 23). The massive flows and lapilli tuffs from the Dixie 150 - 18 sulphide prospect plot individually as high iron tholeiitic basalts with some tholeiitic and calc-alkaline andesites (figures 24, 26 and 27).

Chemical characteristics of the massive flows and lapilli tuffs are difficult to assess because of limited knowledge of the surrounding geology, insufficient outcrop and textural homogenizing effects of later metamorphism. Despite these difficulties, the chemistry and mineralogy may be indicative of primary features inherited within the volcanic rocks during formation or reflect an environment where several factors may have been important in contributing to the changes in cation composition between and within the flows and lapilli tuffs. Suggested primary features and

environmental factors attributing to the chemical characteristics or metasomatic changes within the volcanic rocks are as follows:

(1) Higher sodium concentrations accompanied by low potassium concentrations in the massive flows may have been derived by primary crystallization from magmatic solutions rich in sodium and low in potassium. Similarly, the iron enrichment trend observed for the Dixie 150 - 18 volcanic rocks may indicate a trend of evolution (primary fractionation) similar to the trends of the Skaergaard liquids, Hawaiian tholeiitic suite and the Thingmuli volcanic rocks in Iceland.

(2) Primary differentiation and the formation of cumulates within the magma in the volcanic edifice may explain sympathetic trends between certain elements in the massive flows (figures 17 and 18) and the occurrence of calc-alkaline high alumina massive flows.

(3) Assuming that the flows have been extruded within a marine environment, the inclusion of saline water within the flows offers a specific source of sodium to account for the characteristic compositional features.

(4) The alteration of the deposited tuffaceous debris by submarine reworking and weathering accompanied by addition of clastic sediments (ash) and chemical material (chert and carbonate) from the marine environment may have had a profound effect on the alkali variability within the tuffaceous units. Tuffaceous

rocks tend to be contaminated by the incorporation of mud or ash material and sea water from the marine environment. Thin section studies indicate that the tuffs are locally rich in mud and ash material. The incorporation of mud and ash material into these units can account for the higher potassium concentrations and marked variation characterizing the lapilli tuffs.

(5) The tuffaceous units are also characterized by high iron concentrations. The increased iron concentrations are mineralogically shown by large modal abundances of hornblende, actinolite and biotite comprising the fragments within these units and strongly suggests that iron enrichment has partially resulted from incorporation of those fragments into the lapilli tuffs.

(6) Metamorphic processes resulting in local migrations of trapped meteoric, connate or juvenile saline waters may have caused minor leaching and migration of alkalies in the more porous tuffaceous units.

## SILICEOUS TUFFITE

Four samples selected throughout the siliceous tuffite were collected for major element chemical analyses and presented on figures 16 and 19 to 25. The most distinctive chemical features of the unit are the low concentrations of iron and magnesium and the high concentrations of silica.

The tuffite may have developed during a quiescent period

of volcanism. Accumulation and compaction of volcanic detritus (ash and sediment) derived from weathering and erosion of surrounding volcanic and sedimentary sequences into a restricted basin or lagoon, may have lead to the formation of the siliceous tuffite. The high concentration of silica and potassium probably reflects a large contribution of detrital quartz, potassium feldspar and clay minerals incorporated into the tuffite during the quiescent period.

GREYWACKE

Three greywacke samples were collected for major element chemical analyses. The samples chosen are representative of the abundance and mineralogical type occurring within the sequences. The samples are presented on figures 16 and 19 to 25.

The greywackes and associated volcanic rocks have comparable compositions. The greywackes are slightly enriched in $Na_2O$, $K_2O$ and $Al_2O_3$. The most characteristic feature of greywackes is their excess $Na_2O$ (Pettijohn, 1975). Sample 150 - 18 - 11 - 55 does contain high concentrations of sodium. However, samples 150 - 18 - 1 - 166 and 150 - 18 - 5 - 200 are strongly enriched in potassium and slightly depleted in sodium - a feature not characteristic of greywackes. The excess potassium is reflected in the large modal abundance of potassium feldspar (table V). Sodium

content appears to be primarily associated with plagioclase feldspar which is near albite in composition (sample 150 - 18 - 5 - 200, figure 22).

The high sodium content may be related to the weathering and erosion of the sodium-enriched massive flows found in the vicinity of the greywacke sequences and possible albitization of plagioclase during diagenesis (Blatt et al, 1972). The high alumina content in comparison with the surrounding volcanic rocks may indicate a contribution of clay minerals now represented as numerous thin intercalated bands of biotite found throughout the sequences (table V).

Enrichment in potassium is more difficult to explain. The associated volcanic rocks have $K_2O$ and potassium feldspar concentrations several times lower than that for the greywacke sequences. It is unlikely that excess potassium feldspar could have been derived from the volcanic rocks. The granodiorite intrusions are the only rocks capable of supplying large concentrations of potassium upon weathering and erosion. However, the granodiorite intrusions within the area are stratigraphically younger than the volcanic and greywacke sequences. The possibility exists that the greywackes are arkosic but arkoses are generally restricted in time and environments not found within the study area.

The only explanations remaining to account for the high potassium feldspar concentrations are metamorphic potassium metasomatic processes or rapid deposition and incomplete weathering of the sediment with little or no post

depositional solution and removal of potassium feldspar taking place (Gluskoter, 1964). Finally, potassium can also be adsorbed on various clay minerals contained within the greywacke sequences. Original adsorption of potassium on clay minerals now represents potassium contained within biotite laths and may constitute a large percentage of the potassium concentration in the greywacke sequences.

Generally speaking, the major element chemical analyses do suggest that the greywackes were derived in part from the surrounding volcanic rocks.

## CHEMISTRY OF THE DIXIE 150 - 18 CORDIERITE - ANTHOPHYLLITE ALTERATION ZONE

The cordierite-anthophyllite alteration zone contains altered volcanic rocks that are chemically distinct from all other rock types. The range and average chemical composition for 24 samples throughout the alteration zone are given on figure 16. Figures 28 and 29 contrast the major oxide chemistry of the unaltered volcanic rocks with that of the altered cordierite-anthophyllite volcanic rocks to determine specific chemical changes which occurred as the result of superimposed hydrothermal alteration. Chemical distinctions between the altered cordierite-anthophyllite-bearing and unaltered volcanic rocks are also shown on figures 19 to 21 and 23 to 25.

A comparison of the total FeO / $TiO_2$, MgO / $TiO_2$, $Na_2O$ /

FIGURE 28 PLOT OF TOTAL IRON VERSUS SILICA

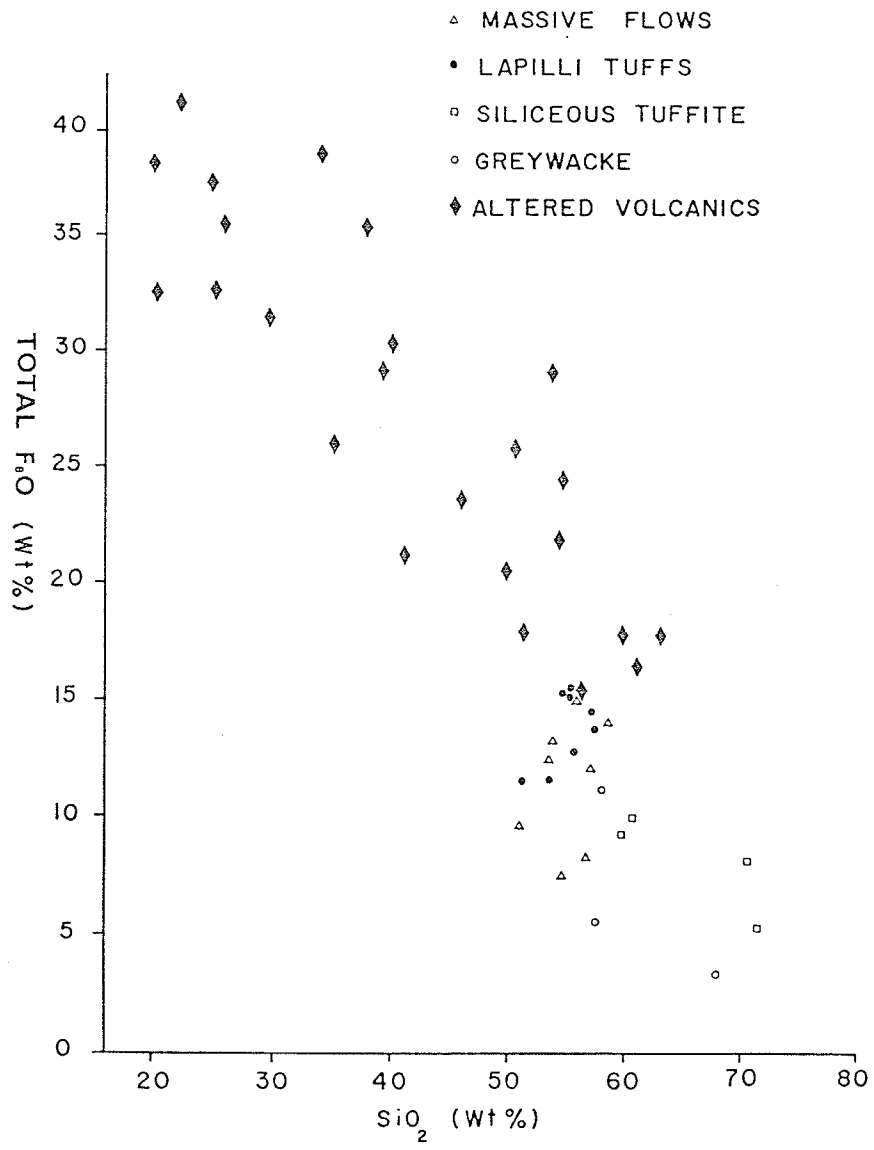

FIGURE 29 PLOT OF MAGNESIUM VERSUS SILICA FOR THE DIXIE VOLCANIC ROCKS

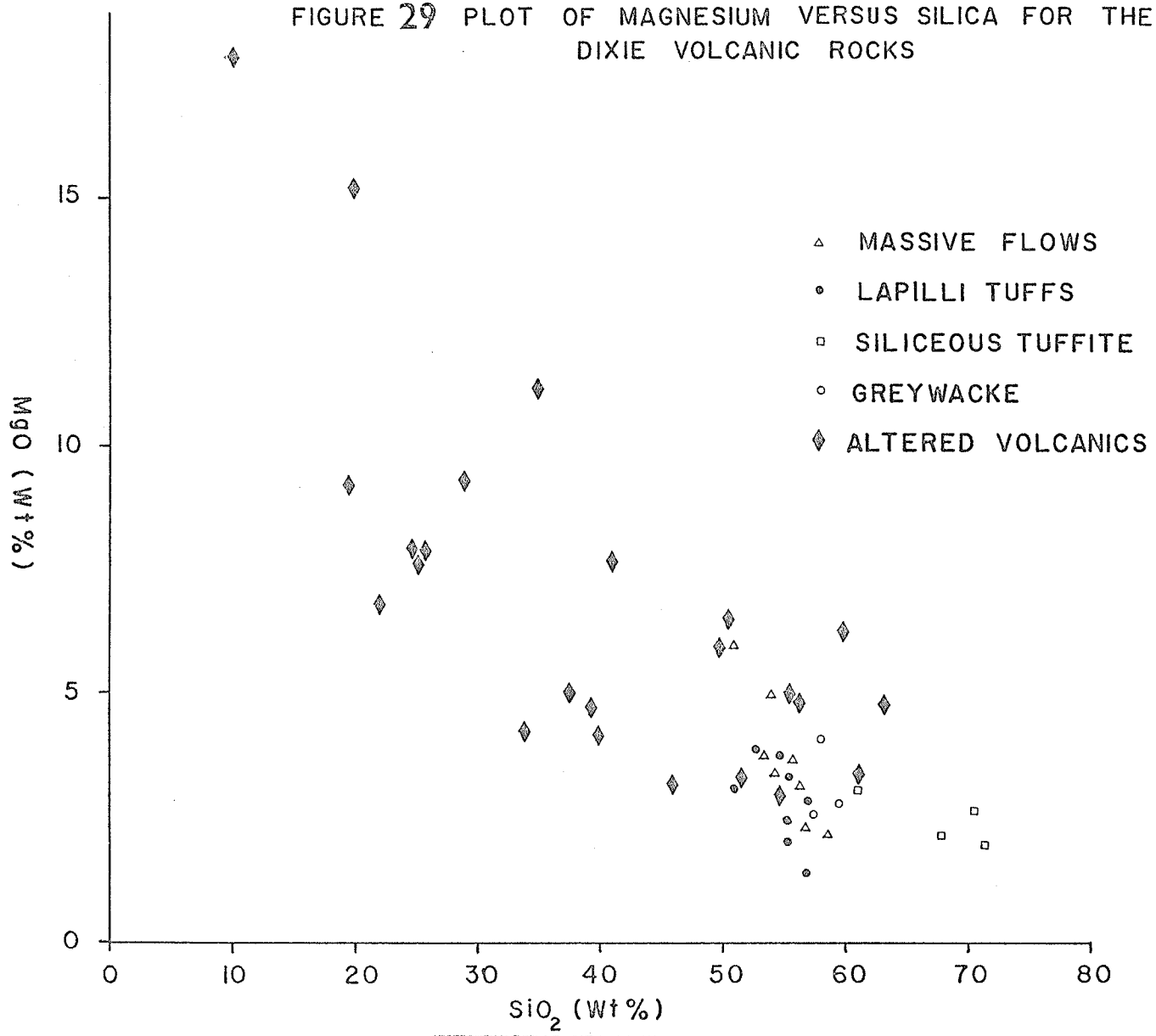

$TiO_2$, $K_2O$ / $TiO_2$ and CaO / $TiO_2$ ratios from the 24 cordierite-anthophyllite alteration samples and from 6 unaltered lapilli tuff samples located along stratigraphically equivalent horizons and above the alteration zone gives the following values:

| ALTERATION ZONE | UNALTERED LAPILLI TUFFS |
|---|---|
| FeO total / $TiO_2$ = 25.26 | FeO total / $TiO_2$ = 12.06 |
| MgO / $TiO_2$ = 5.74 | MgO / $TiO_2$ = 2.54 |
| $Na_2O$ / $TiO_2$ = 0.46 | $Na_2O$ / $TiO_2$ = 2.23 |
| $K_2O$ / $TiO_2$ = 0.32 | $K_2O$ / $TiO_2$ = 0.92 |
| CaO / $TiO_2$ = 2.05 | CaO / $TiO_2$ = 4.68 |

$TiO_2$ is used as a constant when comparing the ratios between the cations in the two rock types because titanium remains relatively constant and has similar ranges of values in both cordierite-anthophyllite altered rocks and unaltered lapilli tuffs (figure 16). Unaltered lapilli tuffs were selected for comparative purposes because the alteration zone is situated within former tuffaceous units.

Distinctive chemical changes have taken place throughout the alteration zone. These changes are as follows:

(1) A strong enrichment in iron, magnesium, sulphur and manganese (the ratios indicate a doubling of iron and magnesium).

(2) A depletion of alumina and silica.

(3) A strong depletion of lime and alkalies (the ratios

indicate substantial losses of calcium, sodium and potassium). (4) A moderate enrichment in water.

Nine cordierite - anthophyllite alteration samples chosen from drill hole 150 - 18 - 18 have been plotted at various distances throughout the entire alteration and mineralized zone (figure 30 and 31). The samples begin in the unaltered hanging wall tuffaceous unit and terminate within relatively unaltered volcanic rocks beneath the alteration zone. All major element oxides for each sample have been plotted along with the characteristic mineralogy from certain sections within the alteration and mineralized zones over a total distance of approximately 90 feet (28 m).

Distinct major element variations are illustrated on figures 30 and 31. Silica exhibits a decrease in concentration away from the unaltered hanging wall tuff throughout the chloritic and first zone of massive sulphides. Silica increases in concentration near the second zone of sulphide mineralization and continues to remain relatively constant throughout the remaining portion of the alteration zone. Alumina reflects a similar trend but exhibits a consistent depletion near both zones of mineralization.

Iron and sulphur exhibit very similar chemical variations throughout the alteration and mineralized zones. Both elements show large increases in concentration corresponding to the zones of massive sulphide deposition with depletion elsewhere. Magnesium concentrations are somewhat similar to the iron and sulphur trends with the highest concentrations superimposed

# CHEMICAL VARIATION THROUGHOUT THE ALTERATION ZONE IN DRILL HOLE 150-18-18

FIGURE 30

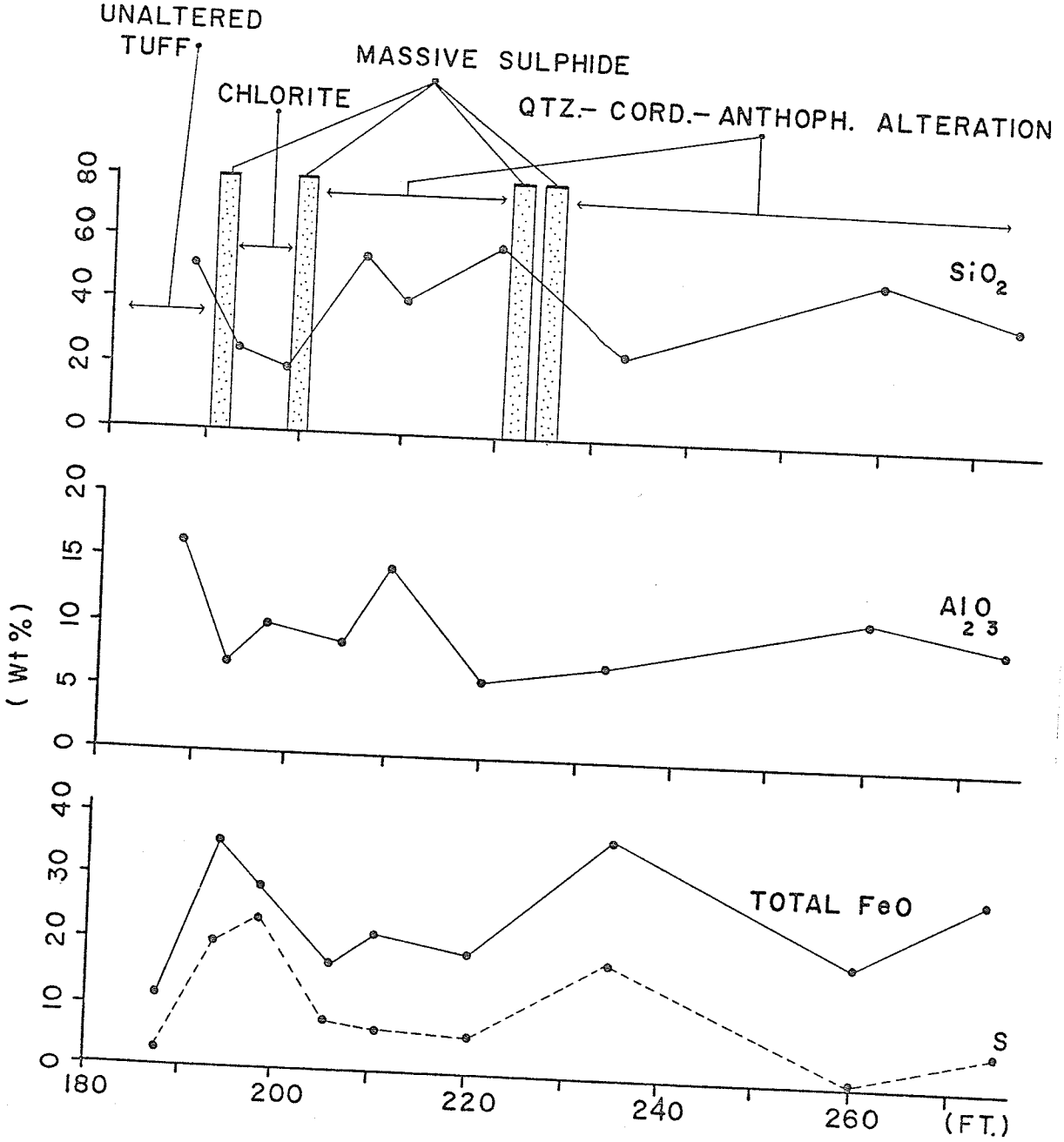

# CHEMICAL VARIATION THROUGHOUT THE ALTERATION ZONE IN DRILL HOLE 150-18-18

FIGURE 31

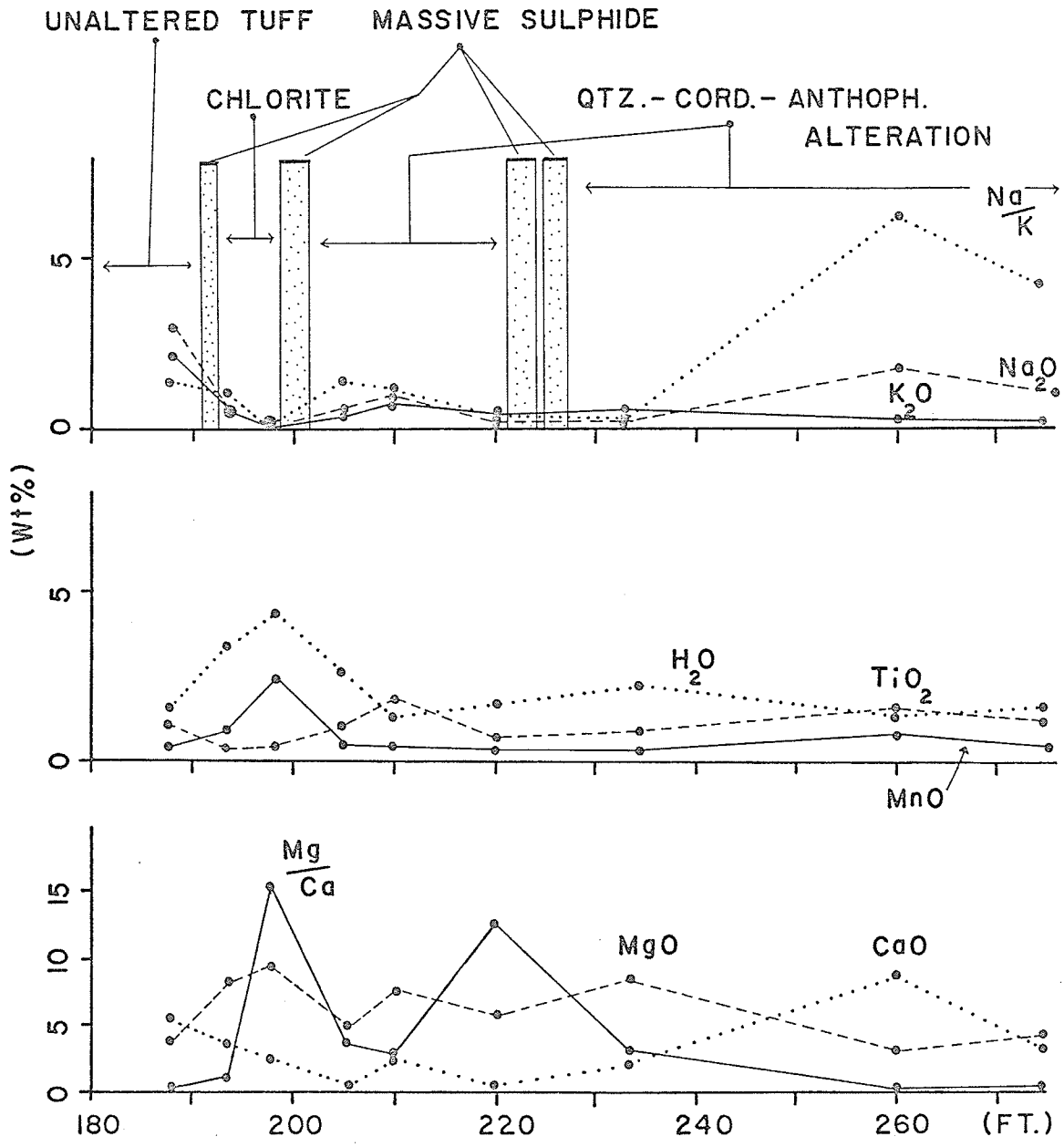

upon mineralization and an overall enrichment throughout the entire alteration zone.

Conversely, calcium exhibits considerable depletion throughout the alteration zone particularly near the zones of sulphide mineralization. Concentrations increase outwards towards less altered volcanic rocks beneath the alteration zone. Magnesium and calcium concentrations also show a strong inverse relationship.

The alkalies show identical trends of considerable depletion away from the unaltered hanging wall tuff towards the zones of sulphide mineralization with gradual enrichment towards less altered volcanic rocks beneath the alteration zone. Manganese and water concentrations exhibit strong enrichment near the first zone of sulphide deposition immediately adjacent to the hanging wall with little variation elsewhere. Titanium appears to have been only slightly depleted near the first zone of sulphide deposition.

## DISCUSSION

From sequential relationships noted from polished sections, megascopic drill core investigations, thin section studies and bulk chemical analyses, the chemical variations observed are directly related to various alteration processes occurring throughout the cordierite - anthophyllite alteration zone. Many of these chemical variations

and alteration processes are reflected in the mineralogy and bulk chemistry.

The increase in iron is mainly attributed to abundant disseminated pyrite, pyrrhotite and chalcopyrite occurring throughout the alteration zone coupled with iron combined in high iron modal minerals such as chlorite, anthophyllite, biotite and minor actinolite. The high $Fe_2O_3$ content is due in part to the presence of the relatively high concentrations of disseminated iron sulphides.

High concentrations of iron within the chlorite zone (figure 30) and very high iron and modal concentrations of chlorite in sample 150 - 18 - 17 - 408 (table A5 appendix and table VI) suggest that the chlorite within the alteration zone is relatively rich in iron. Zones of intense chloritization are commonly associated with massive sulphide deposition. Although retrograde metamorphic production of chlorite is a common feature throughout the alteration assemblages, localized concentrations of massive chlorite immediately adjacent to sulphide deposition strongly suggests that chloritization is locally a major alteration phenomenon associated with the ore-forming processes.

Magnesium enrichment is shown by high modal abundances of anthophyllite, cordierite and possibly chlorite. Similarly, sulphur enrichment is clearly related to the presence of iron, copper and zinc sulphides disseminated throughout the alteration zone. Large concentrations of iron, magnesium and sulphur are associated with sulphide

mineralization and indicate that all three elements were major ore-forming constituents during the phases of mineralization.

Periodic influx of silica is a common feature observed throughout the alteration zone. In some zones, silica is intimately associated with sulphide deposition whereas in others it is completely devoid of any involvement with the mineralizing processes. Silica has been removed from certain sections, remobilized and reconcentrated into others. The inverse relationship between silica and the iron and magnesium concentrations (figures 30 and 31) could be a result of the addition of iron-and magnesium-rich sulphide and silicate minerals such as pyrite, pyrrhotite, chalcopyrite, chlorite, anthophyllite and cordierite during mineralization with coincident removal of silica. Silicification is generally sporadic but is locally related to mineralizing processes throughout certain sections in the alteration zone.

Very low concentrations of sodium, calcium and potassium are reflected in the absence of potassium feldspar, hornblende, calcite and low modal concentrations of plagioclase and actinolite throughout the alteration zone. The strong depletion or leaching of lime and alkalies particularly near the zones of sulphide deposition could have resulted from base exchange of cation reactions involving mineral hydrolysis (hydrogen metasomatism) in the presence of water during the ore-forming processes (Meyer and Hemley, 1967).

Manganese and water enrichment are clearly related to sulphide deposition and are probably derived from mineralizing solutions rich in water and manganese. Manganese enrichment is closely associated with the development of spessartite (sample 150 - 18 - 17 - 393, table A5 appendix and table VI) near the zones of sulphide deposition. Small quantities of manganese may have also been incorporated into the mineralogical structures of chlorite and biotite as manganese commonly substitutes for other cations in the crystal lattices. The moderate enrichment in water may coincide with the development of cordierite, which usually incorporates significant concentrations of water into its mineralogical structure (Lepezin, 1969) and other hydrous minerals such as anthophyllite and biotite.

The progressive increase in $SiO_2$, $Al_2O_3$, CaO, $Na_2O$ and $K_2O$ away from the sulphide mineralization and outwards into relatively unaltered equivalent tuffaceous rocks below the alteration zone reflects the decreasing alteration intensity of the rocks. The most intensely altered volcanic rocks lie within the zones of sulphide mineralization and suggest that the various alteration processes (silicification, hydrolysis, chloritization and biotitization) were more active within the mineralized zones.

# CHAPTER 9

## ORIGIN AND FORMATION OF THE CORDIERITE - ANTHOPHYLLITE ASSEMBLAGES

The Dixie 150 - 18 alteration zone is characterized by cordierite - anthophyllite mineral assemblages. The assemblage is characteristically formed at shallow depths either near or within contact aureoles, middle grades of regional metamorphism or abnormally shallow low pressure regional metamorphism of the Abukuma type (Winkler, 1967). The temperature of metamorphism for these terraines can range from 500 to 800°C but the pressure seldom exceeds 4 to 7 kbars and a rather low 3 to 5 kbars for the Abukuma type metamorphism (Winkler, 1967).

Cordierite - anthophyllite rocks are not widely known hosts for base metal sulphide deposits although well known occurrences have been described from the Rouyn - Noranda district (De Rosen - Spence, 1969), the Coronation Mine in Saskatchewan (Froese, 1969), the Blue Hill district in Maine (Emmons, 1909), the Falum Deposit of central Sweden (Magnusson, 1960), the Orijarvi area in Finland (Eskola, 1914) and the base metal deposits from the Notre Dame Bay area of Newfoundland (Upadhyay and Smitheringale, 1972 and Bachinski, 1976). Numerous concepts concerning the origin and formation of the cordierite - anthophyllite assemblages with base metal deposits have been proposed for these areas. Eskola's classical study in the Orijarvi area in 1914 demonstrated that the composition of the rocks did not corres-

pond to that of any sedimentary or igneous rock and for this reason, their origin was attributed to contact metasomatism involving an increase in iron and magnesium with depletion in calcium and alkalies.

De Rosen - Spence (1969) proposed that the Rouyn - Noranda area deposits obtained their present mineral assemblages through contact metamorphism of pre-existing volcanogenic sulphides in chloritic alteration zones. Froese (1969) demonstrated that the cordierite - anthophyllite rocks from the Coronation Mine represent original zones of chloritization developed at the time of mineralization rather than products of high temperature metasomatism. Bachinski (1976) considered the cordierite - anthophyllite alteration assemblages as isochemical, thermally metamorphosed equivalents of ophiolitic cuperiferous iron sulphide ores and wall rock alterations in the chloritic zones. He found that extraction of iron from the silicate fraction would be required to account for most of the cordierite - anthophyllite assemblages and all of the cordierite - biotite assemblages at Gull Pond, Newfoundland. In contrast, Vallance (1967) suggested that deuteric or subaqueous diagenetic processes might alter basaltic host rocks to compositions suitable for the development of cordierite - anthophyllite rocks.

The most appropriate concept of the origin and formation of the cordierite - anthophyllite assemblages at the Dixie 150 - 18 prospect is an agglomeration of ideas put forth by

De Rosen - Spence (1969), Froese (1969), Upadhyay and Smitheringale (1972), Bachinski (1976), Gilmour (1965) and Whitmore (1969). All of the authors suggest that the rocks acquired their pre-metamorphic mineralogy through the action of hydrothermal fluids enriched in iron and magnesium of volcanogenic origin acting during the mineralizing period. The origin best explains the observed spatial relationship in the field between the cordierite - anthophyllite rocks, unaltered volcanic rocks and the sulphide mineralization.

The cordierite - anthophyllite assemblages of the Dixie 150 - 18 prospect probably acquired their pre-metamorphic mineralogy from the addition of iron and magnesium from hydrothermal fluids of volcanogenic origin coupled with depletion of calcium, sodium and potassium during the mineralizing period. The comparison of FeO total, MgO, $K_2O$, CaO and $Na_2O$ / $TiO_2$ ratios between the stratigraphically equivalent unaltered and altered tuffaceous units demonstrates that enrichment in iron and magnesium accompanied by calcium, sodium and potassium depletion has taken place during the mineralizing processes. This relative enrichment in iron and magnesium and depletion in lime and alkalies was sufficient so that cordierite - anthophyllite assemblages developed within the original chloritic alteration zones during appropriate metamorphic conditions (high temperature and low to moderate pressures). This conclusion is substantiated by the absence of cordierite and anthophyllite in any of the surrounding unaltered volcanic rocks

which possess much lower concentrations of iron and magnesium and have undergone similar grades or conditions of metamorphism.

The metamorphic regime suggested for the isochemical transformation of pre-existing chloritic assemblages into cordierite - anthophyllite assemblages is normal middle grade regional metamorphism (500 to 800°C temperature range and 4 to 7 kbars pressure range). Large igneous intrusions or indication of any igneous intrusive contact aureoles do not occur within the vicinity of the Dixie 150 - 18 sulphide body which could explain the development of the cordierite - anthophyllite assemblages by high temperature contact metamorphic processes. Furthermore, the characteristic andalusite mineral assemblages belonging to very low pressure regional metamorphism of the Abukuma type are absent in the surrounding volcanic rocks and alteration zone.

# CHAPTER 10

# GENETIC ASPECTS AND GEOLOGICAL HISTORY OF THE DIXIE 150 - 18 SULPHIDE PROSPECT

## GENETIC ASPECTS OF THE DIXIE 150 - 18 SULPHIDE PROSPECT

The relative lack of structural deformation and intrusive activity within the area allows a detailed interpretation of ore genesis and geological history of the Dixie 150 - 18 sulphide prospect.

The following significant regional observations have been considered in the interpretation, and all suggest a gross similarity with Archean sulphide deposits in volcanogenic environments.

(1) The common occurrence of several sulphide lenses similar to the Dixie prospect within volcanic rocks of the southwestern extension of the Uchi - Confederation Lake greenstone belt (figure 2) suggests that the occurrences are related to volcanism or at least the same magmatic event responsible for the formation of the volcanic rocks.

(2) Many of these sulphide occurrences (figure 2) are contained within identical sequences of dominantly mafic volcanic rocks (as described for the Dixie prospect) suggesting a stratigraphic control on sulphide deposition.

Similarly, features from the Dixie sulphide body and enclosing stratigraphy also suggest genetic relationships

with Archean sulphide deposits in volcanogenic environments. These features include:

(1) The stratabound sheet-like nature of the sulphide body enclosed within conformable volcanic units.

(2) The sharp relatively unaltered contacts between the sulphide mineralization and hanging wall siliceous tuffite.

(3) The location of the siliceous tuffite unit immediately above the sulphide mineralization and nowhere else within the volcanic stratigraphy.

(4) The presence of tuffaceous units within, overlying and underlying the sulphide mineralization.

(5) The presence of an extensive alteration zone along the footwall which thickens and resembles an alteration pipe beneath the centre of the sulphide body.

(6) Zoning within the sulphide body, although somewhat vague, copper-rich sulphide assemblages do coincide with the approximate location of the alteration pipe indicating the general vicinity of the discharge source of the hydrothermal solutions.

(7) The occurrence of an identical, smaller sulphide body located along strike and at the same stratigraphic horizon as the larger sulphide body.

(8) The chemical changes within the alteration zone, most noticeably iron and magnesium enrichment with calcium, sodium and potassium depletion are identical to that described for numerous Archean sulphide deposits in

volcanogenic environments.

Based upon regional observations and local features pertaining to the sulphide body and enclosing volcanic rocks, the Dixie 150 - 18 sulphide occurrence resembles Archean sulphide occurrences and deposits within volcanogenic environments. However, one major contrasting feature between the Dixie 150 - 18 prospect and most other Archean sulphide deposits is the occurrence of mineralization contained specifically within mafic volcanic rocks such as basalts and andesites. Felsic or rhyolitic volcanic sequences which are almost invariably associated with other Archean sulphide deposits are totally absent within the immediate vicinity of the Dixie 150 - 18 sulphide mineralization.

The occurrence of sulphide mineralization in mafic volcanic sequences as described for the Dixie prospect is rare and unusual. Such occurrences may represent a new environment of sulphide deposition that warrants considerable attention during further exploration activities within the southwestern extension of the Uchi - Confederation Lake greenstone belt and perhaps other greenstone belts.

## GEOLOGICAL SETTING AND HISTORY OF THE DIXIE 150 - 18 SULPHIDE BODY

The interpretation of the geological history and setting of the Dixie sulphide body is based upon the stratigraphic

correlation of the enclosing volcanic units, regional geological correlation from reconnaissance drill holes, chemical considerations and sulphide and metal relationships from the mineralized zones described in previous chapters. The interpretation will undoubtedly need some modifications as future investigations within this region of the Uchi subprovince should provide further amd perhaps more important evidence concerning the localization and genesis of the sulphide mineralization in the proposed models.

Two models of sulphide deposition and localization within a volcanogenic environment are proposed for the Dixie 150 - 18 sulphide occurrences. The first model involves syngenetic (solfataric) deposition of sulphide mineralization contemporaneously with the enclosing volcanic sequences, and the second model involves epigenetic (stratigraphic trapping) emplacement of sulphide mineralization following formation of the volcanic pile.

## SYNGENETIC MODEL

After the close of the major volcanic events responsible for the deposition of andesitic lapilli tuffs with minor intercalated massive andesitic flows (figure 32A) a thin but extensive layer of massive and disseminated iron, zinc and copper sulphides was deposited on an undulating surface. The mechanisms of sulphide deposition were probably similar to

# INTERPRETATION OF GEOLOGICAL HISTORY

## EAST - WEST VERTICAL SECTION
## SYNGENETIC MODEL

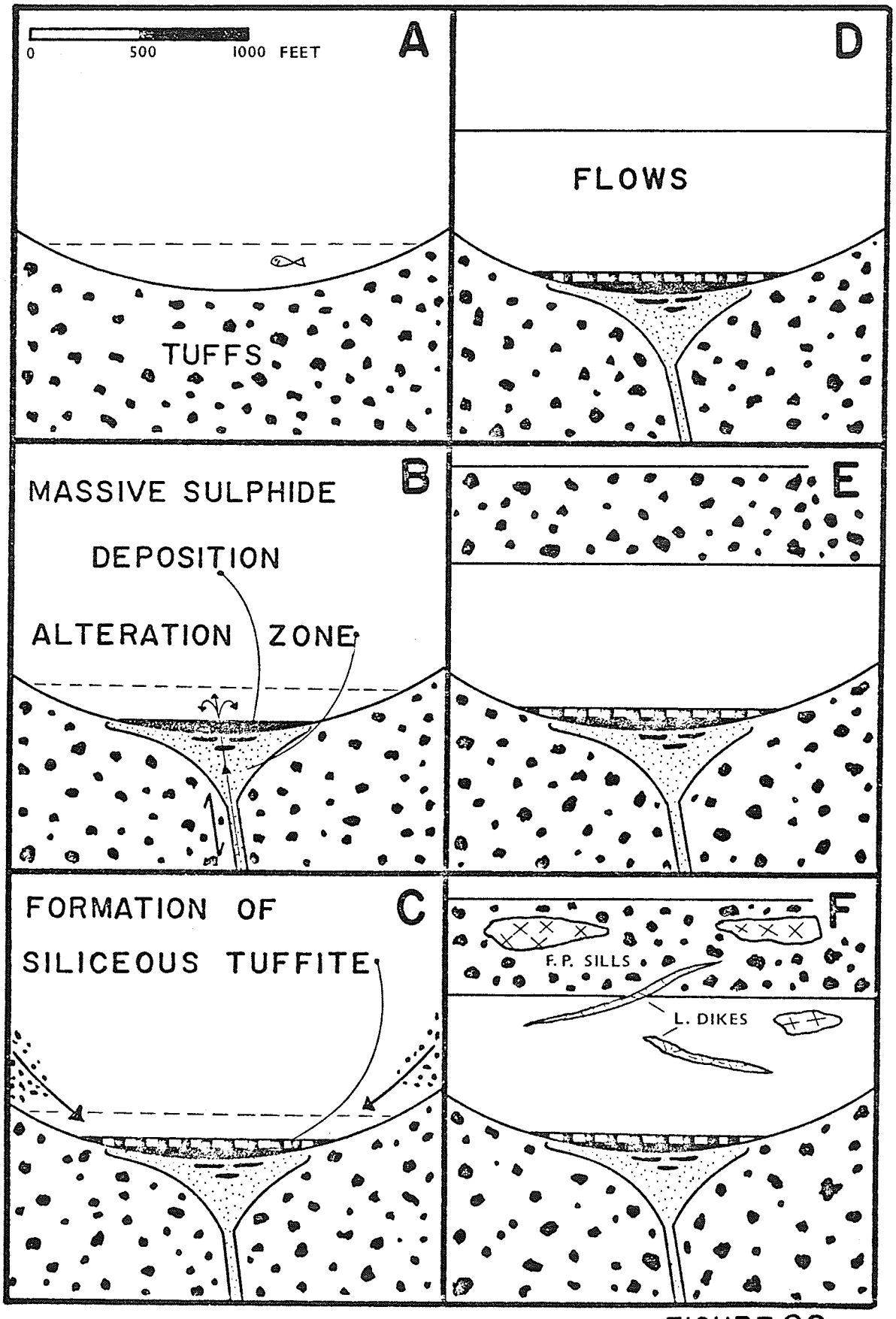


FIGURE 32

present day solfataric (hot spring) activity. The metal-bearing hydrothermal solutions approached the surface through a small structural fissure or fracture system located beneath the central portion of the sulphide body and precipitated within a small subaqueous basin or lagoon located along the flanks of a major volcanic complex (figure 32B). The hydrothermal solutions were enriched in iron, sulphur, magnesium, zinc, copper, silver, manganese and water. High concentrations of copper within the sulphide body indicate the location of the discharge source where the hydrothermal solutions entered the shallow basin or lagoon. The pipe-like cordierite - anthophyllite alteration zones represent the channelways for the ascending ore solutions and the conformable fan-like expression of the alteration zone along the flanks of the sulphide body represents outward percolation of the solutions throughout the porous tuffaceous units near the surface.

Following sulphide deposition, a period of quiescence with resultant subaerial and subaqueous weathering and erosion of topographically higher tuffaceous and volcaniclastic units into the shallow basin or lagoon culminated in the restricted development of the siliceous tuffite immediately above the massive and disseminated sulphides (figure 32C). Renewed mafic volcanism proceeded with the extrusion of dominantly massive and porphyritic andesitic flows (figure 32D) followed by a tuffaceous episode with minor intercalated andesitic flows (figure 32E) over the

entire sulphide body. The deepest location within the basin or lagoon is situated over the central portion of the sulphide body where the thickest and best-developed section of the siliceous tuffite and subsequent greatest accumulations of massive and porphyritic andesitic flows occur.

Subsequent intrusive activity resulted in the emplacement of several small feldspar porphyry sills and lamprophyric dikes (figure 32F).

## EPIGENETIC MODEL

Ore-bearing hydrothermal solutions can be deflected or impeded by slate, shale, clay, siltstone, or other relatively impervious rocks. At the Bushy Creek Mine, Fletcher Mine and Ozark Lead Company Mine within the Viburnum trend, southeast Missouri and in many of the fluorite mines within the Cave in Rock district, Illinois, mudstone, dense dolomite, siltstone and fine grained sandstone act as impervious barriers to ascending mineralizing solutions and have ponded ore solutions at and below their contacts forming major ore bodies (Evans, 1977; Paarlberg and Evans, 1977; Mouat and Clendenin, 1977 and Grogan and Bradbury, 1967). In the Quartz Hill district near Divide, Montana, silver ores occur in short shoots or pipes in fissures in crystalline limestone and as bedded replacement deposits at the contact between the limestone and an overlying

calcareous shale (Taylor, 1942). Where the ore fissures intersect the limestone-shale contact at right angles to the strike of the beds, the ore solutions tend to "mushroom" and follow the intersection of the contact by replacement of the limestone for variable distances on either side of the fissures. With minor exceptions, the ore does not penetrate the calcareous shale contact (Taylor, 1942).

A similar process may have concentrated ascending hydrothermal ore solutions at the Dixie 150 - 18 prospect. The siliceous tuffite is a dense, argillaceous, fine-grained unit and possesses the physical characteristics of a natural, nonporous impermeable barrier. The Dixie 150 - 18 sulphide horizon is contained immediately below the siliceous tuffite and the contact between the mineralization and the unaltered tuffite is sharp. The sulphide mineralization does not penetrate the tuffite contact.

Following the deposition of the siliceous tuffite and overlying volcanic units, metal-bearing hydrothermal solutions may have approached the impervious tuffite through small structural fissures which dissipated within the impermeable unit. The ascending ore solutions were blocked by the impervious tuffite, ponded and began spreading along the impermeable contact and other surfaces of discontinuity to search out various routes or minor channelways through or around the barrier. The greater permeability and pronounced schistosity in the underlying tuffaceous sequences

with a large feldspar porphyry sill.

The dikes are dark gray-green and fine-grained with distinct medium-grained biotite porphyroblasts or concentrations. Biotite is the dominant mafic mineral and occurs throughout the matrix and also as large porphyroblasts. Hornblende and actinolite also occur in the matrix but rarely form porphyroblastic aggregates. Minor concentrations of quartz, plagioclase, carbonate, magnetite and zircon are present. The dikes are highly metamorphosed and intrusive contacts are sharp with well-defined chilled margins.

# CHAPTER 4

## MINERALOGICAL CLASSIFICATION OF THE VOLCANIC ROCKS

The lapilli tuffs, massive flows and porphyritic flows were classified according to their mineral compositions previously shown in tables I, II and IV. Sixteen specimens were classified according to Streckeisen (1967) in the Q A P triangle where Q, A and P represent total quartz, alkali feldspar and plagioclase within the rock. The modal analyses are based upon 1000 point counts throughout a thin section representative of that specific volcanic rock. Five of the sixteen calculations were from the lapilli tuff sequences, six from the massive flows and five from the porphyritic flow sequences directly above and along strike of the Dixie 150 - 18 sulphide body.

The tuffs and flows have similar mineralogical compositions and plot essentially as andesites and basalts with a few specimens of quartz andesite. The plots also correspond to the tholeiitic basalt and andesite fields (figure 7).

## GRADE OF METAMORPHISM

The mafic metavolcanic rocks are characterized by two distinct mineralogical assemblages. The first assemblage comprises colourless to pale green actinolite and hornblende - Ca plagioclase ± chlorite and epidote. The second and more diagnostic mineral assemblage comprises dark green

# CHAPTER 11

# THE DIXIE 150 - 17B and 150 - 19 SULPHIDE PROSPECTS

## THE DIXIE 150 - 19 PROSPECT

The Dixie 150 - 19 grid is located approximately 2.4 km southeast of the Dixie 150 - 18 sulphide body. The horizontal loop electromagnetic survey over this grid outlined a continuous conductor on lines 8E, 12E and 16E (figure 34). Three diamond drill holes have tested the anomaly intersecting scattered low and high grade sections of base metal mineralization.

Drill hole 150 - 19 - 1 on line 8E intersected 0.37% copper, 3.04% zinc and 0.38 ounces of silver per ton along 2 m and drill hole 150 - 19 - 2 on line 12 E intersected 12% copper, 5.16% zinc and 4.25 ounces of silver per ton along 0.6 m. Drill hole 150 - 19 - 3 was drilled on line 16E to test the extension of the zone. This hole intersected a series of narrow but zinc-rich massive veins along a core length of 5.6 m averaging 0.17% copper, 4.75% zinc and 0.05 ounces of silver per ton (figures 35 and 36).

The metavolcanic units enclosing the Dixie 150 - 19 prospect are markedly different from those surrounding the 150 - 18 prospect. A large granodiorite intrusion which lies immediately south of the conductor has completely granitized the metavolcanic sequences into fractured, sheared and highly altered schistose rock units. The metavolcanic rocks consist of a strongly recrystallized assemblage con-

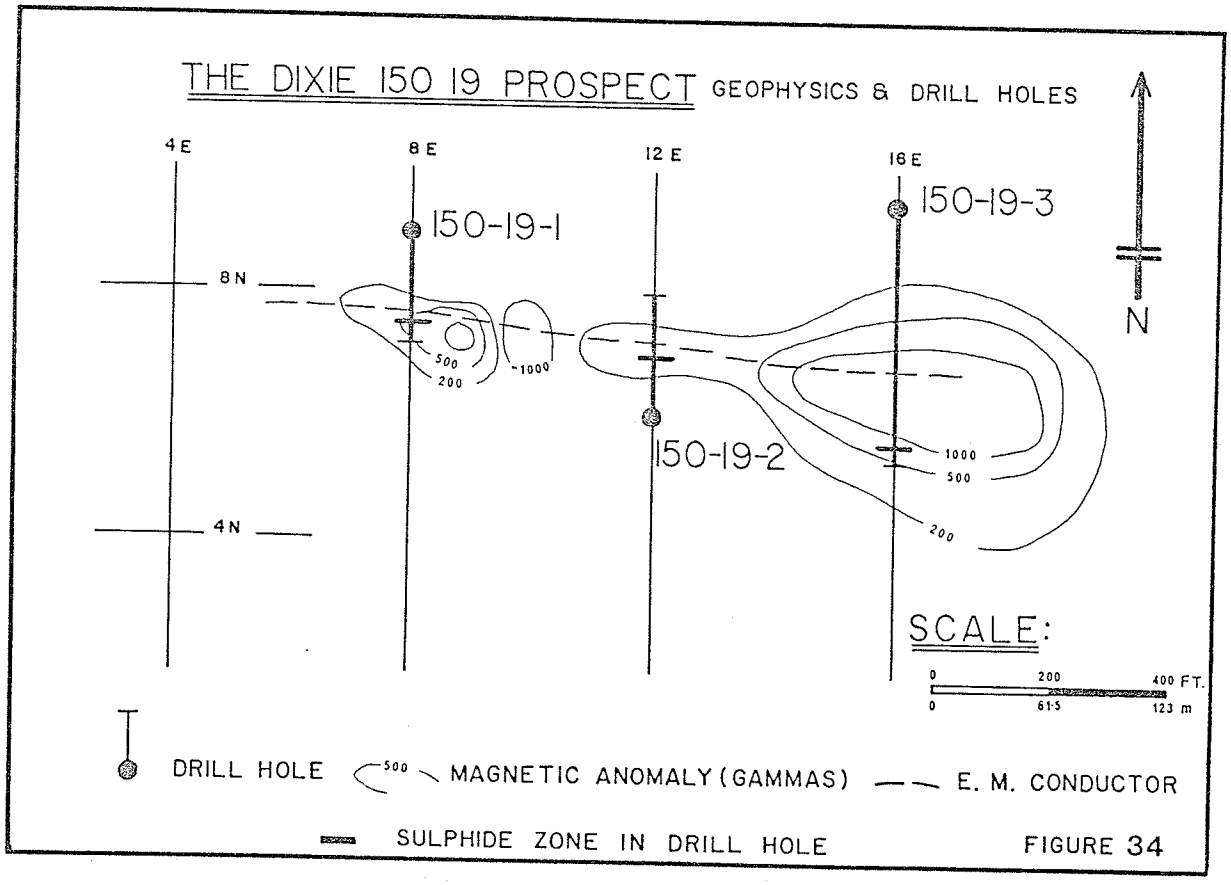
THE DIXIE 150 19 PROSPECT GEOPHYSICS & DRILL HOLES
4E
8E
12E
16E
150-19-1
150-19-3
150-19-2
8N
4N
500
200
1000
1000
500
200
N
SCALE:
0
200
400 FT.
0
61·5
123 m
DRILL HOLE
500
MAGNETIC ANOMALY (GAMMAS)
E. M. CONDUCTOR
SULPHIDE ZONE IN DRILL HOLE

FIGURE 34

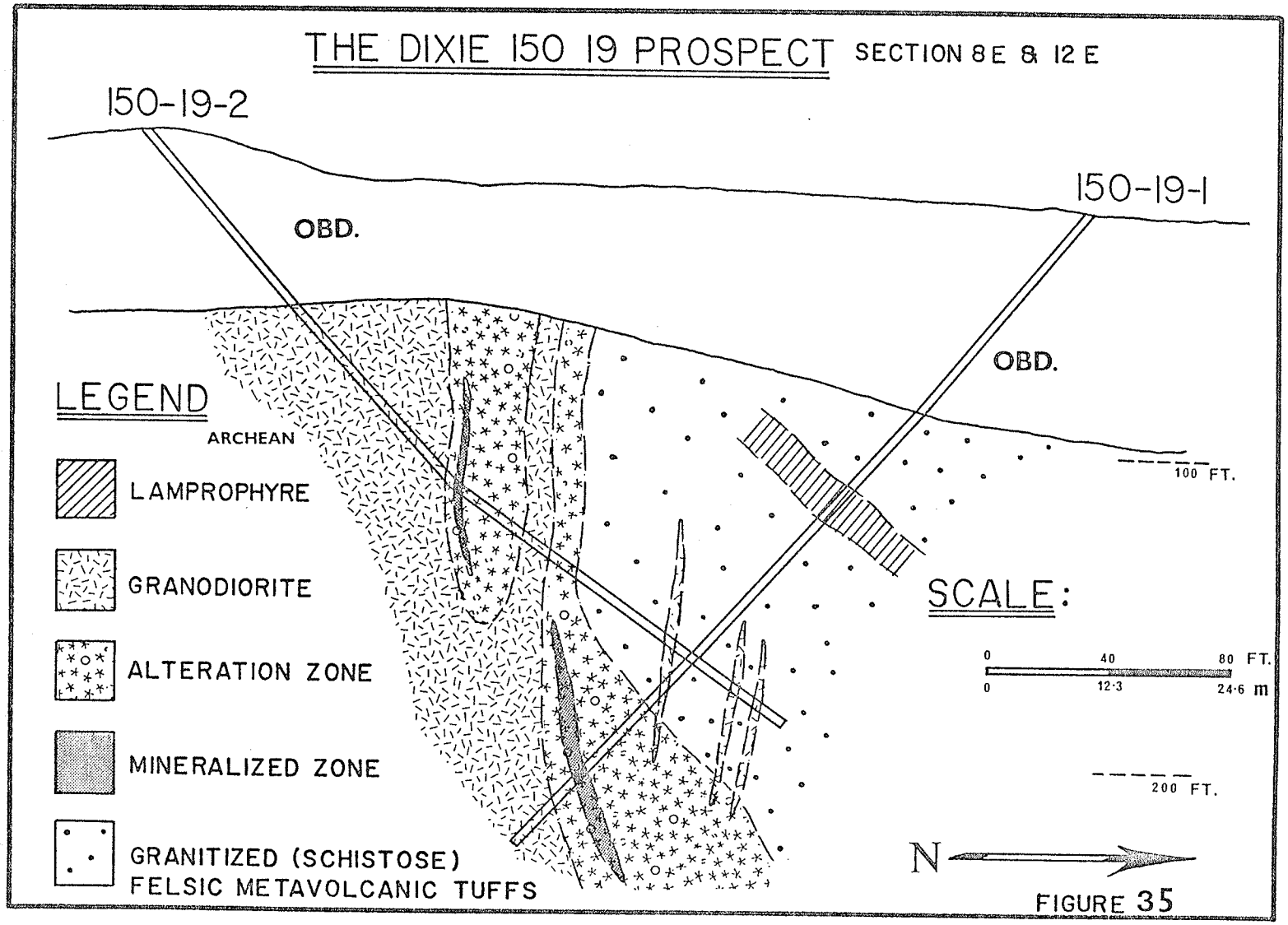
THE DIXIE 150 19 PROSPECT SECTION 8 E & 12 E
150-19-2
150-19-1
OBD.
OBD.
LEGEND
ARCHEAN
LAMPROPHYRE
GRANODIORITE
ALTERATION ZONE
MINERALIZED ZONE
GRANITIZED (SCHISTOSE)
FELSIC METAVOLCANIC TUFFS
100 FT.
SCALE:
0 40 80 FT.
0 12·3 24·6 m
200 FT.
N

FIGURE 35

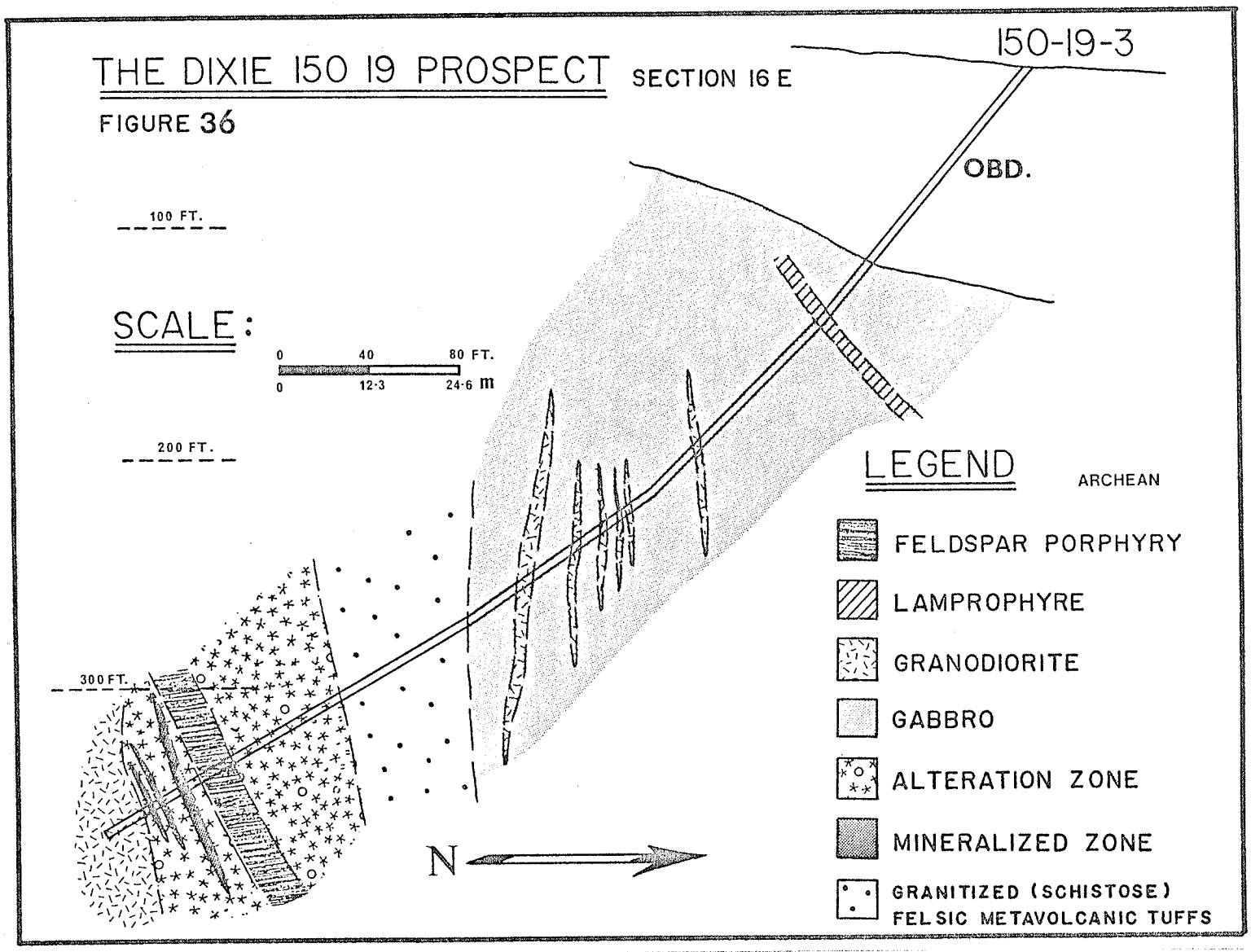
THE DIXIE 150 19 PROSPECT
SECTION 16 E
FIGURE 36
150-19-3
OBD.
100 FT.
SCALE:
0 40 80 FT.
0 12·3 24·6 m
200 FT.
300 FT.
N
LEGEND
ARCHEAN
FELDSPAR PORPHYRY
LAMPROPHYRE
GRANODIORITE
GABBRO
ALTERATION ZONE
MINERALIZED ZONE
GRANITIZED (SCHISTOSE)
FELSIC METAVOLCANIC TUFFS

sisting of fine to medium-grained biotite, chlorite, actinolite, quartz and plagioclase with subordinate microcline. Large poikiloblastic laths of biotite and felted masses of chlorite are contained within a highly polygonized groundmass of plagioclase, microcline and quartz. Actinolite is present in many sections and commonly constitutes as much as 80% of the rock with only minor biotite and quartz or plagioclase. Biotite, chlorite and actinolite always exhibit a strong preferred orientation parallel to foliation and are commonly concentrated into elongated porphyroblastic aggregates. Quartz and plagioclase form an equigranular polygonized groundmass which contains minor epidote, microcline, euhedral magnetite and sericite. Plagioclase and to a lesser extent microcline exhibit varying degrees of alteration to sericite. Sericite accounts for 40% of the groundmass in some sections.

The mineralized zones are contained within a very coarse-grained and extensive alteration zone composed of anthophyllite, actinolite, biotite, chlorite and manganiferous garnet with subordinate sericite, quartz, plagioclase, microcline and associated sulphide minerals. The alteration zone is characterized by an increase in concentration of anthophyllite and actinolite and by a pronounced increase in grain size of all mafic minerals. Biotite and actinolite exhibit extensive alteration to chlorite, and plagioclase is commonly completely replaced by sericite. The alteration zone averages 20 m in width

and lies immediately adjacent to, and mantles, the entire outer margin of the granodiorite intrusion. The contact between the granodiorite and the alteration zone is sharp, although several granodiorite dikes intrude outwards into the metavolcanic sequences.

The granodiorite is a light to medium grayish-pink, moderately foliated and medium to fine-grained rock. Quartz and plagioclase are the dominant minerals although microcline is locally abundant. Biotite is characteristic of the granodiorite and is commonly accompanied by chlorite (pseudomorphic after biotite), magnetite, apatite, zircon, epidote and sericite.

A large body of metagabbro underlies most of the eastern portion of the 150 - 19 grid. The gabbro is a dark green to gray, medium to coarse-grained rock composed of blue-green hornblende and plagioclase. Magnetite, pyrrhotite, pyrite and quartz are present in minor amounts. Secondary epidote and sericite are also present.

Numerous lamprophyric dikes occur throughout the gabbroic and metavolcanic sequences. The dikes are dark grayish-green, fine-grained, and composed of abundant biotite and actinolite with minor plagioclase and quartz. Biotite is the dominant mafic mineral although actinolite is commonly present as part of the groundmass or as porphyroblastic aggregates. Some secondary epidote and sericite are present.

A small medium-grained, grayish-green feldspar porphyry dike was intersected in drill hole 150 - 19 - 3. Well-

zoned euhedral plagioclase phenocrysts as much as 1 cm in diameter with smaller hornblende prisms constitute as much as 35% of the rock. Both phenocrysts are contained within a fine-grained quartz - plagioclase groundmass with secondary epidote, chlorite and sericite.

The mineralized zones consist of massive and disseminated sulphide minerals. The sulphide minerals occur as narrow, but high grade, veins, stringers and lenses of massive sphalerite and chalcopyrite with subordinate pyrite, pyrrhotite and magnetite. The variation of pyrite, pyrrhotite and magnetite to copper, zinc and silver are shown in figure 37 for drill holes 150 - 19 - 1 and 3. Distribution patterns for copper and zinc are indistinct but the zinc content is always much greater than copper. Several high concentrations of zinc are due to narrow vein intersections which are usually devoid of copper. Magnetite is not abundant in the mineralization. Pyrite and pyrrhotite concentrations are low and in many places totally absent from the richest intersections of base metals. Silver content is also low and is not closely associated with the distribution of zinc as in the 150 - 18 sulphide body.

The available geological data suggest that the 150 - 19 mineralization has been emplaced by hydrothermal solutions emanating outward from the granodiorite intrusion. Several factors favouring hydrothermal emplacement are:

(1) The mineralized and alteration zones lie immediately adjacent and parallel to the contact between the

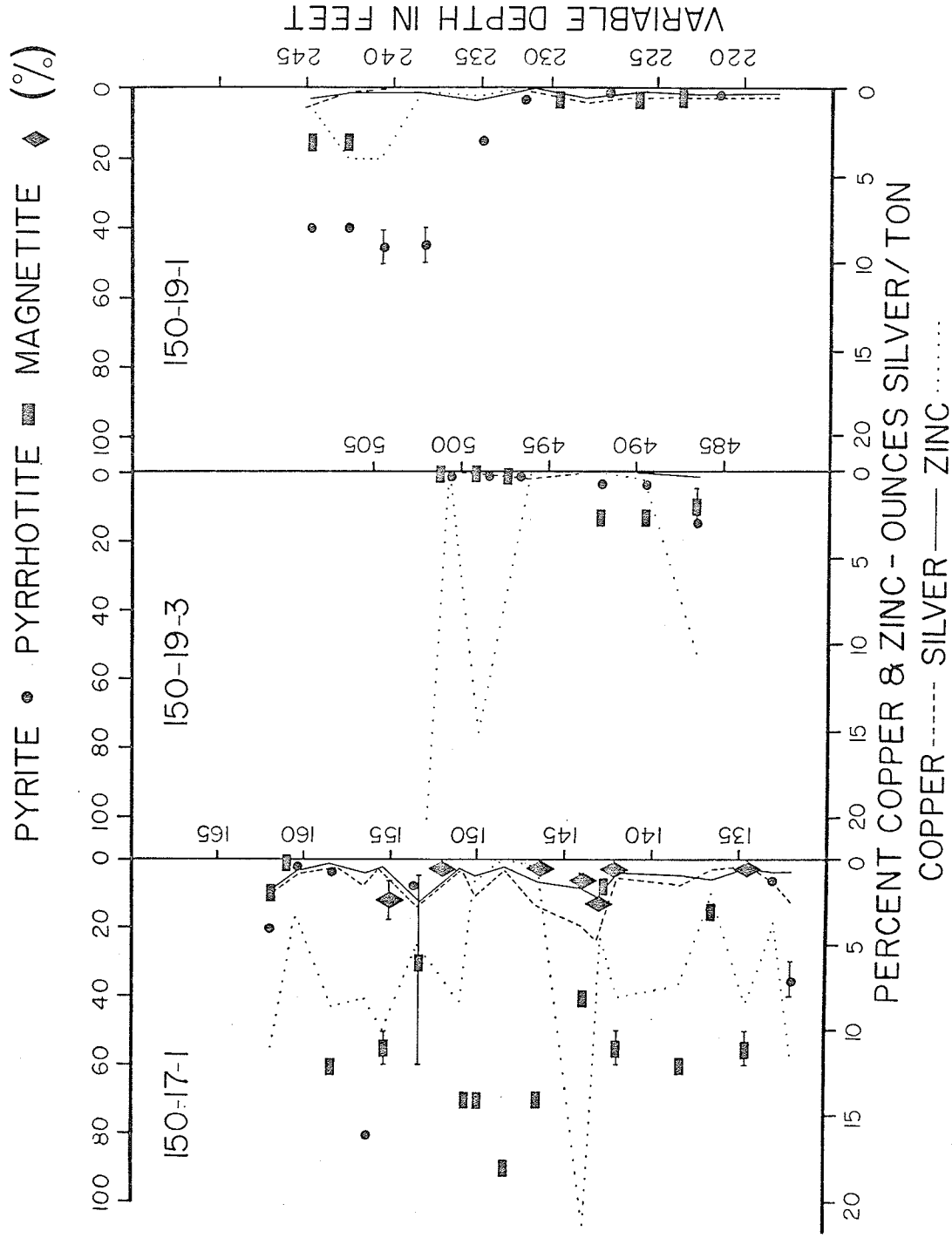


FIGURE 37 PERCENTAGES OF MAGNETITE, PYRRHOTITE AND PYRITE WITH COPPER, ZINC AND OUNCES OF SILVER PER TON FOR THE DIXIE 150-17 & 19 PROSPECTS

intrusion and altered metavolcanic sequences. The metavolcanic sequences are excessively fractured and sheared near the intrusion. The fractured and sheared rock can provide a network along which hydrothermal fluids can migrate. Many of the fractures in the alteration zone are mineralized, clearly indicating that mineralizing solutions have passed through the rocks and deposited remnant mineralization in the fractured and sheared zones.

(2) The sulphide minerals have not undergone metamorphism in the form of recrystallization, cataclastic deformation and extensive replacement. Continuous masses of pyrite are rarely fractured or brecciated and several colloform textures are well preserved - textures not observed in the 150 - 18 sulphide mineralization. Annealed textures in pyritic sections and segregation banding of sphalerite and pyrrhotite are absent - textures which are commonly observed in the 150 - 18 sulphide mineralization. Had the mineralization been introduced into the metavolcanic sequences prior to the granodiorite intrusion, the sulphide mineralization should exhibit textural evidence of similar metamorphic conditions.

(3) In many sections, the metavolcanic sequences represent highly altered (metasomatically granitized) material. The exact concentrations of $SiO_2$, $K_2O$ and $Na_2O$ introduced into the metavolcanic rocks is not known but the

high abundance of microcline and quartz along fractures, and plagioclase and quartz in the groundmass strongly suggest the passage of hydrothermal fluids from the granodiorite intrusion.

(4) Hydrothermal alteration is pervasive throughout the alteration zone and well out into the metavolcanic sequences. Intense chloritization of ferromagnesium minerals (biotite and actinolite) and extensive saussuritization of plagioclase to sericite and epidote are major alteration features in the alteration zone and enclosing metavolcanic sequences. Hydrothermal alteration of this nature is rarely observed in the volcanic units surrounding the 150 - 18 sulphide body and only occurs sporadically throughout the 150 - 18 alteration zone.

In summary, a hydrothermal emplacement origin is suggested for the Dixie 150 - 19 sulphide occurrence. Hydrothermal fluids emanating outwards from the granodiorite intrusion intensely altered and introduced copper - zinc mineralization into extensive sections of metavolcanic sequences.

## THE DIXIE 150 - 17B PROSPECT

The Dixie 150 - 17B sulphide occurrence is situated approximately 1.6 km southwest of the Dixie 150 - 18 pros-

pect (figure 38). The first diamond drill hole put down tested a short, weak conductor and intersected an impressive sulphide zone along 10 m which assayed 1.44% copper, 7.34% zinc and 0.94 ounces of silver per ton. A second drill hole, passing below the first, encountered a much narrower and lower grade sulphide zone at a depth of 61.5 m below the initial intersection. This weaker intersection assayed 0.36% copper, 4.53% zinc and 0.18 ounces of silver per ton along 1 m (figure 39).

The geological setting of the sulphide zone is somewhat similar to that of the 150 - 19 prospect located 3 km along strike to the east. The metavolcanic tuffs consist of a strongly recrystallized assemblage of biotite, chlorite, actinolite, quartz and plagioclase with minor microcline, sericite and epidote. Many of the sequences represent granitized material as another large granodiorite intrusion with several granodiorite dikes intruding the metavolcanic sequences lies northeast of the mineralized zone. A small semi-concordant quartz diorite intrusive body was intersected in both drill holes. The diorite consists of a medium-grained assemblage of hornblende, biotite and plagioclase with subordinate quartz and euhedral magnetite. Several quartz diorite dikes also intrude the metavolcanic sequences.

Important differences occur in the sulphide and alteration assemblages of the 150 - 17B prospect. The alteration zone does not lie immediately adjacent to the granodiorite

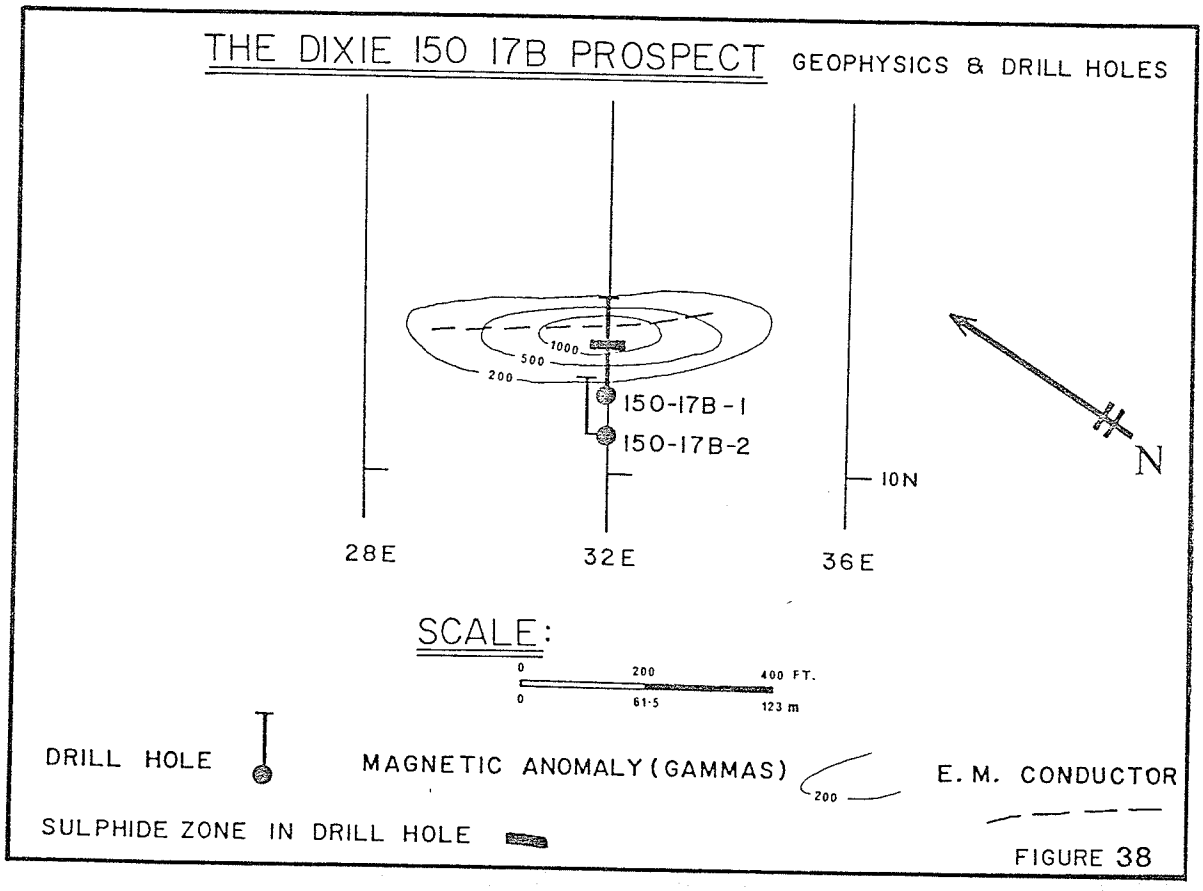
THE DIXIE 150 17B PROSPECT
GEOPHYSICS & DRILL HOLES
1000
500
200
150-17B-1
150-17B-2
28E
32E
36E
10N
N
SCALE:
0
200
400 FT.
0
61·5
123 m
DRILL HOLE
MAGNETIC ANOMALY (GAMMAS)
200
E. M. CONDUCTOR
SULPHIDE ZONE IN DRILL HOLE

FIGURE 38

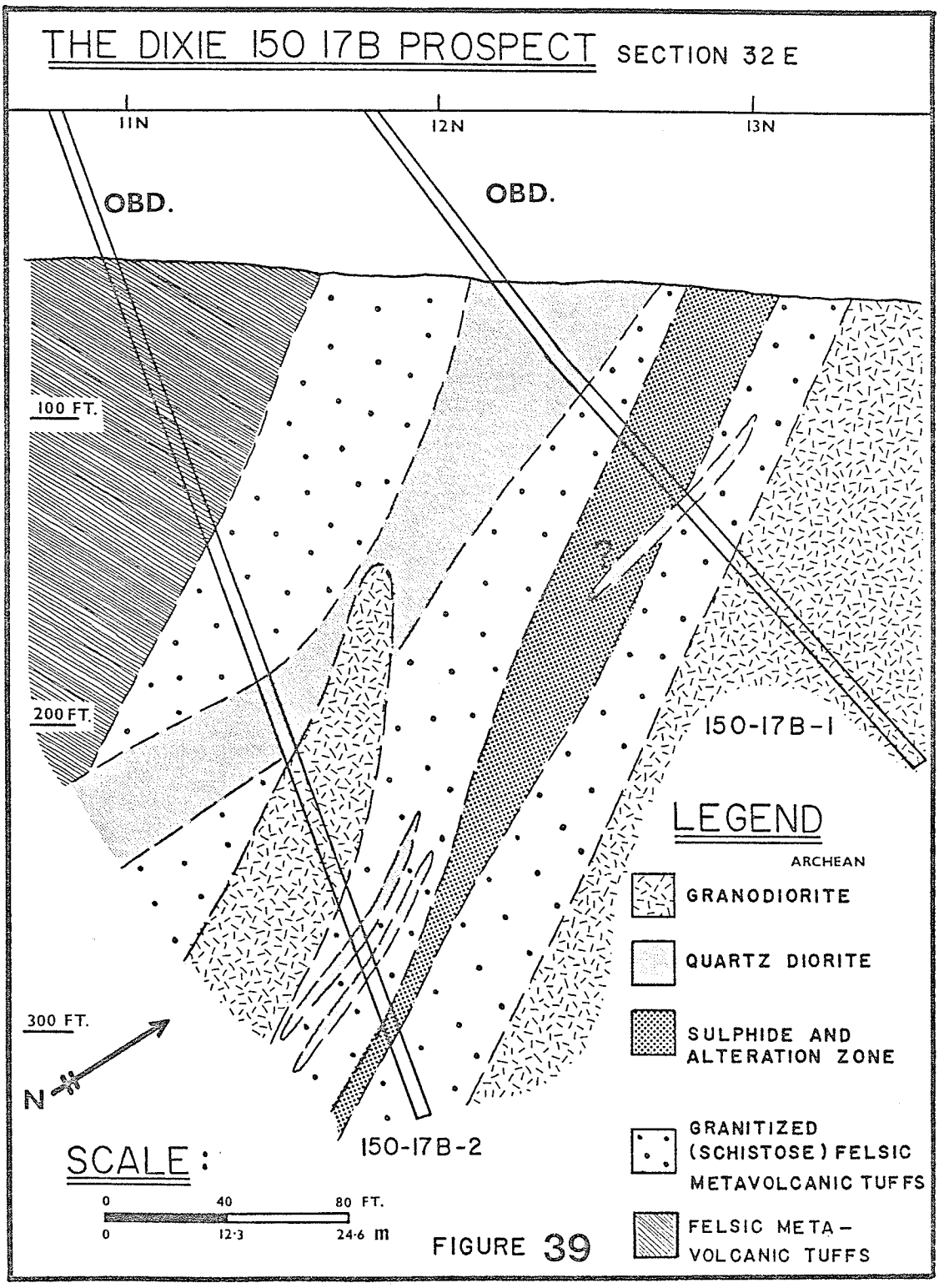
THE DIXIE 150 17B PROSPECT SECTION 32 E
11N
12N
13N
OBD.
OBD.
100 FT.
200 FT.
150-17B-1
150-17B-2
LEGEND
ARCHEAN
GRANODIORITE
QUARTZ DIORITE
SULPHIDE AND ALTERATION ZONE
GRANITIZED (SCHISTOSE) FELSIC METAVOLCANIC TUFFS
FELSIC META-VOLCANIC TUFFS
300 FT.
N
SCALE:
0 40 80 FT.
0 12·3 24·6 m

FIGURE 39

intrusion but occurs as intercalated bands and lenses within the sulphide mineralization. The entire mineralized zone is separated from the granodiorite intrusion by a narrow sequence of granitized metavolcanic tuffs. The alteration bands and lenses are composed of anthophyllite, chlorite, biotite and cordierite with minor quartz, actinolite, sericite and epidote. The sulphide body consists of a large single lens of massive pyrrhotite with pyrite and intercalated alteration assemblages. Sphalerite and chalcopyrite commonly occur as discrete disseminations and replacements in the iron sulphide minerals. Chalcopyrite commonly occurs as exsolution granules in sphalerite and invades fractures and intersticies in the alteration minerals. Magnetite is common throughout the mineralization and occurs as shredded masses and individual anhedral to subhedral grains within the iron sulphide minerals. High grade massive veinlets, lenses or stringers of chalcopyrite and sphalerite do not occur.

Unlike the 150 - 19 mineralization, the sulphide minerals have undergone intense metamorphism in the form of extensive recrystallization, fracturing, shearing, lenticulation and boudinage. Cataclastic deformation of pyrite aggregates, with plicative gneissic textures of pyrrhotite and minor folding of the alteration bands within the sulphide mineralization, are common features seen throughout the 150 - 17B mineralization.

The relative amounts of pyrite, pyrrhotite and magnetite

with copper, zinc and silver for drill hole 150 - 17B - 1 are shown in figure 37. Major metal or iron sulphide distribution patterns are not discernable but some minor features are similar to the 150 - 18 mineralization. The 150 - 17B mineralization contains considerable pyrrhotite, pyrite and magnetite. Zinc forms an enriched core and becomes increasingly richer towards the margins of the sulphide body. Copper and silver, although considerably less than zinc, show a close association with the distribution of zinc throughout the intersection. The highest concentrations of copper and silver occur within the central portion of the sulphide lens where zinc concentrations are in excess of 20% by volume. In general, the sulphide and alteration assemblages are similar to the 150 - 18 mineralization and markedly different from the 150 - 19 mineralization.

The available geological data suggests that two main genetic possibilities account for the 150 - 17B mineralization. The mineralization may have been emplaced by hydrothermal fluids emanating from the granodiorite intrusion as seems to be the case with the 150 - 19 sulphide occurrences, or deposited contemporaneously with the enclosing volcanic sequences.

Several factors favouring the latter genesis are evident and suggest that the mineralization was derived from volcanogenic processes.

(1) The sulphide mineralization has been metamorphosed and reflects similar grades of metamorphism to those of

the enclosing metavolcanic sequences.

(2) The mineralogical composition of the metavolcanic rocks is relatively uniform on either side of the sulphide lens. Megascopic influx of $SiO_2$, $K_2O$ and $Na_2O$ is not evident in the metavolcanic rocks between the granodiorite intrusion and the mineralized zone. Veinlets of fractures composed of microcline or silica were not observed.

(3) Hydrothermal alteration (chloritization of biotite and saussuritization of plagioclase to sericite and epidote) is not pervasive throughout the metavolcanic sequences and only occurs as a minor sporadic assemblage in the alteration zone.

(4) Vein or stringer associated mineralization does not occur and the fractures and shear zones in the metavolcanic sequences enclosing the sulphide mineralization are not mineralized. Some remnant sulphide mineralization would be expected had mineralizing solutions passed through the metavolcanic sequences.

(5) Alteration or sulphide assemblages do not occur immediately adjacent to the granodiorite intrusion. The alteration and mineralized zone is completely enclosed in metavolcanic tuffs and direct genetic association with the intrusion is not apparent.

In summary, a volcanogenic origin is suggested for the Dixie 150 - 17B sulphide occurrence. The sulphide minerali-

zation may have been emplaced as exhalative precipitates during volcanism, or emplaced by hydrothermal fluids related to volcanism, and not the granodiorite intrusion. Evidences confirming or even suggesting emplacement of the sulphide mineralization by hydrothermal fluids emanating from the granodiorite intrusion is lacking.

# CHAPTER 12

# CONCLUSIONS

## THE DIXIE 150 - 18 PROSPECT

(1) The 150 - 18 prospect is contained within upper greenschist to lower amphibolite mineral facies metavolcanic and metasedimentary units comprising massive and porphyritic flows, lapilli tuffs, siliceous tuffite with minor intrusive feldspar porphyry sills and lamprophyric dikes. Primary textures include quartz and plagioclase phenocrysts in flows, graded bedding and sorting of quartz grains in the siliceous tuffite and relict fragments and bedding preserved in the lapilli tuffs.

(2) Metamorphic textures within the volcanic rocks suggest that three phases of deformation have disturbed the volcanic rocks.

(3) The unaltered volcanic sequences have similar mineralogical compositions. The mineralogical compositions of the flows and lapilli tuffs are classified as basalts, andesites and quartz andesites.

(4) The generalized lithological volcanic pile enclosing and the depositional history for the 150 - 18 prospect is as follows:

Unit (a) initial tuffaceous sequence development.

Unit (b) deposition of the siliceous tuffite.

Unit (c) extrusion of massive and porphyritic flows.

Unit (d) deposition of another tuffaceous sequence . sporadic intrusions of feldspar porphyry sills and lamprophyric dikes.

(5) Metasedimentary greywackes, calcareous siltstones and impure limestones occur east and northeast of the sulphide body and suggest an environmental transgression eastward from subaqueous or subaerial conditions into deeper water offshore marine environments.

(6) Major element chemical analyses of the least altered volcanic rocks reveal:

- minimal volatile metasomatism.
- slight alkali metasomatism reflected as sodium enrichment and potassium depletion in flows and an overall variability in the lapilli tuffs.
- a strong iron and slight magnesium enrichment trend for the massive flows and lapilli tuffs.
- an accompanying trend towards alkali enrichment for the massive flows and lapilli tuffs.
- primary differentiation and crystallization of magma in the volcanic edifice may explain the tholeiitic iron enrichment trends and the occurrence of calc-alkaline high alumina massive flows.
- environmental and metamorphic factors may have attributed to metasomatic changes (iron and magnesium enrichment and alkali variations) within the volcanic rocks.
- the volcanic rocks belong to the sub-alkalic field

of volcanic rocks.

- the volcanic rocks plot mainly within the tholeiitic field although high alumina massive flows plot within the calc-alkaline field.
- the flows are individually classified as high-iron tholeiitic basalts and andesites with some calc-alkaline andesites.
- the lapilli tuffs are classified as being basaltic to andesitic in composition.
- greywackes were derived from the surrounding volcanic sequences.
- the siliceous tuffite contains a large detrital component of silica and potassium.

(7) The 150 - 18 sulphide prospect is a zinc-rich sulphide body composed of pyrite, pyrrhotite, sphalerite, chalcopyrite, magnetite and tetrahedrite. Sulphide textures indicate that the mineralization has undergone differential stress, metamorphic recrystallization and mobilization which considerably modified the sulphide mineralization from initial configurations. Primary textures are not preserved and base metal zonations within the sulphide body (although slightly redistributed) may indicate the discharge source for the hydrothermal solutions. Silver shows a close association with high concentrations of zinc throughout the sulphide body.

(8) A large hydrothermal cordierite-anthophyllite altera-

tion zone composed of quartz, cordierite, anthophyllite, chlorite, biotite and actinolite mineral assemblages is situated immediately along the footwall of the sulphide body. The cordierite-anthophyllite alteration zone is conformable along the flanks of the sulphide body but thickens, becomes discordant and resembles an alteration pipe beneath the central portion of the sulphide mineralization. Silicification, chloritization, cation hydrolysis and biotitization were major alteration processes closely associated with sulphide deposition.

(9) Major element chemical analyses throughout the cordierite-anthophyllite alteration zone reveal:

- a strong enrichment in iron, magnesium, sulphur and manganese.
- a strong depletion in lime and alkalies.
- a slight depletion in silica and alumina.
- a moderate enrichment in water.

Leaching of lime and alkalies and enrichment of iron, magnesium, sulphur and manganese is coincident with sulphide mineralization. The mineralizing hydrothermal solutions were enriched in iron, magnesium, zinc, sulphur, copper, silver, water and manganese. The relative enrichment in iron and magnesium and depletion in lime and alkalies within the alteration zone may have been sufficient so that cordierite-anthophyllite assemblages developed within original chloritic altera-

tion zones during high temperature (500 - 800°C)-low to moderate pressure (4 - 7 kbars) regional metamorphism.

(10) The 150 - 18 sulphide mineralization may have been precipitated during syngenetic (solfataric) processes contemporaneously with the enclosing volcanic sequences or as epigenetic emplacement (stratigraphic trapping and replacement) of mineralization beneath the siliceous tuffite following formation of the volcanic pile.

## THE DIXIE 150 - 17B and 19 PROSPECTS

The rocks enclosing the 150 - 17B and 19 prospects are markedly different from those enclosing the 150 - 18 prospect. The metavolcanic sequences are hydrothermally altered, strongly foliated, granitized volcanic sequences. The copper-zinc mineralization associated with both occurrences is small and closely related to large granodiorite intrusions covering large portions of both prospects.

A hydrothermal emplacement origin is suggested for the 150 - 19 sulphide occurrences. Metal-bearing hydrothermal solutions emanating from the granodiorite intrusion introduced copper-zinc mineralization into the volcanic rocks and intensely altered large sections of the metavolcanic sequences.

A volcanogenic origin is suggested for the Dixie 150 - 17B sulphide occurrence. The sulphide mineralization may have

been emplaced as exhalative precipitates during volcanism or emplaced by hydrothermal fluids related to volcanism and not the granodiorite intrusion.

## ECONOMIC RECOMMENDATIONS

(1) The Dixie 150 - 18 sulphide occurrence is contained within the basalt and andesite sequences and may represent a new environment of sulphide deposition in mafic volcanic piles. Geological exploration within the southwestern extension of the Uchi - Confederation Lake greenstone belt has been primarily restricted to geological areas known to contain sulphide occurrences within felsic (siliceous) volcanic rocks, or to other linear trends of volcanic rocks known to contain intercalated felsic (siliceous) volcanic sequences.

However, the occurrence of the Dixie 150 - 18 mineralization in mafic volcanic sequences should warrant considerable geological interest and expand present geological exploration within the Uchi - Confederation Lake greenstone belt to include large and relatively unexplored areas containing mafic volcanic sequences.

(2) Diamond drill holes 150 - 18 - 3, 16 and 17 terminated within cordierite - anthophyllite-bearing rocks of the hydrothermal alteration zone. This central portion of the alteration zone continues to greater depth beyond the drill holes, appears to be thickening and may contain a number of undiscovered sulphide lenses at depth. Further drilling on the

Dixie 150 - 18 prospect should include the extension of drill holes 150 - 18 - 3, 16 and 17.

(3) The highest concentrations of copper in the Dixie 150 - 18 sulphide body occur in samples from drill hole 150 - 18 - 3. The occurrence of high grade copper intersections throughout drill hole 150 - 18 - 3 suggests that the discharge vent or source for the hydrothermal solutions lies within the central portion of the sulphide body.

The approximate location of the discharge vent or source for the hydrothermal solutions becomes a major priority when searching for additional lenses of sulphide mineralization. Chalcopyrite precipitation will tend to occur at the discharge vent or within the hydrothermal (alteration) pipe. Therefore, the extension of the cordierite - anthophyllite alteration zone beneath drill hole 150 - 18 - 3 represents an area that should be favoured in the search for additional copper-rich sulphide lenses.

(4) The highest concentrations of silver and the occurrence of tetrahedrite are closely associated with concentrations of zinc (sphalerite) in excess of 15% by volume. Microprobe analyses of several tetrahedrite grains indicate that tetrahedrite contains substantial quantities of silver.

Therefore, during milling procedures, individual separation and treatment of tetrahedrite and sphalerite should result in greater silver recoveries from the Dixie 150 - 18 sulphide ores.

(5) Chalcopyrite is the only major copper sulphide found

throughout the Dixie 150 - 18 mineralization. Chalcopyrite almost invariably occurs as minute exsolution emulsoid bodies in sphalerite and less commonly as minute veinlet and fracture fillings in gangue silicate minerals, pyrite and pyrrhotite.

Therefore, during milling procedures, separation and treatment of sphalerite should result in greater copper recoveries from the Dixie 150 - 18 sulphide ores although the minute chalcopyrite grain size may cause some initial grinding and separation difficulties.

# REFERENCES

# REFERENCES

Amstutz, G. C. 1974. Spilites and Spilitic Rocks. Internat. Union of Geol. Sci. Series A4, Springer Verlag, N.Y., 482 p.

Ayres, L. D. 1978. Metamorphism in the Superior province of northwestern Ontario and its relationship to crustal evolution. In: Metamorphism in the Canadian Shield. Geol. Surv. Can., Paper 78-10, pp. 25-36.

Bachinski, D. J. 1976. Metamorphism of cupriferous iron sulphide deposits, Notre Dame Bay area, Newfoundland. Econ. Geol., 71, pp. 443-452.

Baragar, W. R. A., Coleman, L. C. and Hall, J. M. 1977. Volcanic regimes in Canada. Geol. Assoc. Can., Special Paper 16, 476 p.

Bastin, E. S. 1950. Interpretation of ore textures. Geol. Soc. Am. Memoir 45, pp. 1-91.

Blatt, H., Middleton, G., and Murray, R. 1972. Origin of Sedimentary Rocks. Prentice Hall, N.J., 634 p.

Carmichael, I. S. E. 1964. The petrology of Thingmuli, a tertiary volcano in eastern Iceland. Jour. Pet., 5, pp. 435-460.

Clark, B. R. and Kelly, W. C. 1973. Sulphide deformation studies; I experimental deformation of pyrrhotite and sphalerite to 200 bars and 500° C. Econ. Geol., 68, pp. 332-352.

Deer, W. A., Howie, R. A. and Zussman, J. 1974. An introduction to the rock forming minerals. Longman, pp. 1-528.

DeRosen-Spence, A. 1969. Genèse des roches à cordiérite-anthophyllite des gisements cupro-zinciferes de la région de Rouyn-Noranda, Quebec, Canada. Can. Jour. Earth Sci., 6, pp. 1339-1345.

Emmons, W. H. 1909. Some regionally metamorphosed ore deposits and the so-called segregation veins. Econ. Geol., 4, pp. 755-781.

Eskola, P. 1914. On the petrology of the Orijarvi region in southwestern Finland. Bull. Comm. Geol. Finlande, No. 40, 277 p.

Evans, L. L. 1977. Geology of the Bushy Creek Mine, viburnum trend, southeast Missouri. Econ. Geol., 72, pp. 381-390.

Froese, E. 1969. Metamorphic rocks from the Coronation Mine and surrounding area. Geol. Surv. Can., Paper 68-5, pp. 55-77.

Gilmour, P. 1965. The origin of massive sulphide mineralization in the Noranda district, northwestern Quebec. Geol. Assoc. Can., 16, pp. 62-82.

Gluskoter, H. J. 1964. Orthoclase distribution and authigenesis in the Franciscan formation of a portion of western Marin County, California. Jour. Sed. Pet., 34, pp. 335-343.

Graf, J. L. Jr. and Skinner, B. J. 1970. Strength and deformation of pyrite and pyrrhotite. Econ. Geol., 65, pp. 200-215.

Grogan, R. M. and Bradbury, J. C. 1967. The origin of stratiform fluorite deposits in southern Illinois. In: Part I Econ. Geol. Monograph No. 3, J. S. Brown editor, pp. 40-51.

Guha, J. and Koo, J. 1975. Role of fluid state mobilization during metamorphism of the Henderson ore bodies, Chibougamau, Quebec, Canada. Can. Jour. Earth Sci., 12, pp. 1516-1523.

Hodgson, C. J. and Lydon, J. W. 1977. Geological setting of volcanogenic massive sulphide deposits and active hydrothermal systems - implications for exploration. Can. Inst. Mining and Met. Bull., October, pp. 95-105.

Hughes, C. J. 1972. Spilites, kerotophyres and the igneous spectrum. Geol. Mag., 109, pp. 513-527.

Irvine, T. N. and Baragar, W. R. A. 1971. A guide to the classification of the common volcanic rocks. Can. Jour. Earth Sci., 8, pp. 523-547.

Jensen, L. S. 1976. A new cation plot for classifying subalkalic volcanic rocks. Ont. Div. of Mines, Misc. Paper 66.

Kalliokoski, J. 1965. Metamorphic features in North American massive sulphide deposits. Econ. Geol., 60, pp. 485-505.

Kanehira, K. 1969. Sulphide ores from the Coronation Mine, Saskatchewan. Geol. Soc. Can., Paper 68-5, pp. 79-135.

_____ and Bachinski, D. J. 1968. Mineralogy and textural relationships from the Whalesback Mine, N.E. Newfoundland. Can. Jour. Earth Sci., 5, pp. 1387-1395.

Large, R. R. 1977. Chemical evolution and zonation of massive sulphide deposits in volcanic terraines. Econ. Geol., 72, pp. 549-572.

Lepezin, G. C. 1969. Importance of $H_2O$ in cordierite in natural mineralogenesis. Dolk. Akad. Nauk. SSR., 186, pp. 122-125.

MacDonald, G. A. and Katsura, T. 1964. Chemical compositions of Hawaiian lavas. Jour. Pet., 5, pp. 82-133.

MaCrea, N. D. 1974. Sulfurization of basalt under thermal metamorphic conditions to produce cordierite bearing rocks. Can. Jour. Earth Sci., 11, pp. 246-253.

Magnusson, N. H. 1960. Iron and sulphide ores of central Sweden. Internat. Geol. Congress, 21st session guide to excursions, No. A26 and C21.

McDonald, J. A. 1967. Metamorphism and its effect on sulphide assemblages. Miner. Deposita, 2, pp. 200-220.

Meyer, C. and Hemley, J. J. 1967. Wallrock alteration. In: Geochemistry of Hydrothermal Ore Deposits. Holt Rinehart, N.Y., pp. 166-235.

Miyashiro, A. 1974. Volcanic rock series in island arc and active continental margins. Amer. Jour. Sci. 274, pp. 321-355.

Mouat, M. M. and Clendenin, C. W. 1977. Geology of the Ozark Lead Company Mine, viburnum trend, southeast Missouri. Econ. Geol., 72, pp. 398-407.

Nunes, P. D. and Thurston, P. C. 1978. Two hundred twenty million years of greenstone evolution in a single belt - a zircon study of the Uchi Lake area, northwestern Ontario. Fourth Internat. Conf. on Geochronology, Cosmochronology and Isotope Geology, Aug. 20-25, Colorado.

Paarlberge, N. L. and Evans, L. L. 1977. Geology of the Fletcher Mine, viburnum trend, southeast Missouri. Econ. Geol., 72, pp. 391-397.

Pettijohn, E. J. 1975. Sedimentary Rocks, Third edition, Harper Internat., 628 p.

Roberts, W. M. B. 1965. Recrystallization and mobilization of sulphides at 2000 ATM. and in the temperature range 50-145° C. Econ. Geol., 60, pp. 168-180

Sangster, D. F. 1972. Precambrian volcanogenic massive sulphide deposits in Canada: a review. Geol. Surv. Can., Paper 72-22.

Sangster, D. F. and Scott, S. D. 1976. Precambrian strata-bound massive Cu-Zn-Pb sulphide ores of North America. Pp. 129-222. In: Wolf, K. H. Handbook of Stratabound and Stratiform Ore Deposits, 6, p. 129-222.

Sato, T. 1972. Behaviors of ore-forming solutions in sea-water. Mining Geol., 22, pp. 31-42.

____ 1973. A chloride complex model for Koroko mineraliza-tion. Geochem. Jour., 7, pp. 245-270.

Shadlum, T. N. 1971. Metamorphic textures and structures of sulphide ores. Soc. Mining Geol. Japan, Spec. issue 3, pp. 241-250.

Shklanka, R. 1970. Geology of the Bruce Lake area, district of Kenora. Ont. Div. of Mines, Geological Report 82.

Simmons, B. D. 1973. Geology of the Millenbach massive sulphide deposit, Noranda, Quebec. Can. Inst. Mining and Met. Bull., 66, pp. 67-78.

Stanton, R. L. 1960. General features of the conformable "pyritic" orebodies. Part 1, Field association, pp. 24-29, Part 2, Mineralogy, pp. 66-74. Can. Inst. Mining and Met. Bull., LXII.

Stauffer, M. R., Mukherjee, A. C. and Koo, J. 1975. The Amisk group: an Aphebian (?) island arc deposit. Can. Jour. Earth Sci., 12, pp. 2021-2035.

Streckeisen, A. 1967. Classification and nomenclature of igneous rocks. N. Jb. Mineral, Abh., 107, pp. 144-240.

Suffel, G. G., Hutchinson, R. W. and Ridler, R. H. 1971. Metamorphism of massive sulphides at Manitouwadge, Ontario, Canada. Soc. Mining Geol. Japan, Spec. issue 3, pp. 235-240.

Taylor, A. V. 1942. Quartz Hill district, near Divide, Montana. In: Ore Deposits as Related to Structural Features, W. H. Newhouse, editor, pp. 215-217.

Thurston, P. C. and Breaks, F. W. 1978. Metamorphic and tectonic evolution of the Uchi-English River subprovince. In: Metamorphism in the Canadian Shield. Geol. Surv. Can., Paper 78-10, pp. 49-62.

_____, Wan, J., Squair, H. S., Warburton, A. F. and Wierzbicki, V. W. 1978. Volcanology and mineral deposits of the Uchi-Confederation Lakes area, northwestern Ontario. Geol. Assoc. Can., Toronto 78 Field trips Guidebook, edited by A. L. Currie and W. O. Mackasey, pp. 302-324.

Upadhyay, H. D. and Smitheringale, W. G. 1972. Geology of the Gullbridge copper deposit, Newfoundland. Volcanogenic sulphides in cordierite-anthophyllite rocks. Can. Jour. Earth Sci., 9, pp. 1061-1073.

Vallance, T. G. 1967. Mafic rock alteration and isochemical development of some cordierite-anthophyllite rocks. Jour. Pet., 8, pp. 84-96.

Vokes, F. M. 1968. A review of metamorphism of sulphide deposits. Earth Sci. Review, 5, pp. 99-143.

Wager, L. R. and Brown, G. M. 1968. Layered Igneous Rocks. Freeman, San Francisco.

Whitmore, D. R. E. 1969. Geology of the Coronation copper deposit. Geol. Surv. Can., Paper 68-5, pp. 37-53.

Wilson, H. D. B., Andrews, P., Moxham, R. L. and Ramlal, K. 1965. Archean volcanism of the Canadian Shield. Can. Jour. Earth Sci., 2, pp. 161-175.

Winkler, H. J. F. 1967. Petrogenesis of Metamorphic Rocks. First edition, Springer Verlag, N.Y.

_____. 1976. Petrogenesis of Metamorphic Rocks. Fourth edition, Springer Verlag, N.Y.

# APPENDIX

# TABLE A1

MAJOR ELEMENT CHEMISTRY– MASSIVE FLOWS

| D. D. H. | 18-13-379 | 18-10-77 | 18-4-126 | 18-14-123 | 18-1-131 | 18-7-56 | 18-7-128 | 18-9-38 |
|---|---|---|---|---|---|---|---|---|
| $SiO_2$ | 54.05 | 53.50 | 54.40 | 55.80 | 51.10 | 56.50 | 56.90 | 58.60 |
| $Al_2O_3$ | 12.95 | 13.20 | 18.12 | 12.82 | 15.60 | 18.80 | 13.40 | 11.51 |
| $Fe_2O_3$ | 3.61 | 3.31 | 2.64 | 3.02 | 1.72 | 1.66 | 2.10 | 5.24 |
| FeO | 10.08 | 9.52 | 5.04 | 10.16 | 7.96 | 5.00 | 10.24 | 9.42 |
| MgO | 5.05 | 3.85 | 3.45 | 3.72 | 7.05 | 3.18 | 2.30 | 2.12 |
| CaO | 7.28 | 8.86 | 9.30 | 7.14 | 9.75 | 7.95 | 6.00 | 5.42 |
| $Na_2O$ | 2.75 | 2.85 | 3.72 | 2.90 | 2.53 | 4.25 | 4.07 | 3.57 |
| $K_2O$ | 0.31 | 0.41 | 0.54 | 0.36 | 0.26 | 0.21 | 0.16 | 0.43 |
| $H_2O$ | 1.14 | 1.19 | 1.25 | 1.21 | 1.56 | 0.78 | 0.98 | 0.98 |
| $CO_2$ | 0.05 | 0.16 | 0.24 | 0.09 | 0.38 | 0.22 | 0.13 | 0.23 |
| $TiO_2$ | 2.16 | 2.20 | 0.72 | 1.74 | 0.86 | 0.52 | 1.72 | 1.35 |
| $P_2O_5$ | 0.24 | 0.26 | 0.14 | 0.28 | 0.088 | 0.068 | 0.24 | 0.37 |
| MnO | 0.42 | 0.36 | 0.22 | 0.40 | 0.19 | 0.15 | 0.43 | 0.45 |
| TOTAL | 100.09 | 99.68 | 99.78 | 99.64 | 99.05 | 99.29 | 98.67 | 99.69 |

# TABLE A2

MAJOR ELEMENT CHEMISTRY– LAPILLI TUFFS

| D. D. H. | 18-8-97 | 18-17-317 | 18-12-201 | 18-13-172 | 18-18-187 | 18-4-296 | 18-16-52 | 18-8-157 |
|---|---|---|---|---|---|---|---|---|
| $SiO_2$ | 55.75 | 57.10 | 51.75 | 57.10 | 53.45 | 55.50 | 55.65 | 54.85 |
| $Al_2O_3$ | 11.92 | 12.98 | 16.28 | 12.40 | 16.20 | 13.19 | 12.42 | 11.96 |
| $Fe_2O_3$ | 2.17 | 2.57 | 2.10 | 4.16 | 2.32 | 4.04 | 4.16 | 4.25 |
| FeO | 13.52 | 11.52 | 9.58 | 10.94 | 9.56 | 11.60 | 11.44 | 11.50 |
| MgO | 3.32 | 2.85 | 3.15 | 1.45 | 3.78 | 2.48 | 2.02 | 3.82 |
| CaO | 4.35 | 6.02 | 10.42 | 5.80 | 5.50 | 5.98 | 4.85 | 6.98 |
| $Na_2O$ | 2.58 | 3.03 | 2.38 | 3.05 | 2.93 | 2.67 | 3.40 | 1.42 |
| $K_2O$ | 1.50 | 0.66 | 1.10 | 1.02 | 2.00 | 0.75 | 1.02 | 0.68 |
| $H_2O$ | 1.62 | 1.14 | 1.41 | 1.34 | 1.57 | 1.20 | 0.98 | 1.13 |
| $CO_2$ | 1.05 | 0.60 | 0.55 | 0.65 | 1.09 | 0.16 | 1.01 | 1.76 |
| $TiO_2$ | 1.28 | 0.72 | 1.14 | 1.40 | 0.98 | 1.81 | 1.71 | 0.66 |
| $P_2O_5$ | 0.32 | 0.17 | 0.14 | 0.44 | 0.16 | 0.30 | 0.64 | 0.14 |
| MnO | 0.38 | 0.46 | 0.24 | 0.28 | 0.24 | 0.45 | 0.37 | 0.32 |
| TOTAL | 99.76 | 99.82 | 99.64 | 100.03 | 99.78 | 100.13 | 99.67 | 99.47 |

# TABLE A3

MAJOR ELEMENT CHEMISTRY

| | SILICEOUS TUFFITE | | | | | GREYWACKE | | |
|---|---|---|---|---|---|---|---|---|
| D. D. H. | 18-8-260 | 18-17-376 | 18-4-148 | 18-17-384 | | 18-1-166 | 18-5-200 | 18-11-55 |
| $SiO_2$ | 71.65 | 70.15 | 59.60 | 60.95 | | 58.00 | 67.90 | 57.75 |
| $Al_2O_3$ | 12.36 | 12.58 | 13.98 | 13.95 | | 13.32 | 15.84 | 19.56 |
| $Fe_2O_3$ | 1.48 | 0.54 | 2.18 | 2.46 | | 1.13 | 0.26 | 0.95 |
| FeO | 4.00 | 6.04 | 6.76 | 8.20 | | 10.20 | 3.00 | 4.70 |
| MgO | 1.98 | 2.75 | 2.80 | 3.12 | | 4.15 | 2.18 | 2.62 |
| CaO | 2.12 | 2.08 | 4.72 | 2.62 | | 3.20 | 2.48 | 5.28 |
| $Na_2O$ | 2.78 | 2.25 | 3.03 | 2.95 | | 2.37 | 5.25 | 1.78 |
| $K_2O$ | 1.63 | 1.67 | 1.74 | 1.51 | | 2.48 | 1.02 | 4.41 |
| $H_2O$ | 1.02 | 0.92 | 1.24 | 2.40 | | 1.21 | 0.91 | 1.36 |
| $CO_2$ | 0.09 | 0.08 | 2.63 | 0.78 | | 1.44 | 0.16 | 0.57 |
| $TiO_2$ | 0.46 | 0.52 | 0.72 | 0.77 | | 0.58 | 0.52 | 0.52 |
| $P_2O_5$ | 0.11 | 0.088 | 0.11 | 0.12 | | 0.17 | 0.15 | 0.11 |
| MnO | 0.11 | 0.18 | 0.23 | 0.17 | | 0.12 | 0.093 | 0.12 |
| TOTAL | 99.79 | 99.85 | 99.74 | 100.00 | | 98.37 | 99.76 | 99.73 |

| TABLE A4 | MAJOR ELEMENT CHEMISTRY | | | | | ALTERATION ZONE | | | |
|---|---|---|---|---|---|---|---|---|---|
| D. D. H. | 18-3-171 | 18-3-176 | 18-3-186 | 18-3-219 | 18-6-120 | 18-6-126 | 18-6-136 | 18-10-231 | 18-16-523 |
| $SiO_2$ | 25.00 | 22.10 | 54.75 | 63.35 | 54.10 | 61.05 | 46.00 | 50.65 | 34.00 |
| $Al_2O_3$ | 14.44 | 11.10 | 7.06 | 6.20 | 11.20 | 8.98 | 10.50 | 6.75 | 5.50 |
| $Fe_2O_3$ | 10.41 | 12.25 | 8.66 | 3.63 | 7.79 | 7.75 | 9.99 | 5.78 | 16.44 |
| FeO | 23.26 | 29.48 | 16.64 | 14.52 | 14.92 | 9.50 | 14.68 | 20.56 | 23.76 |
| MgO | 7.70 | 6.78 | 2.95 | 4.80 | 4.85 | 3.25 | 3.25 | 6.55 | 4.30 |
| CaO | 1.50 | 1.90 | 1.12 | 0.50 | 1.38 | 1.20 | 6.35 | 1.58 | 1.68 |
| $Na_2O$ | 0.68 | 0.51 | 0.18 | 0.21 | 0.58 | 0.81 | 1.18 | 0.18 | 0.47 |
| $K_2O$ | 1.04 | 0.03 | 0.33 | — | 0.12 | 0.56 | 0.27 | 0.24 | 0.17 |
| $H_2O$ | 3.30 | 1.53 | 0.80 | 0.31 | 0.74 | 2.04 | 1.64 | 1.24 | 1.02 |
| $CO_2$ | — | — | — | — | — | — | — | — | — |
| $TiO_2$ | 2.02 | 1.42 | 0.94 | 0.74 | 1.50 | 1.24 | 1.38 | 0.85 | 0.66 |
| $P_2O_5$ | 0.32 | 0.09 | 0.04 | 0.07 | 0.20 | 0.12 | 0.21 | 0.09 | 0.01 |
| MnO | 0.26 | 0.41 | 0.035 | 0.12 | 0.46 | 0.19 | 0.61 | 0.11 | 0.11 |
| $SO_2$ | 15.05 | 18.70 | 10.21 | 4.30 | 4.08 | 4.30 | 3.33 | 8.92 | 19.46 |
| CuO | 0.41 | 0.71 | 0.28 | 0.15 | 0.12 | 0.11 | 0.12 | 0.16 | 0.71 |
| ZnO | 1.47 | 1.66 | 0.06 | 1.62 | 0.12 | 0.62 | 0.04 | 0.04 | 0.62 |
| TOTAL | 99.78 | 99.99 | 99.06 | 99.51 | 100.23 | 100.03 | 97.97 | 99.29 | 99.28 |

| TABLE A5 | MAJOR ELEMENT CHEMISTRY — ALTERATION ZONE | | | | | | |
|---|---|---|---|---|---|---|---|
| D. D. H. | 18-16-528 | 18-17-393 | 18-17-408 | 18-17-416 | 18-17-419 | 18-17-421 | 18-17-449 |
| $SiO_2$ | 37.50 | 39.95 | 20.00 | 49.60 | 29.00 | 35.00 | 53.55 |
| $Al_2O_3$ | 5.76 | 10.06 | 12.11 | 9.05 | 9.94 | 10.50 | 3.94 |
| $Fe_2O_3$ | 16.48 | 7.88 | 12.72 | 13.08 | 20.58 | 17.34 | 5.01 |
| FeO | 20.66 | 23.20 | 21.16 | 8.84 | 12.96 | 10.42 | 24.54 |
| MgO | 5.02 | 4.18 | 15.20 | 6.02 | 9.30 | 11.20 | 3.00 |
| CaO | 1.80 | 0.92 | 1.30 | 2.25 | 1.30 | 1.92 | 0.38 |
| $Na_2O$ | 0.26 | 0.26 | 0.061 | 0.59 | 0.30 | 0.50 | 0.09 |
| $K_2O$ | 0.70 | 0.26 | 0.02 | 0.16 | 0.64 | 0.17 | 1.64 |
| $H_2O$ | 0.86 | 0.74 | 7.35 | 2.01 | 2.19 | 1.89 | 0.63 |
| $CO_2$ | — | — | — | — | — | — | — |
| $TiO_2$ | 0.72 | 0.46 | 1.88 | 1.17 | 1.30 | 1.44 | 0.42 |
| $P_2O_5$ | 0.06 | — | 0.36 | 0.13 | 0.12 | 0.19 | — |
| MnO | 0.12 | 1.84 | 0.48 | 0.26 | 1.55 | 1.32 | 0.048 |
| $SO_2$ | 16.88 | 11.82 | 12.79 | 10.10 | 16.02 | 11.93 | 12.15 |
| CuO | 0.29 | 1.51 | 0.20 | 0.19 | 0.22 | 0.14 | 0.44 |
| ZnO | 0.67 | 1.99 | 0.80 | 0.81 | 0.66 | 0.85 | 0.56 |
| TOTAL | 99.50 | 100.57 | 100.19 | 99.62 | 98.78 | 99.72 | 99.73 |

| TABLE A6 | MAJOR ELEMENT CHEMISTRY | | | | ALTERATION ZONE | | | |
|---|---|---|---|---|---|---|---|---|
| D. D. H. | 18-18-194 | 18-18-198 | 18-18-206 | 18-18-210 | 18-18-220 | 18-18-234 | 18-18-260 | 18-18-274 |
| $SiO_2$ | 25.60 | 19.50 | 55.75 | 41.10 | 59.80 | 24.75 | 51.65 | 39.20 |
| $Al_2O_3$ | 7.10 | 9.80 | 7.90 | 14.68 | 6.10 | 7.58 | 11.86 | 9.82 |
| $Fe_2O_3$ | 22.24 | 30.38 | 9.90 | 12.78 | 3.08 | 26.62 | 5.61 | 12.42 |
| FeO | 15.42 | 10.80 | 7.36 | 9.82 | 15.02 | 13.36 | 12.90 | 18.46 |
| MgO | 7.85 | 9.25 | 5.00 | 7.65 | 6.28 | 7.90 | 3.28 | 4.75 |
| CaO | 3.65 | 0.52 | 1.28 | 2.58 | 0.42 | 2.58 | 8.28 | 7.18 |
| $Na_2O$ | 0.36 | 0.018 | 0.54 | 0.99 | 0.12 | 0.24 | 1.81 | 1.08 |
| $K_2O$ | 0.34 | — | 0.36 | 0.80 | 0.38 | 0.64 | 0.27 | 0.21 |
| $H_2O$ | 3.22 | 4.38 | 2.26 | 1.24 | 1.77 | 2.14 | 1.28 | 1.51 |
| $CO_2$ | — | — | — | — | — | — | — | — |
| $TiO_2$ | 0.42 | 0.42 | 1.08 | 1.78 | 0.74 | 0.82 | 1.48 | 1.31 |
| $P_2O_5$ | 0.06 | 0.09 | 0.10 | 0.09 | 0.07 | 0.12 | 0.21 | 0.18 |
| MnO | 0.91 | 2.32 | 0.20 | 0.26 | 0.38 | 0.38 | 0.71 | 0.66 |
| $SO_2$ | 19.46 | 23.44 | 7.96 | 7.20 | 6.56 | 18.92 | 0.14 | 6.24 |
| CuO | 0.36 | 0.19 | 1.50 | 0.22 | 0.37 | 0.19 | 0.03 | 0.06 |
| ZnO | 1.78 | 0.15 | 1.78 | 0.73 | 0.97 | 1.54 | 0.04 | 0.05 |
| TOTAL | 99.34 | 99.51 | 99.16 | 99.26 | 99.56 | 98.91 | 99.54 | 99.64 |

| TABLE A7 BARTH NORMS MASSIVE FLOWS | | | | | | | | |
|---|---|---|---|---|---|---|---|---|
| D.D.H. | 18-13 397 | 18-10 77 | 18-4 126 | 18-14 123 | 18-1 131 | 18-7 56 | 18-7 128 | 18-9 38 |
| Q | 9.8 | 9.88 | 5.76 | 13.32 | 1.53 | 7.09 | 11.99 | 18.86 |
| C | | | | | | | | |
| Or | 1.9 | 2.6 | 3.25 | 2.25 | 1.6 | 1.25 | 0.95 | 2.70 |
| Ab | 25.75 | 26.9 | 34.1 | 27.4 | 23.35 | 38.75 | 38.5 | 34.0 |
| An | 22.98 | 23.0 | 31.8 | 21.93 | 31.25 | 32.05 | 18.78 | 14.85 |
| Ne | | | | | | | | |
| Lc | | | | | | | | |
| Wo | 5.24 | 8.56 | 5.78 | 5.36 | 8.22 | 3.08 | 4.38 | 4.4 |
| En | 2.74 | 4.42 | 3.72 | 2.5 | 5.34 | 1.82 | 1.46 | 1.66 |
| Fs | 2.5 | 4.14 | 2.06 | 2.86 | 2.88 | 1.26 | 2.92 | 2.74 |
| Di | 10.78 | 17.12 | 11.56 | 10.72 | 16.44 | 6.16 | 8.76 | 8.8 |
| En | 11.82 | 6.76 | 6.02 | 8.3 | 14.7 | 7.12 | 5.24 | 4.54 |
| Fs | 10.72 | 6.3 | 3.36 | 9.6 | 7.96 | 4.96 | 10.46 | 7.62 |
| Hy | 22.54 | 13.06 | 9.38 | 17.9 | 22.66 | 12.08 | 15.7 | 12.16 |
| Fo | | | | | | | | |
| Fa | | | | | | | | |
| Ol | | | | | | | | |
| Ac | | | | | | | | |
| Mt | 3.95 | 3.65 | 2.82 | 3.32 | 1.85 | 1.77 | 2.31 | 5.81 |
| Hm | | | | | | | | |
| Il | 3.12 | 3.22 | 1.02 | 2.54 | 1.22 | 0.74 | 2.52 | 1.98 |
| Py | | | | | | | | |
| Ap | 0.51 | 0.56 | 0.29 | 0.61 | 0.10 | 0.12 | 0.53 | 0.83 |
| Cc | | | | | | | | |
| $H_2O$ | | | | | | | | |
| $CO_2$ | | | | | | | | |
| PLAG. COMP. | An 47 | An 46 | An 48 | An 44 | An 57 | An 45 | An 33 | An 30 |
| TOTAL | 101.03 | 99.99 | 99.98 | 99.99 | 100.01 | 100.01 | 100.04 | 99.99 |

| TABLE A8 BARTH NORMS LAPILLI TUFFS | | | | | | | | |
|---|---|---|---|---|---|---|---|---|
| D. D. H. | 18-8 97 | 18-17 317 | 18-12 201 | 18-13 172 | 18-18 187 | 18-4 296 | 18-16 52 | 18-8 157 |
| Q | 12.22 | 12.26 | 3.99 | 16.88 | 5.12 | 15.06 | 14.02 | 17.96 |
| C | | | | | | | | |
| Or | 9.55 | 4.1 | 6.85 | 6.45 | 12.4 | 4.7 | 6.4 | 4.35 |
| Ab | 24.9 | 28.75 | 22.45 | 29.25 | 27.65 | 25.4 | 32.6 | 13.85 |
| An | 17.63 | 20.9 | 31.93 | 18.25 | 26.25 | 23.05 | 16.65 | 26.33 |
| Ne | | | | | | | | |
| Lc | | | | | | | | |
| Wo | 1.3 | 3.8 | 8.94 | 3.78 | 0.50 | 1.54 | 1.84 | 4.14 |
| En | 0.44 | 1.18 | 3.78 | 0.92 | 0.22 | 0.86 | 0.56 | 1.76 |
| Fs | 0.86 | 2.62 | 5.16 | 2.86 | 0.28 | 1.68 | 1.28 | 2.38 |
| Di | 2.6 | 7.6 | 17.88 | 7.56 | 1.0 | 4.08 | 3.68 | 8.28 |
| En | 9.4 | 7.14 | 5.34 | 3.36 | 10.72 | 6.4 | 5.4 | 9.74 |
| Fs | 18.62 | 15.94 | 7.28 | 10.54 | 12.52 | 12.52 | 12.64 | 13.34 |
| Hy | 28.02 | 23.08 | 12.62 | 13.9 | 23.24 | 18.92 | 18.04 | 23.08 |
| Fo | | | | | | | | |
| Fa | | | | | | | | |
| Ol | | | | | | | | |
| Ac | | | | | | | | |
| Mt | 2.45 | 2.84 | 2.31 | 4.65 | 2.55 | 4.46 | 4.65 | 4.83 |
| Hm | | | | | | | | |
| Il | 1.92 | 1.06 | 1.66 | 2.08 | 1.44 | 2.66 | 2.54 | 1.00 |
| Py | | | | | | | | |
| Ap | 0.72 | 0.37 | 0.29 | 0.99 | 0.35 | 0.67 | 1.44 | 0.32 |
| Cc | | | | | | | | |
| $H_2O$ | | | | | | | | |
| $CO_2$ | | | | | | | | |
| PLAG. COMP. | An 41 | An 45 | An 59 | An 38 | An 49 | An 48 | An 34 | An 66 |
| TOTAL | 100.01 | 100.00 | 99.98 | 100.01 | 100.00 | 99.00 | 100.02 | 100.00 |

TABLE A9 BARTH NORMS SILICEOUS TUFFITE & GREYWACKE

| D. D. H. | 18-8 260 | 18-17 376 | 18-4 148 | 18-17 384 | | 18-1 166 | 18-5 200 | 18-11 55 |
|---|---|---|---|---|---|---|---|---|
| Q | 37.93 | 36.18 | 16.37 | 23.32 | | 14.75 | 21.49 | 11.6 |
| C | 2.75 | 3.94 | | 3.43 | | 6.12 | 2.12 | 2.8 |
| Or | 10.0 | 10.3 | 10.95 | 9.45 | | 14.35 | 6.05 | 26.95 |
| Ab | 26.0 | 21.1 | 29.0 | 28.1 | | 20.85 | 47.6 | 16.5 |
| An | 10.2 | 10.15 | 20.6 | 12.95 | | 14.45 | 11.4 | 26.35 |
| Ne | | | | | | | | |
| Lc | | | | | | | | |
| Wo | | | 1.44 | | | | | |
| En | | | 0.64 | | | | | |
| Fs | | | 0.8 | | | | | |
| Di | | | 2.88 | | | | | |
| En | 5.7 | 7.9 | 7.6 | 9.14 | | 11.24 | 6.08 | 7.48 |
| Fs | 4.88 | 8.9 | 9.68 | 8.16 | | 10.38 | 3.94 | 6.32 |
| Hy | 10.58 | 16.8 | 17.28 | 17.3 | | 21.62 | 10.02 | 13.8 |
| Fo | | | | | | | | |
| Fa | | | | | | | | |
| Ol | | | | | | | | |
| Ac | | | | | | | | |
| Mt | 1.61 | 0.59 | 2.43 | 2.73 | | 1.16 | 0.27 | 1.02 |
| Hm | | | | | | | | |
| Il | 0.68 | 0.76 | 1.06 | 3.78 | | 0.78 | 0.74 | 0.74 |
| Py | | | | | | | | |
| Ap | 0.24 | 0.19 | 0.24 | 0.27 | | 0.35 | 0.32 | 0.24 |
| Cc | | | | | | | | |
| $H_2O$ | | | | | | | | |
| $CO_2$ | | | | | | | | |
| PLAG. COMP. | An 28 | An 32 | An 42 | An 32 | | An 41 | An 19 | An 61 |
| TOTAL | 99.99 | 100.01 | 100.81 | 100.33 | | 100.00 | 100.01 | 100.00 |